Advances in Olefin Metathesis: Water Sensitivity and Catalyst Synthesis

Adrian Botti

Thesis submitted to the
Faculty of Graduate and Postdoctoral Studies
University of Ottawa
in partial fulfillment of the requirements for the degree of

Master of Science in Chemistry

Center for Catalysis Research and Innovation
Department of Chemistry and Biomolecular Science
Ottawa-Carleton Chemistry Institute
Faculty of Science
University of Ottawa

Table of Contents

List of Figures

List of Schemes

Abstract

Olefin metathesis is the most powerful, versatile reaction in current use for the formation of new carbon-carbon bonds. While metathesis has been known for over 60 years, it has only recently been implemented into pharmaceutical and specialty chemical manufacturing. The slow uptake of olefin metathesis can be attributed in part to low catalyst productivity, a consequence of short catalyst lifetime. Improving catalyst activity is critical for the advancement of metathesis. This improvement can be achieved through greater understanding of the catalysts and their limitations.

The ability to perform metathesis in aqueous media is desirable, but as yet largely unrealized, for the modification of water-soluble, biologically-relevant substrates. At present, high catalyst loadings are necessary even for less demanding metathesis reactions in water. The limited mutual solubility of the catalyst and substrate in water are one limitation. Examined in this thesis are more fundamental challenges associated with catalyst deactivation by water. The impact of water on catalyst productivity was assessed for both the second-generation Grubbs catalyst **GII**, and the phosphine-free Hoveyda catalyst **HII**, in ring-closing and cross-metathesis reactions. Water was shown to have a negative impact on metathesis productivity, owing to catalyst decomposition. The decomposition pathway was catalyst-dependent: **GII** was found to decompose through a pathway in which water accelerated abstraction of the methylidene ligand by dissociated phosphine. For **HII**, water was found to decompose the metallacyclobutane intermediate. A β-hydride transfer mechanism was proposed, to account for the organic decomposition products observed.

Chapter 4 focuses on problems encountered during the synthesis of ruthenium catalysts, and presents improved methods. An updated method was developed for the synthesis of phenyldiazomethane, the principal source of the alkylidene ligand required in synthesis of **GI**. Challenges in use of the phosphine-scavenging resin Amberlyst-15 resin are discussed. Improving synthetic routes to the important first- and second-generation Grubbs catalysts will aid in expansion of olefin metathesis methodologies, particularly in the industrial context, in which batch-to-batch reproducibility is paramount.

Acknowledgements

I would first like to sincerely thank my supervisor Prof. Deryn Fogg for her guidance. You have given me opportunities that have allowed me to not only develop as a better scientist but also as a person. The experience and skills I have learned from you will serve me for the rest of my career and I am very thankful for that.

I would also like to thank the technical experts at the University of Ottawa, Dr. Glenn Facey (UOttawa NMR Facility) and Roxanne Clement (CCRI High-Throughput Facility), who helped with the work described in the thesis.

To my current lab-mates Carolyn, Gwen, Billy, Stephanie and Emma and past members Jenn, Bianca, Justin, Ben and Nikita: I am very happy I had the opportunity to work with all of you. Carolyn, Gwen and Emma, thank you for all the discussions we had in the lab and the help you provided me, which were greatly appreciated. Billy, it was a pleasure getting to work with you and to go for our morning coffees. I would also like to thank all my friends outside of the lab, who have supported me through this journey.

To my parents, who supported me every step of the way and provided me with life skills that allowed me to develop into who I am: I appreciate everything you have done for me and for all your guidance.

Finally, to Jerrika, I cannot thank you enough for all the support you have given me. This would not have been possible without you, whether it was to talk about my day or try to make things better when something did not work out. You are an amazing person and I admire all your hard work, which has pushed me to work harder.

List of Compounds

Organic and main group compounds

H_2IMes	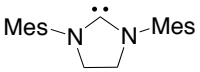	IMes	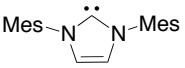
1	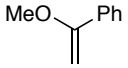	**2**	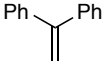
3	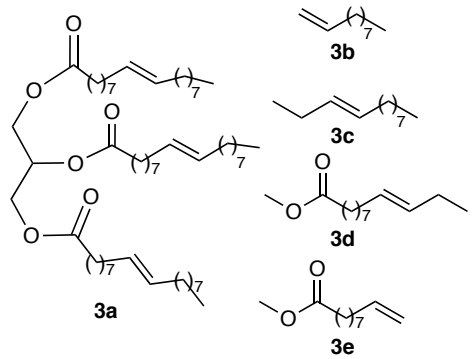	**4**	$[MePCy_3]Cl$
		5	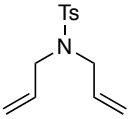
		6	$TBSO(H_2C)_4$
		7	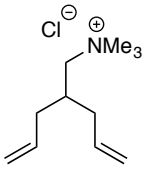
8	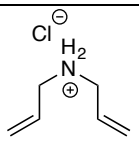	**9**	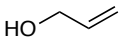
10	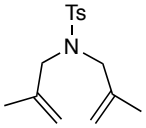	**11**	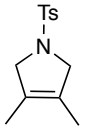
12	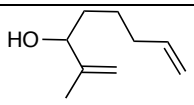	**13**	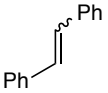
14	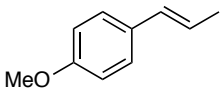	**15**	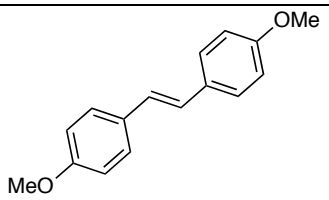
16	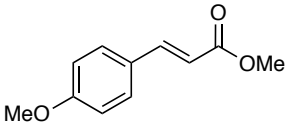	**17**	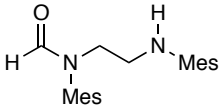
18a		**18b**	

18c	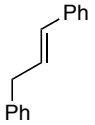	**19**	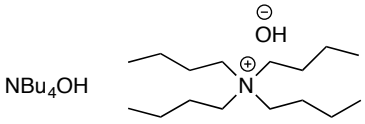
20		**21**	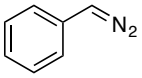
22	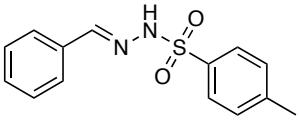	**23**	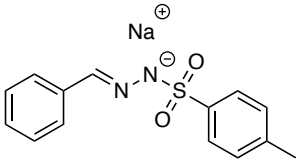
24		**25**	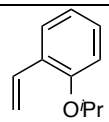
DDM	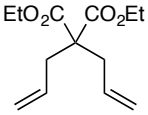	**DMT**	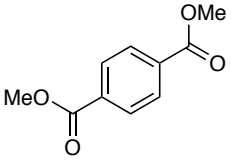
MA	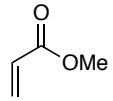		

Metal complexes

GI	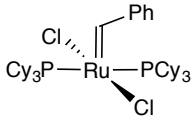	**GII**	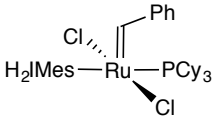
uGII	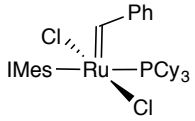	**GIIm**	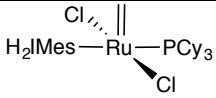
G0	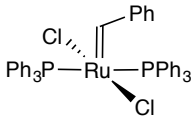	**HI**	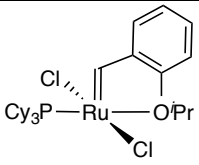
HII	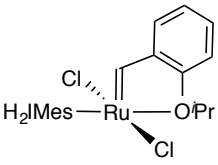	**uHII**	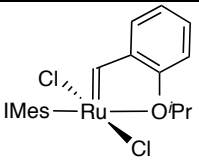

HII-(OH)	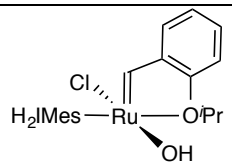	**HII-(OH)$_2$**	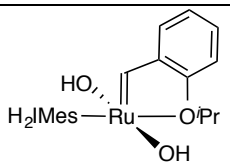
M1	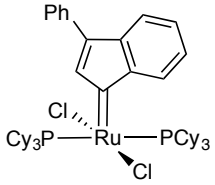	**M2**	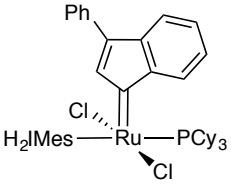
Caz1	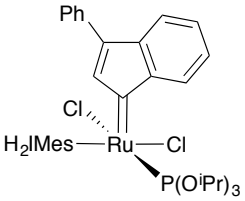	**Ru-1**	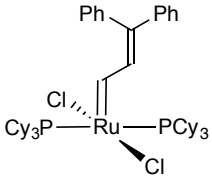
Ru-2	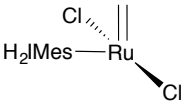	**Ru-3**	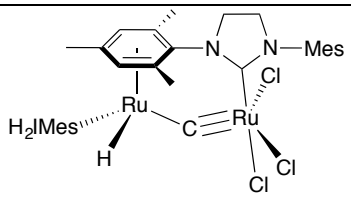
Ru-4	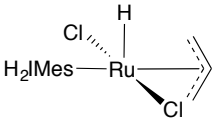	**Ru-5**	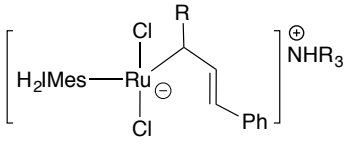
Ru-6	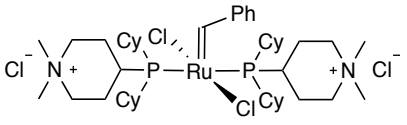	**Ru-7**	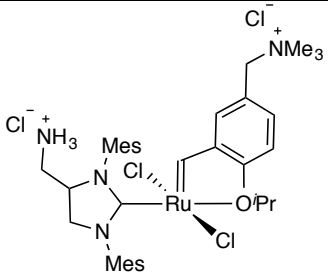
Ru-8	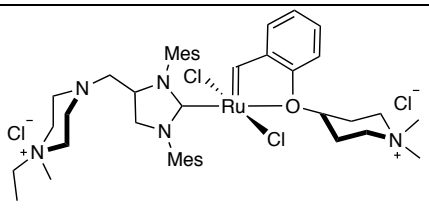	**Ru-9**	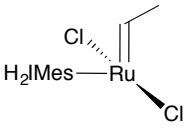
Ru-10	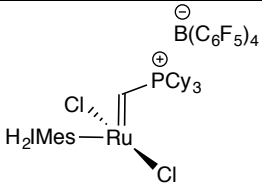	**Ru-11**	$RuCl_2(PPh_3)_3$

Ru-12	$RuHCl(PPh_3)_3$	**Ru-13**	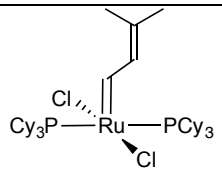
Ru-14	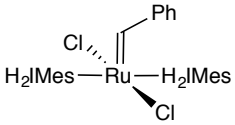	**Ru-15**	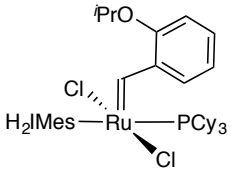

MCB	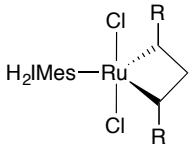	**W-1**	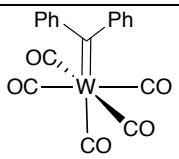
W-2	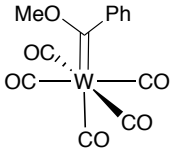	**W-3**	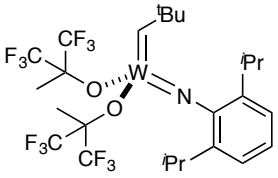
Ta-1	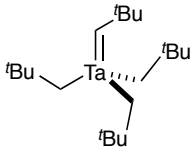	**Mo-1**	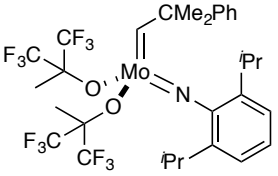

Abbreviations

ADMET	Acyclic diene metathesis
Ar	Aryl
CM	Cross metathesis
COSY	Correlation spectroscopy
DDM	Diethyl diallylmalonate
DMT	Dimethyl terephthalate
EI	Electron impact
equiv	Equivalents
FID	Flame ionization detector
GC	Gas chromatography
H_2IMes	1,3-bis-(2,4,6-trimethylphenyl)imidazolin-2-ylidene
HCV	Hepatitis C virus
HMBC	Heteronuclear multiple bond correlation
HMQC	Heteronuclear multiple quantum coherence
Hz	Hertz
IMes	1,3-bis-(2,4,6-trimethylphenyl)imidazol-2-ylidene
IS	Internal standard
KTp	Potassium hydrotris(pyrazolyl)borate
L	Neutral ligand donor
MA	Methyl acrylate
MCB	Metallacyclobutane
Mes	Mesityl
MeOH	Methanol
MS	Mass spectrometry
NHC	*N*-heterocyclic carbene
NMR	Nuclear magnetic resonance
NOE(SY)	Nuclear Overhauser effect (spectroscopy)
ppm	Parts per million
RCM	Ring closing metathesis
ROMP	Ring opening metathesis polymerization
RT	Room temperature

SM	Self-metathesis
THF	Tetrahydoafuran
TMS	Tetramethylsilane
TON	Turnover number

Chapter 1. Introduction

1.1. Catalysis

A catalyst is defined as a substance that lowers the activation energy of a reaction without being consumed in the process.[1] Because catalysts are not consumed during the reaction, they are able to "turn over" multiple cycles during the reaction (Figure 1.1). Catalysts are responsible for an enormous variety of chemical transformations, the scope and power of which have been recognized with 15 Nobel Prizes since 1901.[2] Catalysis enables faster production of target molecules, commonly in fewer steps than stoichiometric routes.[3] Environmental impacts can be reduced in consequence: not only is the overall mass of material reduced, but eliminating the need for intervening steps reduces the waste associated with workup, particularly solvent demands.[4] Highly stable and active catalysts are highly sought after, as a means of achieving higher turnover numbers (TON), which translates into catalyst productivity.

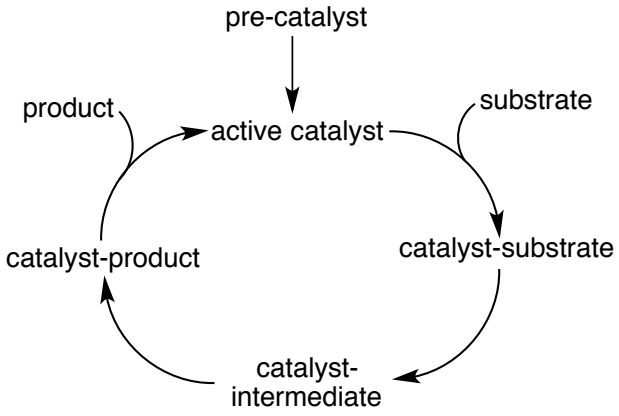

Figure 1.1 General pathway for a catalytic cycle.

A vast amount of research has focused on catalyst development for both homogeneous and heterogeneous catalysis.[1] Among the most important such synthetic reactions is the formation of new carbon-carbon bonds, which form the skeletal structures of complex organic molecules.[5]

References page 13

Catalyst design for carbon-carbon forming reactions has focused on the opportunities that transition-metal complexes create for tuning catalyst steric, electronic, and chiral properties. Two Nobel Prizes in chemistry were awarded in the last decade for the advancement of carbon-carbon bond-forming reactions via homogeneous catalysis. In 2005, Chauvin,[6] Grubbs[7] and Schrock[8] were recognized for their pioneering work in olefin metathesis. In 2010, Heck, Negishi[9] and Suzuki[10] were honoured for the development of palladium-catalyzed cross-coupling reactions. This thesis will focus on olefin metathesis: on catalyst decomposition, and synthetic routes to olefin metathesis catalysts.

1.2 Olefin Metathesis

1.2.1 History and Overview of Olefin Metathesis

Olefin metathesis is a powerful synthetic tool that enables construction of carbon-carbon double bonds. It has had a massive impact on the academic sector and, more recently, pharmaceutical and specialty-chemical manufacturing, affording access to products that would be difficult to synthesize via stoichiometric processes. Olefin metathesis encompasses transformations ranging from ring-closing metathesis (RCM) to cross-metathesis (CM), ring-opening metathesis polymerization (ROMP), and acyclic diene metathesis (ADMET) (Figure 1.2).

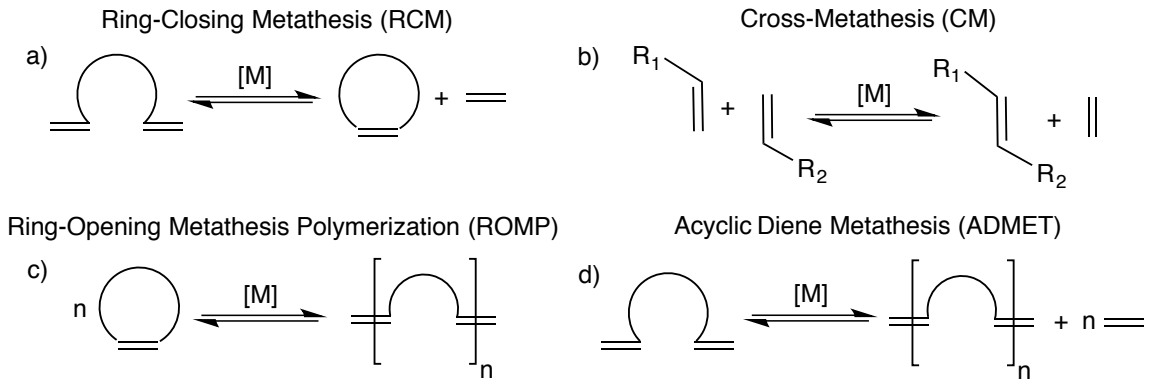

Figure 1.2 Examples of the common types of olefin metathesis reactions.

The first reported example of olefin metathesis was documented in a patent filed by researchers at Du Pont in 1956.[11] In this patent, the polymerization of norbornene was observed using $TiCl_4$ as the catalyst, although the mechanistic details were unknown. In 1964, Phillips Petroleum described the disproportionation of propylene into ethylene and 2-butene using molybdenum and tungsten catalysts.[12] It was not until 1967 that it was determined that the breaking and re-forming of the carbon-carbon double bonds were responsible for this phenomenon.[13] The identity of the active catalyst or the mechanism of this process was unknown as the metal complex was simply WCl_6. Using 2-pentene, a 1:2:1 mixture of 2-butene, 2-pentene, and 3-hexene in ethanol was obtained, confirming carbon-carbon double bonds were breaking and re-forming.

In a seminal report in 1971, Chauvin proposed that olefin metathesis occurs via a [2+2] cyclo-addition between a metal alkylidene and an olefin, forming a metallacyclobutane (**MCB**) intermediate.[14] Subsequent cyclo-reversion of the **MCB** results in the formation of new olefinic products (Scheme 1.1). Experimental evidence from several groups, particularly relating to product distributions, supported the Chauvin mechanism over the other mechanistic hypotheses, such as a metallacyclopentane intermediate or reaction of a cyclobutane with a metal complex.[15]

Key evidence included work from Katz and co-workers on the molybdenum-catalyzed reaction of cyclooctene with 2-butene and 4-octene, which afforded 2,10-tetradecadiene, a product consistent only with the Chauvin mechanism.[16] Early isotopic labeling studies employed by Grubbs, using deuterium-labeled and unlabeled 1,7-octadiene, revealed ethylene-d_2 as one of the products.[17,18] The observation of ethylene-d_2 was significant in that the only explanation for its production was via a metal carbene complex and the **MCB** intermediate

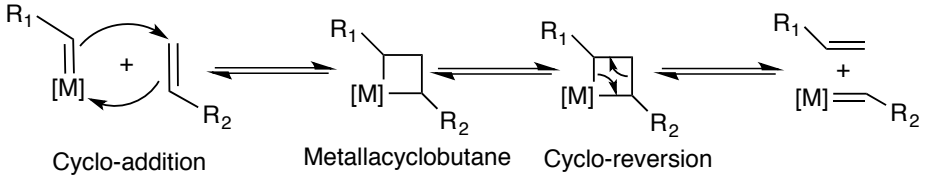

Scheme 1.1 The Chauvin mechanism for olefin metathesis, highlighting the steps involved.

1.2.2 Well-defined Metal Alkylidene Complexes for Olefin Metathesis

Essential to the Chauvin mechanism is the formation of two key organometallic species: a metal carbene complex and the **MCB** intermediate. Early attempts to isolate a metal carbene were described by Casey and Burkhardt in 1974.[19] In this study, a reactive (and unstable) tungsten carbene (**W-1**) underwent stoichiometric reaction with 1-methoxy-1-phenylethylene **1** to afford new olefinic product **2** and metal carbene **W-2**, confirming alkylidene transfer to the olefin (Scheme 1.2). Again, these data supported the Chauvin mechanism.

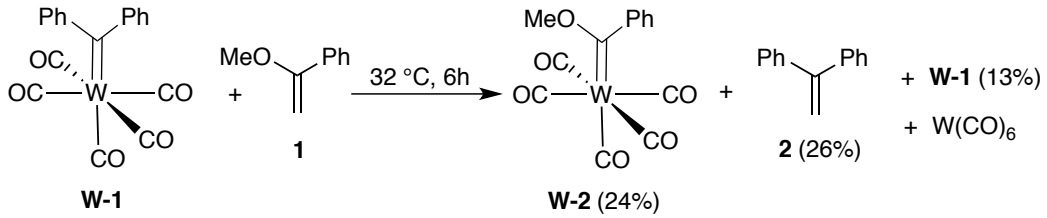

Scheme 1.2 Reaction of **W-1** with 1-methoxy-1-phenylethylene (**1**) to generate a new olefin (**2**) and metal carbene (**W-2**) complex.

In 1974, Schrock achieved the first synthesis of the putative metal alkylidene complex.[20] This tantalum alkylidene (**Ta-1**, Figure 1.3) was not only synthesized and isolated, but was shown to initiate the metathesis of 1-butene. Multiple turnovers of the catalyst were achieved, consistent with the Chauvin mechanism.[21] Further modification of these Schrock alkylidene complexes afforded molybdenum and tungsten catalysts such as **Mo-1** and **W-3** (Figure 1.3).[22-24] These catalysts exhibited remarkable activity and tunability, leading to their eventual commercial availability. A limitation, however, lies in their high oxophilicity, which results in difficulties in handling, owing to decomposition by air, moisture, and protic functional groups such as alcohols, aldehydes and carboxylic acids.[25]

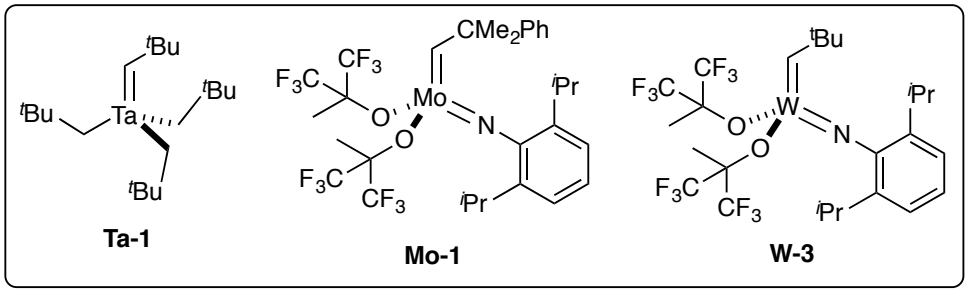

Figure 1.3 Group 5 and 6 metal alkylidene complexes.

1.2.3 Ruthenium Olefin Metathesis Catalysts

The ruthenium catalysts initially discovered by Grubbs are much less sensitive to air, moisture, and protic functional groups, making them easier to handle than the Schrock catalysts.[26] Grubbs reported the first well-defined ruthenium metathesis catalyst in 1992 (**Ru-1**, Figure 1.4),[27] but it was the so-called first-generation Grubbs catalyst **GI** (Figure 1.4),[28] that led to high popularity. The reactivity of **GI** was limited relative to the Schrock catalysts, however. A breakthrough in reactivity resulted on replacing one of the PCy_3 ligands of **GI** with a more strongly σ-donating

N-heterocyclic carbene (NHC) ligand. The first such ligand was unsaturated **IMes**, incorporated within the Grubbs catalyst **uGII** (where u signifies unsaturated) by Nolan and co-workers (Figure 1.4).[29] Almost simultaneously, Grubbs reported the **H_2IMes** analogue **GII** (Figure 1.4).[30,31] Slower initiation was reported for **GII** compared to **GI**, but higher metathesis activity.[32] Our group recently uncovered the basis of the inverse trans effect that decreases the lability of the PCy_3 ligand in **GII**, tracing the slow phosphine dissociation required for catalyst initiation to Ru→PCy_3 backbonding.[33]

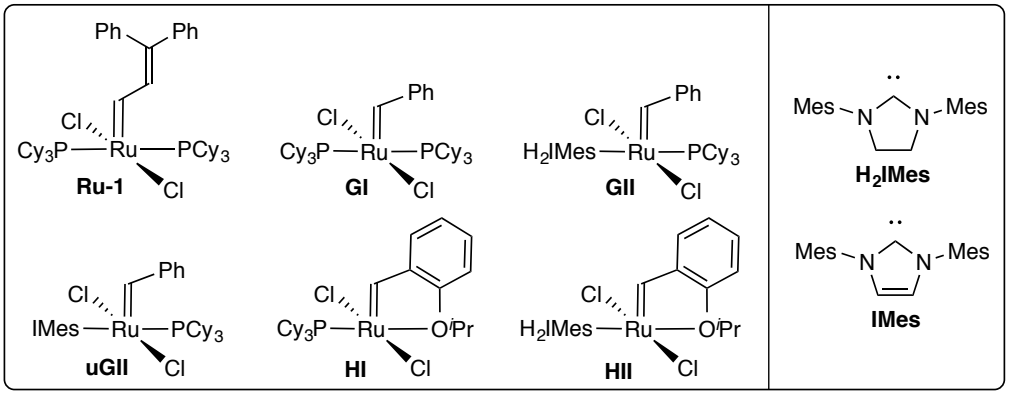

Figure 1.4 Ruthenium metathesis catalysts of the Grubbs and Hoveyda types.

Catalyst modification has garnered much attention, as there are many tunable sites on the complexes including the alkylidene, the neutral ligands and the anionic ligands. Substituting the benzylidene moiety on **GI** and **GII** with a chelating styrenyl ether afforded the Hoveyda catalysts (**HI** and **HII**, Figure 1.4).[34,35] The key difference resides in their phosphine-free character, which enables faster entry into the catalytic cycle.[36] An associative pathway has been proposed in some cases.[36-38] ^{13}C-Labelling studies confirmed that recapture of the styrenyl ether ligand regenerates **HII** as the off-cycle, resting-state species.[36]

Although **GII** remains the most dominant catalyst used in metathesis, the popularity of **HII** has increased in recent years. Other variants on these catalysts include modification of the NHC ligand and replacement of the chloride ligands.[39]

1.2.4 Uptake of Olefin Metathesis in Industrial Processes

While hundreds of ruthenium metathesis catalysts have been developed, of which many are now commercially available,[40] industrial examples of olefin metathesis using molecular catalysts are only 2 years old.[41] Notwithstanding the importance of cross-metathesis in the SHOP process, and of specialty polymers prepared via ROMP, it has taken almost 60 years for the fine-chemicals and pharmaceutical sectors to embrace olefin metathesis. In 2005, a report from Boehringer Ingelheim described the first pilot-scale RCM synthesis of an active pharmaceutical ingredient (API).[42] The large-scale synthesis of Ciluprevir (Figure 1.5), a HCV protease inhibitor, utilized metathesis to form the 15-membered macrocyclic ring. While Ciluprevir failed in clinical trials, it was the first report of metathesis being used on large scale, and paved the way for other macrocyclic drug candidates to be synthesized using olefin metathesis as a key step. The first RCM-enabled industrial process was the production of the HCV protease inhibitor Simeprevir, developed by Janssen Pharma, which came on stream in 2014.[43]

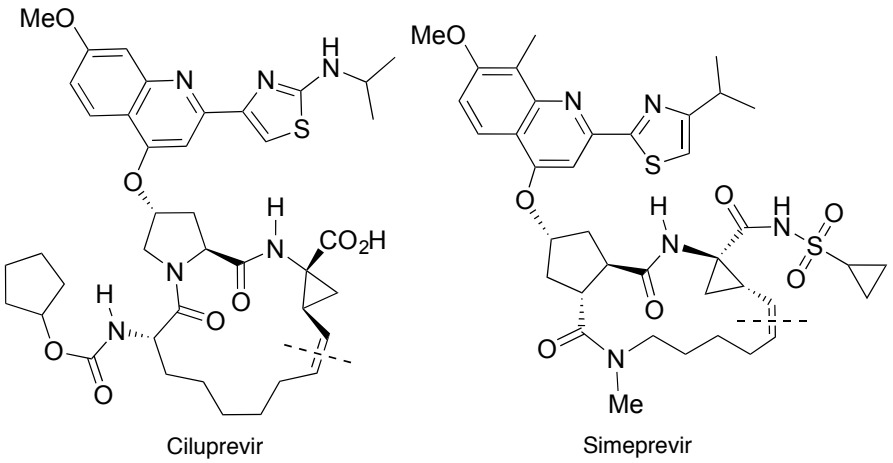

Figure 1.5 HCV protease inhibitors synthesized using RCM.

While the pharmaceutical industry is increasingly open to RCM macrocyclization as a route to valuable drug candidates, CM processes are less established. The first reported (2013) industrial process implementing CM was a joint venture between Elevance Renewable Sciences and Wilmar International. Specialty chemicals are reportedly manufactured from renewable feedstocks via sequential CM and transesterification (Scheme 1.3). Vegetable-oil triglycerides **3a** (predominantly from palm oil) are converted into products **3b-e** for which applications as lubricants, synthetic oils, fuels, waxes, and precursors to fine chemicals are claimed.[41,44,45]

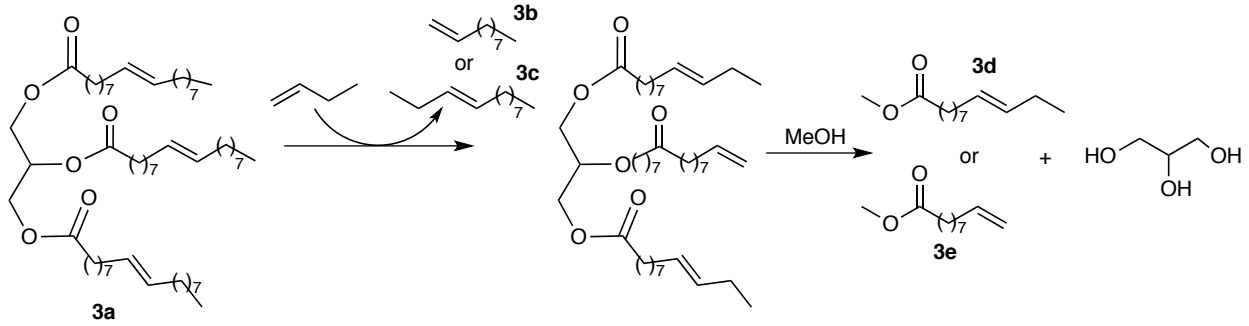

Scheme 1.3 Conversion of triglycerides by sequential CM and transesterification to precursors of specialty chemicals.

One limitation on industrial uptake of these molecular olefin metathesis is catalyst decomposition, which limits productivity. Even the relatively robust ruthenium catalysts are prone to decomposition, especially in the presence of both Brønsted and Lewis bases, as our group has shown.[46-53] Decomposition may be triggered by contaminants in technical-grade solvents, residues from previous synthetic steps, or indeed functionalities present on the substrate.[42,54-56] Improved understanding of the nature of such problems is key to developing solutions, whether by changing reaction conditions or by catalyst design to increase productivity and lifetime.

While several reports describe decomposition of precatalysts,[29,53,57-59] the species generated during metathesis are generally more vulnerable. For the Grubbs catalyst, the key species that warrant more extensive study are the resting-state methylidene complex **GIIm**, and the metallacyclobutane **MCB** (Figure 1.6). The Hoveyda catalysts have been less studied, but the **MCB** and the four-coordinate methylidene intermediates are likely most vulnerable.

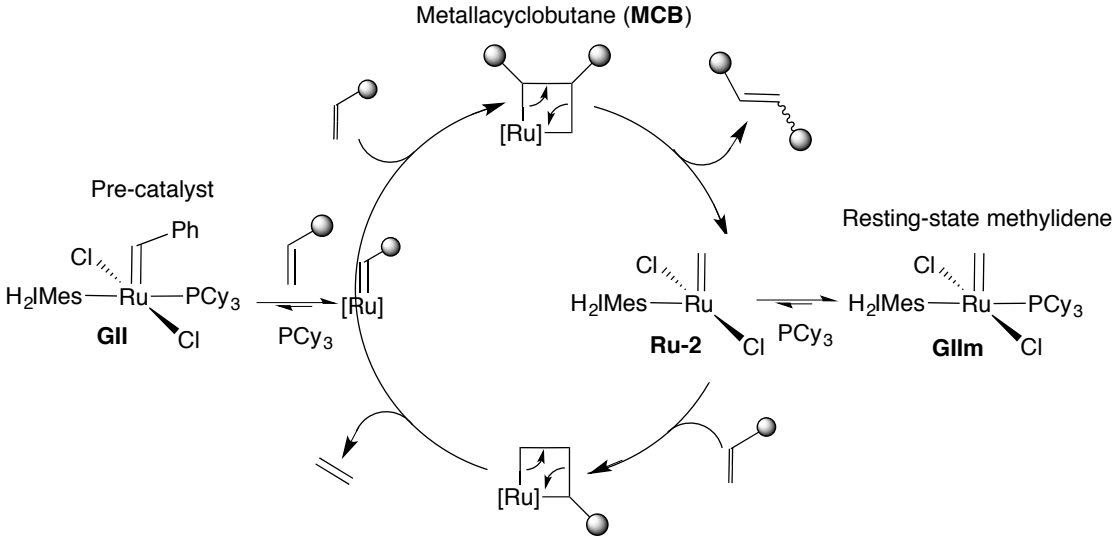

Figure 1.6 Catalytic cycle for **GII**, highlighting key species in the cycle.

1.2.5 Decomposition Studies on GIIm

The off-cycle species in the catalytic cycle, **GIIm**, is formed via re-coordination of PCy_3 to the active species. Dr. Justin Lummiss of this research group developed the first high-yield route to this complex, an enabling advance that facilitates examination of the decomposition pathways to which **GIIm** is subject, including its vulnerability to impurities.[60] In 2004, Hong and Grubbs reported thermolysis of **GIIm** in the absence of substrate, resulting in the dinuclear ruthenium species **Ru-3**,[61] isolated in 46% yield, with observation of $[MePCy_3]Cl$ **4**. Dissociation of PCy_3 and methylidene abstraction was proposed (Scheme 1.4). While these authors proposed that hydride complex **Ru-3** was the principal cause of competing isomerization during intended metathesis reactions,[62] subsequent studies showed that this species is not kinetically competent for the suggested purpose.[63]

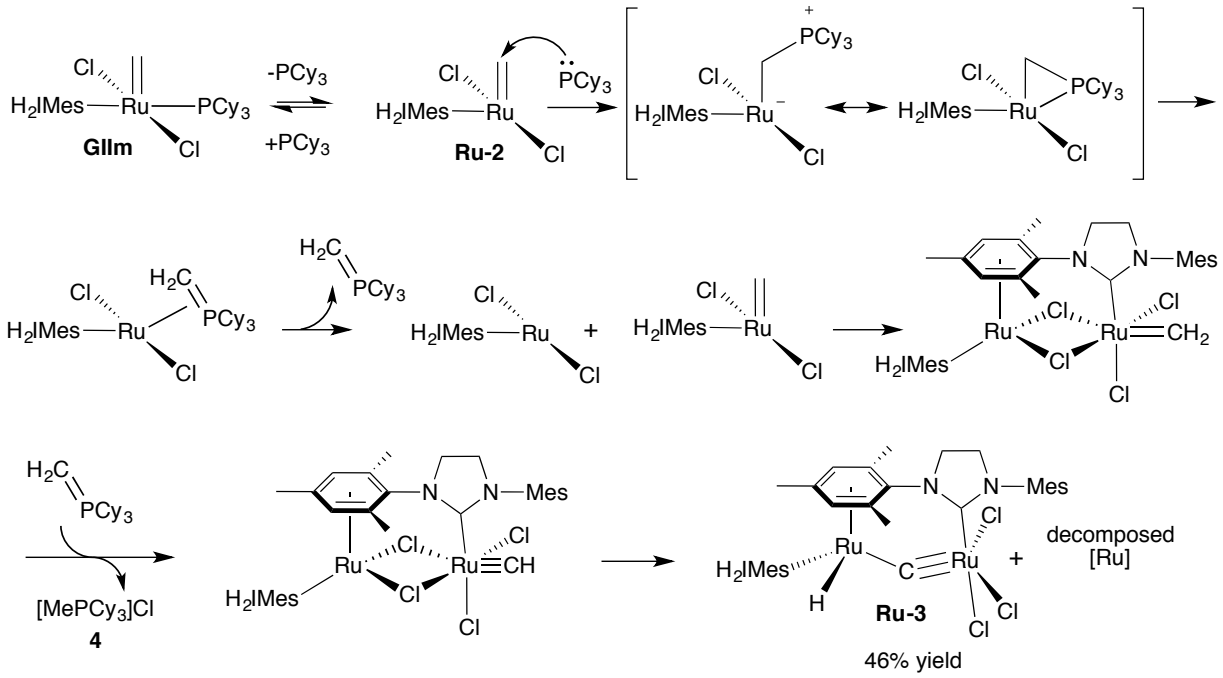

Scheme 1.4 Proposed mechanism for the thermolysis of **GIIm** to produce $[MePCy_3]Cl$ and **Ru-3**.

The long reaction time required for this decomposition pathway (72 h) casts doubt on its relevance to catalyst decomposition during metathesis. The more important finding in this experiment was the nucleophilic attack of PCy_3 on the methylidene complex. This pathway of PCy_3 attack on the **GIIm** has been extensively studied within the Fogg group, and the generality of this pathway has been demonstrated in recent work by Mr William McClennan.[46] Sterically accessible Lewis donors (i.e. many common impurities) were shown to greatly accelerate loss of PCy_3, owing to associative reaction with **GIIm** (Scheme 1.5). We have termed this decomposition pathway donor-accelerated decomposition.[46,49-51] Recent findings demonstrated that the ruthenium byproducts can terminate in isomerization-active ruthenium nanoparticles. Given the vulnerability of **GIIm** to donors, it is important that the presence of these donors be reduced during metathesis, to protect catalyst productivity.

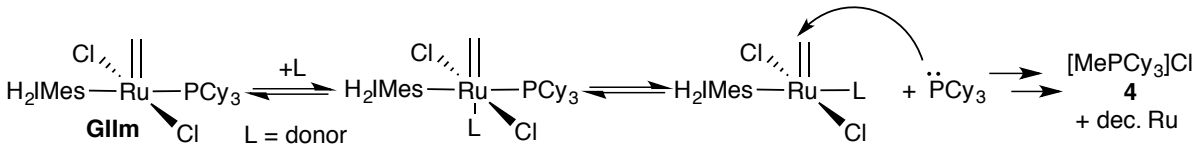

Scheme 1.5 General mechanism for donor-accelerated decomposition.

1.2.6 Reported Decomposition of MCB Complex for Olefin Metathesis Catalysts

A 2005 report by van Rensburg and co-workers at Sasol described the decomposition of **GIIm** under ethylene, with formation of propylene and unidentified ruthenium by-products.[64] The proposed mechanism (Scheme 1.6) involved β-hydride elimination from the **MCB** through a ruthenium allyl-hydride intermediate (**Ru-4**). Interestingly, the imidazolium salt $[H_2IMesH]Cl$ was observed in 11% yield, a rare report on NHC decoordination.

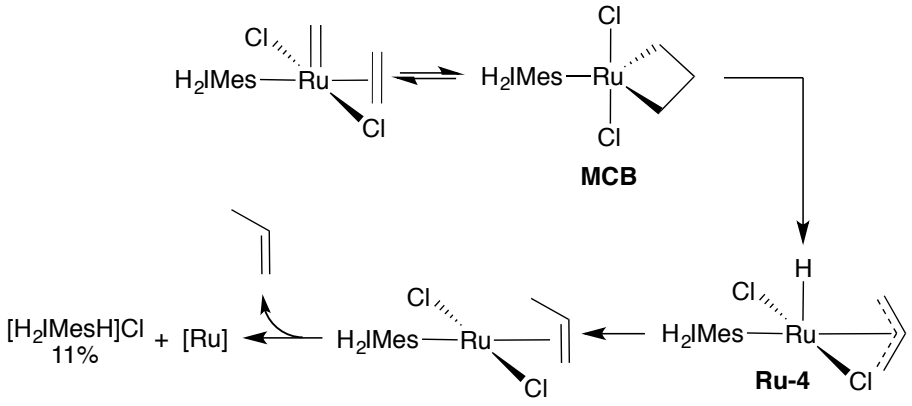

Scheme 1.6 Proposed decomposition pathway of **GIIm** under ethylene by β-hydride elimination.

Bespalova and co-workers subsequently reported that decomposition of **HII** with ethylene likewise generated propylene (as well as 2-butene, proposed to form from the CM of propylene under the reaction conditions: 55 °C, C_6D_6, 24 h).[65]

Recent work by Dr. Benjamin Ireland of the Fogg group examined the effect of amines during self-metathesis of styrene by **HII**. Deprotonation of the **MCB** by the amines was proposed due to the observation of organic products containing the three metallacyclobutane carbons (Scheme 1.7). Given the low acidity of the MCB protons, the potential for alternative routes involving activation of the mesityl methyl groups may present an alternative pathway. Such bond activation has been described for ruthenium complexes formed by decomposition of metathesis catalysts.[59,61,66,67]

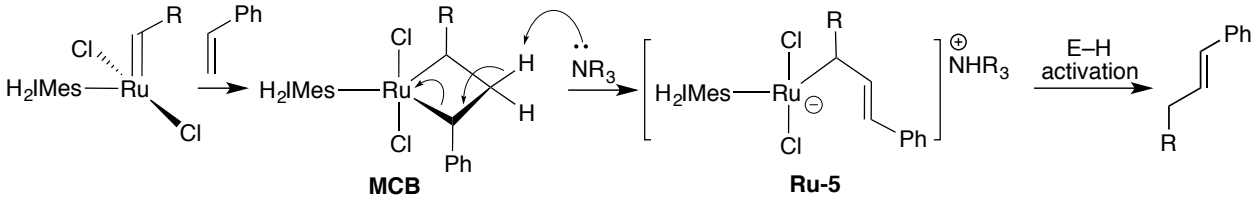

Scheme 1.7 Proposed mechanism for deprotonation of **MCB** complex by amines in metathesis.

1.3 Scope of Thesis Work

Increasing the lifetime and productivity of olefin metathesis catalysts is essential to advance the field. To that end, better understanding of catalyst decomposition pathways during metathesis is required, with the goal of redesigning catalyst structures and/or reaction conditions.

Chapter 2 of this thesis presents the experimental procedures used. Chapter 3 examines the negative impact of water during metathesis, an issue that has gone largely overlooked. Any deleterious effects associated with water are highly important, as water is a ubiquitous contaminant. Better understanding provides the opportunity to develop new catalysts or conditions to promote catalyst longevity, and may ultimately contribute to the development of metathesis catalysts that operate efficiently for challenging reactions in aqueous media. Chapter 4 outlines unexpected issues associated with the literature routes to access the Grubbs catalysts. Improved synthetic are presented, which limit the proportion of impurities that may affect the catalysts at the stage of use. Finally, Chapter 5 reviews the key advances in this thesis, and future directions.

1.4 References

(1) Rothenberg, G., *Catalysis*. Wiley-VCH: Weinheim, 2008.
(2) Thayer, A. M. *Chem. Eng. News,* **2013**, *91*, 68.
(3) Sheldon, R. A. *Green Chem.* **2007**, *9*, 1273–1283.
(4) Anastas, P.; Eghbali, N. *Chem. Soc. Rev.* **2010**, *39*, 301–312.
(5) Blaser, H.-U., Applications of Transition Metal Catalysis in Drug Discovery and Development: An Industrial Perspective. Crawley, M. L.; Trost, B. M., Eds. John Wiley & Sons 2012.
(6) Chauvin, Y. *Angew. Chem. Int. Ed.* **2006**, *45*, 3741–3747.
(7) Grubbs, R. H. *Angew. Chem. Int. Ed.* **2006**, *45*, 3760–3765.
(8) Schrock, R. R. *Angew. Chem. Int. Ed.* **2006**, *45*, 3748–3759.
(9) Negishi, E.-i. *Angew. Chem., Int. Ed.* **2011**, *50*, 6738–6764.
(10) Suzuki, A. *Angew. Chem., Int. Ed.* **2011**, *50*, 6722–6737.

(11) Anderson, A. W.; Merckling, N. G. Polymeric bicyclo[2.2.1]hept-2-ene. U.S. Patent No. 2721189, 1955.
(12) Banks, R. L.; Bailey, G. C. *Ind. Eng. Chem. Prod. Res. Dev.* **1964**, *3*, 170–173.
(13) Calderon, N.; Chen, H. Y.; Scott, K. W. *Tetrahedron Lett.* **1967**, 3327–3329.
(14) Hérisson, J. L.; Chauvin, Y. *Makromol. Chem.* **1971**, *141*, 161–176.
(15) Calderon, N.; Ofstead, E. A.; Ward, J. P.; Judy, W. A.; Scott, K. W. *J. Am. Chem. Soc.* **1968**, *90*, 4133–4140.
(16) Katz, T. J.; McGinnis, J. *J. Am. Chem. Soc.* **1975**, *97*, 1592–1594.
(17) Grubbs, R. H.; Burk, P. L.; Carr, D. D. *J. Am. Chem. Soc.* **1975**, *97*, 3265-3267.
(18) Grubbs, R. H.; Carr, D. D.; Hoppin, C.; Burk, P. L. *J. Am. Chem. Soc.* **1976**, *98*, 3478–3483.
(19) Casey, C. P.; Burkhardt, T. J. *J. Am. Chem. Soc.* **1974**, *96*, 7808-7809.
(20) Schrock, R. R. *J. Am. Chem. Soc.* **1974**, *96*, 6796–6797.
(21) Schrock, R.; Rocklage, S.; Wengrovius, J.; Rupprecht, G.; Fellmann, J. *J. Mol. Catal.* **1980**, *8*, 73–83.
(22) Schrock, R. R.; DePue, R. T.; Feldman, J.; Schaverien, C. J.; Dewan, J. C.; Liu, A. H. *J. Am. Chem. Soc.* **1988**, *110*, 1423–1435.
(23) Schrock, R. R.; Murdzek, J. S.; Bazan, G. C.; Robbins, J.; DiMare, M.; O'Regan, M. *J. Am. Chem. Soc.* **1990**, *112*, 3875–3886.
(24) Fox, H. H.; Lee, J. K.; Park, L. Y.; Schrock, R. R. *Organometallics* **1993**, *12*, 759–768.
(25) Schrock, R. R. *Chem. Rev.* **2009**, *109*, 3211–3226.
(26) Trnka, T. M.; Grubbs, R. H. *Acc. Chem. Res.* **2001**, *34*, 18–29.
(27) Nguyen, S. T.; Johnson, L. K.; Grubbs, R. H.; Ziller, J. W. *J. Am. Chem. Soc.* **1992**, *114*, 3974–3975.
(28) Schwab, P.; Grubbs, R. H.; Ziller, J. W. *J. Am. Chem. Soc.* **1996**, *118*, 100–110.
(29) Huang, J.; Stevens, E. D.; Nolan, S. P.; Petersen, J. L. *J. Am. Chem. Soc.* **1999**, *121*, 2674–2678.
(30) Scholl, M.; Ding, S.; Lee, C. W.; Grubbs, R. H. *Org. Lett.* **1999**, *1*, 953–956.
(31) Ackermann, L.; Fürstner, A.; Weskamp, T.; Kohl, F. J.; Herrmann, W. A. *Tetrahedron Lett.* **1999**, *40*, 4787–4790.
(32) Sanford, M. S.; Love, J. A.; Grubbs, R. H. *J. Am. Chem. Soc.* **2001**, *123*, 6543–6554.
(33) Lummiss, J. A. M.; Higman, C. S.; Fyson, D. L.; McDonald, R.; Fogg, D. E. *Chem. Sci.* **2015**, *6*, 6739–6746.
(34) Kingsbury, J. S.; Harrity, J. P. A.; Bonitatebus, P. J.; Hoveyda, A. H. *J. Am. Chem. Soc.* **1999**, *121*, 791–799.
(35) Garber, S. B.; Kingsbury, J. S.; Gray, B. L.; Hoveyda, A. H. *J. Am. Chem. Soc.* **2000**, *122*, 8168–8179.
(36) Bates, J. M.; Lummiss, J. A. M.; Bailey, G. A.; Fogg, D. E. *ACS Catal.* **2014**, *4*, 2387−2394.
(37) Thiel, V.; Hendann, M.; Wannowius, K.-J.; Plenio, H. *J. Am. Chem. Soc.* **2012**, *134*, 1104–1114.
(38) Ashworth, I. W.; Hillier, I. H.; Nelson, D. J.; Percy, J. M.; Vincent, M. A. *ACS Catal.* **2013**, *3*, 1929-1939.
(39) Vougioukalakis, G. C.; Grubbs, R. H. *Chem. Rev.* **2010**, *110*, 1746–1787.
(40) Grela, K., *Olefin Metathesis-Theory and Practice*. Wiley: Hoboken, NJ, 2014.

(41) Higman, C. S.; Lummiss, J. A. M.; Fogg, D. E. *Angew. Chem., Int. Ed.* **2016**, *55*, 3552–3565.
(42) Nicola, T.; Brenner, M.; Donsbach, K.; Kreye, P. *Org. Process Res. Dev.* **2005**, *9*, 513–515.
(43) Rosenquist, Å.; Samuelsson, B.; Johansson, P.-O.; Cummings, M. D.; Lenz, O.; Raboisson, P.; Simmen, K.; Vendeville, S.; de Kock, H.; Nilsson, M.; Horvath, A.; Kalmeijer, R.; de la Rosa, G.; Beumont-Mauviel, M. *J. Med. Chem.* **2014**, *57*, 1673−1693.
(44) Chikkali, S.; Mecking, S. *Angew. Chem., Int. Ed.* **2012**, *51*, 5802−5808.
(45) Dubois, J.-L., Refinery of the future: Feedstock, process, products. In *Biorefinery: from Biomass to Chemicals and Fuels*, Aresta, M.; Dibenedetto, A.; Dumeignil, D., Eds. Walter de Gruyter: Berlin, 2013; Vol. 2.
(46) McClennan, W. L.; Rufh, S.; Lummiss, J. A. M.; Fogg, D. E. *ACS Catal.* **2016**, in preparation.
(47) Ireland, B. J.; Dobigny, B. T.; Fogg, D. E. *ACS Catal.* **2015**, *5*, 4690−4698.
(48) Bailey, G. A.; Fogg, D. E. *J. Am. Chem. Soc.* **2015**, *137*, 7318–7321.
(49) Lummiss, J. A. M.; McClennan, W. L.; McDonald, R.; Fogg, D. E. *Organometallics* **2014**, *33*, 6738–6741.
(50) Lummiss, J. A. M.; Ireland, B. J.; Sommers, J. M.; Fogg, D. E. *ChemCatChem* **2014**, *6*, 459–463.
(51) Lummiss, J. A. M.; Botti, A. G. G.; Fogg, D. E. *Catal. Sci. Technol.* **2014**, *4*, 4210–4218.
(52) Beach, N. J.; Lummiss, J. A. M.; Bates, J. M.; Fogg, D. E. *Organometallics* **2012**, *31*, 2349–2356.
(53) Beach, N. J.; Camm, K. D.; Fogg, D. E. *Organometallics* **2010**, *29*, 5450–5455.
(54) Lübbe, C.; Dumrath, A.; Neumann, H.; Schäffer, M.; Zimmermann, R.; Beller, M.; Kadyrov, R. *ChemCatChem* **2014**, *6*, 684–688.
(55) Wang, H.; Goodman, S. N.; Dai, Q.; Stockdale, G. W.; Clark, W. M. *Org. Process Res. Dev.* **2008**, *12*, 226–234.
(56) Farina, V.; Horváth, A., Ring-Closing Metathesis in the Large-Scale Synthesis of Pharmaceuticals. In *Handbook of Metathesis*, Grubbs, R. H.; Wenzel, A. G., Eds. Wiley-VCH: Weinheim, 2015; Vol. 2, pp 633–658.
(57) Dinger, M. B.; Mol, J. C. *Organometallics* **2003**, *22*, 1089–1095.
(58) Dinger, M. B.; Mol, J. C. *Eur. J. Inorg. Chem.* **2003**, 2827–2833.
(59) Trnka, T. M.; Morgan, J. P.; Sanford, M. S.; Wilhelm, T. E.; Scholl, M.; Choi, T.-L.; Ding, S.; Day, M. W.; Grubbs, R. H. *J. Am. Chem. Soc.* **2003**, *125*, 2546–2558.
(60) Lummiss, J. A. M.; Beach, N. J.; Smith, J. C.; Fogg, D. E. *Catal. Sci. Technol.* **2012**, *2*, 1630–1632.
(61) Hong, S. H.; Day, M. W.; Grubbs, R. H. *J. Am. Chem. Soc.* **2004**, *126*, 7414–7415.
(62) Alcaide, B.; Almendros, P.; Luna, A. *Chem. Rev.* **2009**, *109*, 3817–3858.
(63) Higman, C. S.; Plais, L.; Fogg, D. E. *ChemCatChem* **2013**, *5*, 3548-3551.
(64) van Rensburg, W. J.; Steynberg, P. J.; Meyer, W. H.; Kirk, M. M.; Forman, G. S. *J. Am. Chem. Soc.* **2004**, *126*, 14332–14333.
(65) Nizovtsev, A. V.; Afanasiev, V. V.; Shutko, E. V.; Bespalova, N. B., Metathesis Catalysts Stability And Decomposition Pathway. In *NATO Sci. Ser. II*, Imamoglu, Y.; Dragutan, V., Eds. Springer Verlag: Berlin, 2007; Vol. 243, pp 125–135.
(66) Endo, K.; Grubbs, R. H. *J. Am. Chem. Soc.* **2011**, *133*, 8525–8527.
(67) Endo, K.; Herbert, M. B.; Grubbs, R. H. *Organometallics* **2013**, *32*, 5128-5135.

Chapter 2. Experimental Methods

2.1 General procedures

2.1.1 Reaction conditions

Reactions were carried out under N_2 (BOC Gases, industrial grade) in an MBraun glovebox or using standard Schlenk techniques, unless otherwise stated. The N_2 stream was dried by passage through a column of activated (blue) Drierite. Reactions above RT were carried out using a thermostatted silicone oil bath. All glassware was cleaned and oven-dried prior to use (150 °C) and allowed to cool under vacuum. Flash column chromatography was carried out in air using silica gel (60 Å, Aldrich) as the stationary phase.

2.1.2 Reagents

The following materials were prepared according to literature procedures: 2-methylocta-1-7-dien-3-ol **12**,[1] benzaldehyde tosylhydrazone **22**,[2] 1,3-bis-(2,4,6-trimethylphenyl)imidazolin-2-ylidene **H_2IMes**,[3] 1,3-bis-(2,4,6-trimethylphenyl)imidazol-2-ylidene **IMes**,[3] $RuCl_2(PPh_3)_3$ **Ru-11**,[4] $RuCl_2(PCy_3)_2(=CHPh)$ **GI**,[5] $RuCl_2(H_2IMes)(PCy_3)(=CHPh)$ **GII**,[6] $RuCl_2(IMes)(PCy_3)(=CHPh)$ **uGII**,[7] $RuCl_2(H_2IMes)(PCy_3)(=CH_2)$ **GIIm**,[8] $RuCl_2(CH(C_6H_4–O^iPr))(H_2IMes)$ **HII**,[6] and $RuCl_2(CH(C_6H_4–O^iPr))(IMes)$ **uHII**.[9]

Reagents were used as received with the exception of olefin substrates, which were degassed as described below. Magnesium turnings (99.9+%) were purchased from Acros Organics. Potassium hydroxide (99%) was purchased from Fisher Scientific. Sodium hydride (95%), potassium chloride (≥99%), tetrabutylammonium hydroxide (40 wt% solution in H_2O) **19**, dimethyl terephthalate (≥99%) (DMT), styrene (>99%), *trans*-anethole **14** (99%), methyl

acrylate **MA** (99%, with ≤100 ppm monomethyl ether hydroquinone as inhibitor), diethyl diallylmalonate **DDM** (98%), phosphorus pentoxide (powder, ACS reagent, ≥98%), iodine (ACS reagent, ≥99.8%), and decane (anhydrous, 99%) were purchased from Aldrich. Potassium tris(pyrazolyl)borate was purchased from TCI Chemicals (KTp; >97%). Ethylene (grade 3.0) was purchased from Linde and used as received.

All liquid substrates such as 2-methylocta-1-7-dien-3-ol **12**, *trans*-anethole **14**, styrene, methyl acrylate **MA**, and diethyl diallylmalonate **DDM** were subjected to five freeze-pump-thaw degassing cycles prior to storage in the glovebox freezer (–35 °C) protected from light. Decane was used as an internal standard in gas chromatography (GC) experiments, DMT as an internal standard for NMR experiments.

2.1.3 Solvents

Oxygen- and water-free hexanes, toluene, C_6H_6, CH_2Cl_2, and THF were obtained using a Glass Contour or Anhydrous Engineering solvent purification system, and stored in the glovebox. Other solvents were purified and degassed by standard distillation methods:[10] methanol over magnesium, and pentane (Fisher ACS grade) was pre-dried over $MgSO_4$ (12 h) at room temperature and reflux and was then refluxed a second time over phosphorus pentoxide (6 h) prior to distillation. Water was degassed by five consecutive freeze-pump-thaw cycles and stored in a sealed Kontes flask or in the freezer at -35 °C. All organic solvents were stored in the glovebox over activated Linde 4 Å molecular sieves, except methanol (3 Å sieves).

2.1.4 Deuterated solvents

Deuterated solvents (Cambridge Isotope Laboratories, Ltd.) were used as received for NMR analysis of air-stable species. Deuterated solvents, used for analysis of oxygen- or moisture-sensitive compounds, were dried and degassed. C_6D_6 was degassed by five freeze-pump-thaw cycles and stored over Linde 4 Å molecular sieves. THF-d_8 (Cambridge Isotope Laboratories, Ltd.) was purchased as ampules under N_2 and used after storing over Linde 4 Å molecular sieves for minimum six hours. To prevent contamination of the NMR solvents, the glovebox atmosphere was purged for 10 min to remove vapors prior to opening these storage vessels.

2.1.5 NMR spectroscopy

^{1}H (300 or 500 MHz), $^{13}C\{^{1}H\}$ (75.5 or 125.5 MHz), and $^{31}P\{^{1}H\}$ (121.5 or 202 MHz) NMR spectra were recorded on Bruker Avance-300 or Avance-500 spectrometers at 298 K. Spectra were referenced to the residual proton or carbon signals of the deuterated solvent (^{1}H, ^{13}C NMR) or externally to 85% H_3PO_4 (^{31}P) at 0 ppm. Spectra of organometallic compounds were measured under anaerobic conditions in NMR tubes equipped with J. Young valves or Rotoflo NMR tubes with PTFE/silicon septum caps.

2.1.6 Gas chromatography

GC quantification was performed on samples diluted with CH_2Cl_2 (ACS reagent grade) on an Agilent 7890A Series GC equipped with a flame ionization detector (FID), an Agilent 7683B Series autosampler and an Agilent HP-5 polysiloxane column (30 m length, 320 μm diameter), using an inlet split ratio of 10:1, an inlet temperature of 250 °C, and helium (UHP grade) as the

carrier gas to maintain column pressure at 11.512 psi. The FID response was maintained between 50-2000 ρA, using analyte concentrations of ca. 5 mM. Retention times for dienes and products were confirmed with samples authenticated by GC-MS and NMR analysis. GC-FID quantification was established by constructing calibration curves of peak area vs. concentration in the relevant concentration regime, to account for the dependence on detector response for substrates, products, and decane. Decane was used as internal GC standard. Yields in catalytic runs were determined from the integrated t_0 peak areas, referenced against decane, and compared to the initial integration ratio of substrate to internal standard.

2.1.7 GC-MS

Gas chromatography (GC) coupled to electron ionization mass spectrometry (EI-MS) was performed using an Agilent Technologies 5975B inert XL EI/CL MSD equipped with a CTC analytics auto-sampler and a polysiloxane column. Samples were diluted to ca. 1 mg/mL using CH_2Cl_2 under N_2 and kept sealed in 1.5 mL sample vials equipped with rubber septa prior to analysis. No calibration for ionization efficiency was applied. Analytes were identified by comparison of mass spectra to literature sources (as cited), and/or by comparison to authentic samples.

2.2 Synthesis of Ligands

2.2.1 Synthesis of Sodium Tosylhydrazone Salt (23) Using Methanol[11]

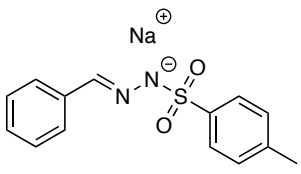

A fresh solution of sodium methoxide was prepared in the glovebox by adding 150 mL of dry MeOH to solid sodium (3.427g, 0.15 mol) at RT in a 250 mL round-bottom flask. Once the solid sodium was fully

dissolved, the solution of sodium methoxide was added to a 500 mL round-bottom flask containing a stirring solution of benzaldehyde tosylhydrazone **22** (40 g, 0.146 mol, 1 equiv) in 150 mL MeOH. The reaction was stirred at RT for 30 minutes, resulting in a pale beige solution with no remaining solid. The reaction was brought out of the glovebox and the solvent was removed on the rotary evaporator. A white powder was isolated and dried under vacuum overnight and wrapped in aluminum foil to protect the isolated solid from photo-induced decomposition. The solid was used without further purification or characterization. Yield: 41.5 g (96%).

2.2.2 Revised Synthesis of Sodium Tosylhydrazone Salt (23) Using THF

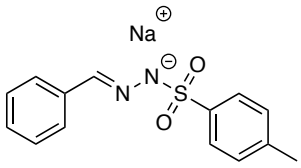

In the glovebox, benzaldehyde tosylhydrazone **22** (6.04 g, 0.022 mol, 1.05 equiv) was dissolved in a 250mL round-bottom flask with 100 mL THF. Solid NaH (0.4980g, 0.021 mol, 1 equiv) was slowly added to the flask and a white precipitate could be seen forming in the flask with excessive bubbling. The reaction was stirred at RT for 30 minutes and once the bubbling had ceased the flask was brought out of the glovebox. The solution was filtered off using a Buchner funnel with a white solid isolated. The solid was dried under vacuum overnight and wrapped in aluminum foil to protect the compound from photo-induced decomposition. The solid was used without further purification or characterization. Yield: 6.15 g (100%).

2.2.3 Synthesis of Phenyldiazomethane (21) by Vacuum Pyrolysis[11]

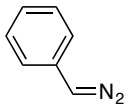

The sodium salt of tosylhydrazone **23** (36.4 g, 0.123 mol) was added to a 100 mL Schlenk round-bottom flask charged with a stir bar. To this flask, 45 mL of nujol oil was added and the flask was placed under vacuum and stirred overnight to degas the nujol oil. The next day, the vacuum pyrolysis apparatus was assembled (see Appendix D) and the

flask containing the salt was placed in an oil bath set at 50 °C and the receiving flask, connected to the vacuum pump, was placed in a dry ice/acetone bath. The temperature in the oil bath was increased 10 °C every 15 minutes and at 90 °C a red oil could be seen condensing in the receiving flask. The slow increase in the oil bath temperature is crucial as **21** is potentially explosive.[2] The temperature of the oil bath was brought to a final temperature of 110 °C, after which a large amount of the red oil could be seen in the receiving flask. Any red oil condensed in the connecting glass piece was heated with a heat gun to move it into the receiving flask. Once the production of red oil forming had ceased, the flask was removed from dry ice/acetone bath and warmed to RT. The flask was quickly weighed (9.43 g, 65% yield) and a solution of hexanes (20 mL) was added to the flask. The resulting red solution was added to a stirred solution of **$RuCl_2(PPh_3)_3$** in CH_2Cl_2 at -78 °C, and the rest of the **GI** synthesis was carried out as previously reported.[5]

2.3 Synthesis of Ruthenium Complexes

2.3.1 $Ru(OH)_2(H_2IMes)(=CH\text{-}2\text{-}O^iPrC_6H_4)$, HII-$(OH)_2$.

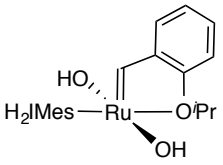

In the glovebox, a 250 mL Schlenk round-bottom flask equipped with a stir bar was charged with **HII** (410 mg, 0.65 mmol) and THF (30 mL). To the resulting green solution, N^nBu_4OH **19** as a 40% wt solution in H_2O (0.89 mL, 1.37 mmol, 2.1 equiv) was added and the reaction mixture turned light brown within 30 seconds. The reaction was stirred for 10 minutes, after which an aliquot was removed confirming complete consumption of **HII** to a single new alkylidene (14.02 ppm) by NMR analysis. The solvent was removed under vacuum to give a brown solid with visible white residues around the flask. This material was dissolved in benzene and filtered through Celite to remove the residual salts. The Celite was extracted with benzene (5 x 2 mL), and the combined washings were

stripped to dryness. Re-precipitation from toluene-hexanes at -35 °C afforded an orange powder, which was filtered off and dried. Yield: 315 mg (82%). Calcd: C 63.0%, H 7.00%, N 4.74%. Found: C 61.4%, H 6.57%, N 4.31%.

^{1}H NMR (300.1 MHz, C_6D_6): δ 14.04 (s, 1H, Ru=C*H*-2-O^{i}PrC_6H_4), 7.14 (dd, $^{3}J_{HH}$ = 7.75 Hz, $^{4}J_{HH}$ = 1.63 Hz, 1H, Ar*H*) 6.94 (td, $^{3}J_{HH}$ = 7.71 Hz, $^{4}J_{HH}$ = 1.54 Hz, 1H, Ar*H*), 6.93 (s, 4H, Mes *m*-C*H*), 6.83 (t, $^{3}J_{HH}$ = 7.45 Hz, 1H, Ar*H*), 6.37 (d, $^{3}J_{HH}$ = 8.01 Hz, 1H, Ar*H*), 4.37 (sept, $^{3}J_{HH}$ = 6.30 Hz, 1H, CH_3CHCH_3), 3.42 (s, 4H, NHC CH_2), 2.52 (s, 12H, *o*-CH_3), 2.23 (s, 6H, *p*-CH_3), 1.25 (d, $^{3}J_{HH}$ = 6.00 Hz, 6H, CH_3CHCH_3), 1.12 (s, 2H, O*H*; exchanges with D_2O).

^{13}C{^{1}H} NMR (C_6D_6, 75.5 MHz) δ 235.3 (Ru=*C*H-2-O^{i}PrC_6H_4), 218.3 (C_{NHC}), 151.5 (Mes *i*-*C*), 144.8 (*Ar*H), 138.7 (Mes *o*-*C*), 138.3 (*Ar*H), 137.8 (Mes *p*-*C*), 129.5 (Mes *m*-*C*), 123.6 (*Ar*H), 122.9 (*Ar*H) 121.3 (*Ar*H), 112.4 (*Ar*H), 73.9 (CH_3CHCH_3), 51.4 (NHC CH_2), 21.2 (Mes *p*-CH_3), 21.0 (CH_3CHCH_3), 18.9 (Mes *o*-CH_3).

2.3.2 Updated Synthesis of GII

Synthesis of **GII** was performed according to the van Lierop procedure,[6] with a slight modification to increase the proportion of resin. The reaction was carried out using **GI** (500 mg, 0.604 mmol), and once no further **GI** remained, Amberlyst-15 (780 mg, 3.62 mmol, 6 equiv) was added. The reaction was stirred for 2 h, then filtered to remove the resin, which was rinsed with THF. The THF was then removed by vacuum to afford GII. Yield: 468 mg (91%) ^{1}H and ^{31}P{^{1}H} NMR data were consistent with literature values.[6]

2.3.3 Updated Synthesis of HI

Synthesis of **HI** was performed on 1 g scale of **GI** (1.22 mmol), according to the literature procedure,[6] with a slight modification. Thus, the proportion of Amberlyst-15 added at the beginning of the reaction was increased (1.5 g, 7.30 mmol, 6 equiv). The reaction was stirred at 50 °C for 3 h and worked up as above. Yield: 662 mg (91%) ^{1}H and $^{31}P\{^{1}H\}$ NMR spectroscopy data were consistent with literature values.[6]

2.3.4 Updated Synthesis of HII

Synthesis of **HII** was performed according to the literature procedure[66] with a slight modification. On a 550 mg scale of **HI** (0.916 mmol), 6 equivalents of Amberlyst-15 (1.12 mg, 5.49 mmol) was added once it was confirmed that no **HI** remained in solution and stirred at 40 °C for 2h. The crude product was then filtered through a silica column using 3:1 hexanes to methylene chloride to remove a ^{31}P impurity at 37 ppm in C_6D_6. Once **HII** was completely loaded on the column the green band can be eluted from the column using 100% methylene chloride. Yield: 445 mg (78%) ^{1}H NMR spectroscopy data was consistent with literature values.[6]

2.4 Catalytic Reactions

2.4.1 Representative Procedure for Ring-Closing Metathesis

A 4 mL vial was loaded with a stir bar, diethyl diallylmalonate (**DDM**) (48 mg, 0.2 mmol), decane (29 mg, 0.2 mmol) and toluene (1.91 mL). A ca. 10 μL aliquot was removed for GC-FID analysis to establish the starting ratio of substrate to decane. **HII** (2.8 μL, 0.01 μmol, 0.005 mol%); stock solution 11 mg in 5 mL toluene (3.5 mM) was then added. The reaction was heated in a thermostatted oil bath at 60 °C and the reaction was stirred open to the well-purged glovebox atmosphere for 24 h. Aliquots were taken from the stirred reaction at specific time intervals,

quenched with KTp (10 μL, 10 mg/mL in THF), diluted with CH_2Cl_2, and analyzed by GC-FID. Identical amounts were used for water-spiked reactions with the exception of H_2O (2.6 μL, 0.144 mmol) added to the reaction before the catalyst was added.

2.4.2 Representative Procedure for Cross Metathesis

Reaction carried out as above, with the following changes: anethole (30 mg, 0.2 mmol), in 1.81 mL toluene, with the addition of methyl acrylate (103 mg, 1.20 mmol, 6 equiv), and **HII** as catalyst (12.5 μL, 0.1 μmol, 0.05 mol%); stock solution 10 mg in 2 mL toluene (8 mM). The reaction was heated in a thermostatted oil bath open to the glovebox atmosphere, and analyzed as above. Identical amounts were used for water-spiked reactions with the exception of H_2O (2.6 μL, 0.144 mmol) added to the reaction before the catalyst was added.

2.5 Identifying Vulnerable Species Towards Water

2.5.1 Representative Reaction for Stability of Pre-Catalysts Towards Water

In the glovebox, two J. Young NMR tubes were charged with **HII** (10 mg, 0.016 mmol), DMT (ca. 2.0 mg) and 0.77 mL C_6D_6. The samples were removed from the glovebox and a ^1H NMR spectrum was taken to establish the **HII** to DMT ratio at t_0 for both samples. The NMR tubes were returned to the glovebox and the solutions were transferred to a 4 mL vial loaded with a stir bar in a thermostatted oil bath set at 60 °C. H_2O (29 μL, 1.6 mmol, 10 equiv) was added to one of the vials and a ^1H NMR spectrum was collected at 10 minutes and 24 hours for both samples.

2.5.2 Reaction of GIIm with 10 Equivalents of Water

In the glovebox, two J. Young NMR tubes were charged with **GIIm** (10 mg, 0.0138 mmol), DMT (ca. 1.0 mg) and 0.69 mL C_6D_6. The samples were removed from the glovebox and a ^1H NMR spectrum was taken to establish the **GIIm** to DMT ratio at t_0 for both samples. The NMR

tubes were returned to the glovebox and H_2O (2.5 μL, 0.138 mmol, 10 equiv) was added to one of them. The sample was shaken vigorously, then both tubes were removed to a 60 °C oil bath (thermocouple-equipped; ±1.5 °C). ^1H and ^{31}P NMR spectra were recorded at 10 minutes and seven hours. For RT experiments, samples were stored at ambient temperature (23 °C ±1.5 °C) and at 24 h, ^1H and ^{31}P NMR spectra were collected. Identical amounts were used in the reaction with 100 equiv of H_2O except the amount of H_2O was increased to 25 μL (1.38 mmol, 100 equiv).

2.5.3 Representative Reaction for Monitoring Decomposition of HII with DDM in the Presence of Water

In the glovebox, a 20 mM stock solution of **HII** (12.5 mg, 0.02 mmol), DMT (ca. 2.0 mg) and 1.0 mL C_6D_6 was made in a 4 mL vial. An aliquot in a J. Young NMR tube from the stock solution was removed and a ^1H NMR spectrum was taken to establish the **HII** : DMT ratio at t_0. In a separate 4 mL vial, a 1 M stock solution of **DDM** (147 mg, 0.6117) in 0.46 mL C_6D_6 was prepared. Next, 75 μL of the 1 M stock solution of **DDM** (100 mM) and 0.66 mL C_6D_6 was added to two separate 4 mL vials loaded with a stir bar in a thermostatted oil bath set at 60 °C. H_2O (1.4 μL, 0.78 mmol, 100 equiv) was added to one of the vials and finally 38 μL of the 20 mM stock solution of **HII** (1 mM) was added to each vial. An aliquot was removed after 10 minutes and a ^1H NMR spectrum was collected to determine how much **HII** remained.

2.6 Identifying Decomposition Products Generated During Metathesis

2.6.1 Identifying GII Decomposition Products Formed by Self-Metathesis of Styrene in the Presence of Water

A solution of **GII** (20 mg, 0.024 mmol) and DMT (ca. 1 mg) was prepared in 1.20 mL C_6D_6. An

aliquot (0.60 mL, 0.012 mmol **GII**) was transferred to a J. Young NMR tube. H_2O (4.3 μL, 0.24 mmol, 20 equiv) was added, and a ^1H NMR spectrum was collected to determine the ratio of **GII** relative to DMT at t_0. Styrene (14 μL, 0.12 mmol, 200 mM, 10 equiv) was then added. The remaining solution was likewise treated with styrene, and used as a control reaction. Both reactions were heated in a thermostatted oil bath at 60 °C, for 24 h and then ^1H and ^{31}P NMR spectra were collected to determine the amount of **GII** remaining, along with any decomposition markers.

2.6.2 Identifying HII Decomposition Products Formed by Self-Metathesis of Styrene in the Presence of Water

A solution of **HII** (15 mg, 0.024 mmol) and DMT (ca. 1 mg) was prepared in 1.20 mL C_6D_6. An aliquot (0.60 mL, 0.012 mmol **HII**) was transferred to a J. Young NMR tube. H_2O (4.3 μL, 0.24 mmol, 20 equiv) was added, and a ^1H NMR spectrum was collected to determine the ratio of **HII** relative to DMT at t_0. Styrene (14 μL, 0.12 mmol, 200 mM, 10 equiv) was then added. The remaining solution was likewise treated with styrene, and used as a control reaction. Both reactions were heated in a thermostatted oil bath at 60 °C, for 24 h and then a ^1H NMR spectrum was collected to determine the amount of **HII** remaining, along with any decomposition markers.

2.7 Measuring Rate of Decomposition for HII Under Ethylene in the Presence of Water

A solution of **HII** (15 mg, 0.024 mmol) and DMT (ca. 3 mg) was prepared in 1.20 mL C_6D_6. An aliquot (0.60 mL, 0.012 mmol **HII**) was transferred to a J. Young NMR tube, and water (4.3 μL, 0.24 mmol, 20 equiv) was added. The remaining solution was used as a control reaction. A ^1H NMR spectrum was collected to determine the integration ratio of **HII** relative to DMT at t_0. To saturate the solutions in ethylene, each sample was freeze-pump-thaw degassed (5 x), then thawed under static vacuum. 1 atm of C_2H_4 was introduced at RT, samples were shaken

vigorously, and a timer was started. ^{1}H NMR spectra were collected at specific time points over 24 h.

2.8 Syntheses of Ruthenium Hydroxide Species

2.8.1 Attempted Synthesis of HII-$(OH)_2$ Using KOH

In the glovebox, a 100 mL Schlenk round-bottom flask loaded with a stir bar was charged with **HII** (110 mg, 0.18 mmol) and THF (5 mL). To the resulting green solution, a 1 M aqueous solution of KOH (0.9 mL, 0.9 mmol, 5 equiv) was added and the reaction was stirred for 4 h, after which a colour change from green to light brown was observed. An aliquot was removed confirming complete consumption of **HII** to a single new alkylidene (14.2 ppm) by ^{1}H NMR analysis. The solvent was removed under vacuum to give a brown solid with visible white residues around the flask. This material was dissolved in benzene and filtered through Celite to remove the residual salts. The Celite was extracted with benzene (5 x 1 mL), and the combined washings were stripped to dryness. Re-precipitation from toluene-hexanes at -35 °C afforded an orange powder, which was filtered off and dried. Yield: 54 mg (52%). ^{1}H NMR values are consisted with shifts reported in section 2.3.1.

2.8.2 Representative Reaction of HII With Aqueous KOH Solution

In the glovebox, a 4 mL vial loaded with a stir bar was charged with **HII** (15.0 mg, 0.024 mmol) and 1.2 mL of THF. A 1 M solution of KOH was also prepared by dissolving KOH (10 mg, 0.18 mmol) in 0.18 mL of H_2O. 24 μL (0.024 mmol, 1 equiv) of the 1 M KOH solution was added to the stirred solution of **HII** in THF and ^{1}H NMR spectra were collected at 3 h or 16 h to determine the ratio of **HII** : **HII-(OH).**

2.8.3 Procedure to Determine the Amount of Decomposition in the Synthesis of HII-$(OH)_2$

The reaction was performed according to the procedure described above with the exception of using THF-d_8 as the solvent and DMT (ca. 3 mg) as the internal standard. A ^{1}H NMR spectrum was collected before adding the KOH to determine the initial ratio of **HII** to DMT. After 4 h, the solution was transferred to a J. Young NMR tube and a ^{1}H NMR spectrum was acquired to determine the total amount of alkylidene signal remaining. The NMR tube was brought back into the glovebox and the THF was removed by vacuum with the resulting solid re-dissolved in C_6D_6 and filtered through Celite. A ^{1}H NMR spectrum for this solution was also collected to compare the amount of remaining alkylidene signal with the amount after 4h.

2.9 References

(1) McGrath, N. A.; Lee, C. A.; Araki, H.; Brichacek, M.; Njardarson, J. T. *Angew. Chem. Int. Ed.* **2008**, *47*, 9450-9453.
(2) Creary, X. *Org. Synth.* **1986**, *64*, 207–216.
(3) Arduengo, A. J.; Krafczyk, R.; Schmutzler, R.; Craig, H. A.; Goerlich, J. R.; Marshall, W. J.; Unverzagt, M. *Tetrahedron* **1999**, *55*, 14523–14534.
(4) Hoffman, P. R.; Caulton, K. G. *J. Am. Chem. Soc.* **1975**, *97*, 4221–4228.
(5) Schwab, P.; Grubbs, R. H.; Ziller, J. W. *J. Am. Chem. Soc.* **1996**, *118*, 100–110.
(6) van Lierop, B. J.; Reckling, A. M.; Lummiss, J. A. M.; Fogg, D. E. *ChemCatChem* **2012**, *4*, 2020–2025.
(7) Huang, J.; Stevens, E. D.; Nolan, S. P.; Petersen, J. L. *J. Am. Chem. Soc.* **1999**, *121*, 2674–2678.
(8) Lummiss, J. A. M.; Beach, N. J.; Smith, J. C.; Fogg, D. E. *Catal. Sci. Technol.* **2012**, *2*, 1630–1632.
(9) Suessner, M.; Plenio, H. *Chem. Commun.* **2005**, 5417–5419.
(10) Armarego, W. L. F.; Perrin, D. D., *Purification of Common Laboratory Chemicals*. 4th Ed. ed.; Butterworth-Heinemann: Oxford, 1997.
(11) Kaufman, G. M.; Smith, J. A.; Stouw, G. G. V.; Shechter, H. *J. Am. Chem. Soc.* **1965**, *87*, 935–937.

Chapter 3. Exploring the Impact of Water on Ru-Catalyzed Olefin Metathesis

3.1 Introduction

Metathesis in water is of enormous interest, most significantly for its potential capacity to enable modification of biologically relevant, water-soluble substrates in their native media. RCM in water could, for example, improve access to stapled peptides (Scheme 3.1), a class of constrained peptides under development by Aileron Therapeutics.[1,2] In the more general context of "green metathesis", water is often presumed to be desirable as a partial or complete replacement for the organic solvents normally used. A central requirement for these applications is the stability of the metal-alkylidene catalyst in water. Even from the perspective of standard use, this issue has important implications for the viability of relaxed solvent drying requirements.

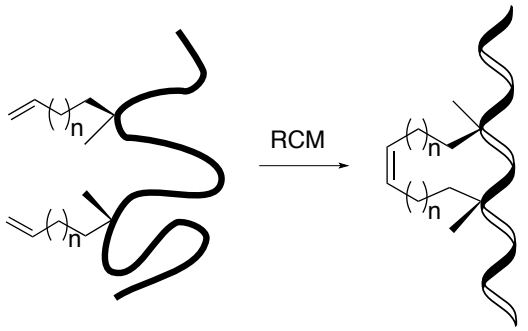

Scheme 3.1 Synthesis of stapled peptides using RCM.

Olefin metathesis has indeed been successfully carried out in water.[3-5] Even for ROMP of strained monomers, however, limiting factors have been noted under the conditions required to achieve mutual solubility of the substrate and catalyst.[6] More challenging yet are RCM or CM reactions (which do not benefit from release of ring strain), especially if these involve hydrophobic substrates. In one such study, Grela and co-workers described RCM of the benchmark substrate diethyldiallylmalonate (**DDM**) in water using the PCy_3-stabilized catalysts

GII or **M2**. Here ultrasonification was used to promote emulsion metathesis of the hydrophobic reagents.[7] RCM was quantitative for Thorpe-Ingold–favoured substrates such as **DDM**, but required high catalyst loadings (5 mol%). For the CM reaction shown in Figure 3.1, yields ranged from 56-86%.

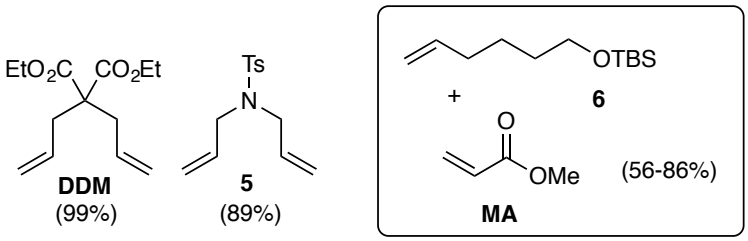

Figure 3.1 Substrates examined in ultrasonification-enabled aqueous metathesis. Yields are shown in parentheses.

Over a dozen well-defined, water-soluble metathesis catalysts have now been reported.[4] As shown in the representative examples of Figure 3.2, the neutral ligand sites have typically been modified to impart solubility. Early efforts focused on use of a variant on the first-generation Grubbs catalysts, in which one cyclohexyl group of the PCy_3 ligand was replaced with *N*,*N*-dimethylpiperidine (**Ru-6**)[8]. Catalysts functionalized at both the NHC and the styrenyl ether sites (**Ru-7**, **Ru-8**) were reported in 2007 by Grubbs, and in 2012 by Grela.[9,10] These catalysts effected RCM of the water-soluble substrates shown in Figure 3.3, at high loadings (2.5-10 mol% Ru). Self-metathesis yields were low in comparison, perhaps a function of deactivation pathways operative for allylic alcohols,[11,12] as well as the increased difficulty of CM over RCM. The majority of substrates used to demonstrate the feasibility of metathesis in water, however, are readily-cyclized RCM targets. While offering some benefit in terms of technology development, these do not reflect the level of difficulty involved for biological applications. Also notable is the fact that high catalyst loadings are required even for "easy" metathesis reactions.

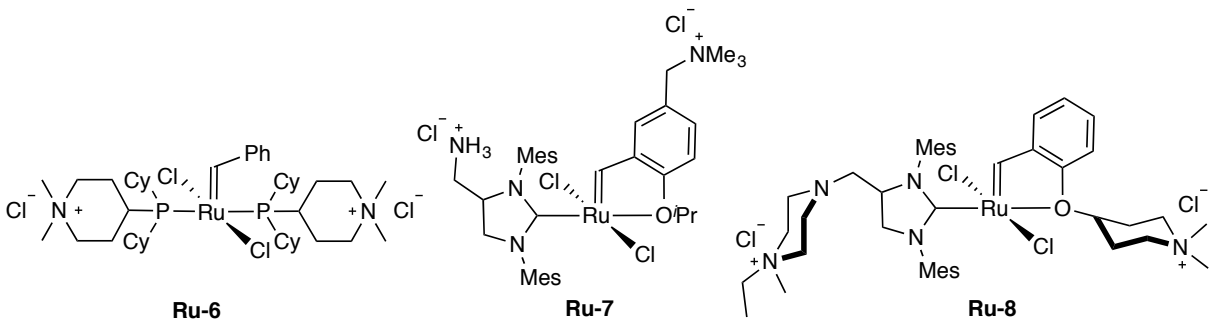

Figure 3.2 Selected water-soluble metathesis catalysts.

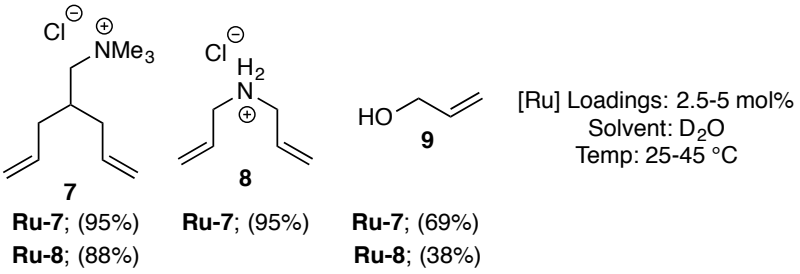

Figure 3.3 Water-soluble substrates used to investigate the feasibility of RCM (**7**, **8**) or self-metathesis (**9**) in aqueous media using the catalysts of Figure 3.2.

Elevated catalyst loadings enable high yields irrespective of catalyst deactivation, and hence mask issues of catalyst longevity. However, a 2015 study by Cazin and co-workers at low catalyst loadings (0.1 mol%) points toward a role for water in promoting catalyst decomposition. The principal goal of the Cazin study was to assess the feasibility of Ru-catalyzed olefin metathesis in air, and indeed it demonstrated that metathesis can out-compete decomposition at high temperatures (refluxing toluene; 110 °C). More relevant in the present context, however, is a portion of the study that examined the specific impact on catalyst productivity of water, vs. CO_2, oxygen, or air. In RCM of the model substrate **10**, the detrimental impact of water was significantly greater (Table 3.1) for the three catalysts tested. With the Hoveyda catalyst **HII**, the turnover number (TON) dropped from 700, out of a maximum TON of 1,000, to just 350. The

productivity of the phosphine / phosphite catalysts **M2** and **CazI** suffered to an even greater extent.

This is an important finding, which raises the possibility that the high catalyst loadings required for aqueous metathesis are due to catalyst decomposition, rather than solubility issues. However, the origin of the detrimental role of water was not examined, nor was it established for substrates other than **10**. The question of substrate generality is important because metathesis is typically carried out using vinylic olefins, and the steric challenges involved in metathesis of geminally-disubstituted olefins such as **10**[12,13] would enhance the negative impact of trace water.

Table 3.1 Reported impact of additives on RCM productivity. Reactions containing N_2, O_2, CO_2 were carried out under an atmosphere of the gas; that in the presence of water involved 100 μL H_2O in 1.5 mL (7% by volume, or ca. 20,000 equiv H_2O vs. Ru).

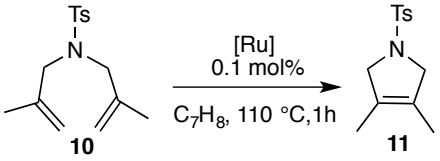

	Catalyst [Ru] (TON)		
Additive	**HII**	**M2**	**Caz1**
N_2 (control)	700	700	900
O_2	600	500	850
CO_2	550	550	800
air	400	250	600
H_2O	350	100	150

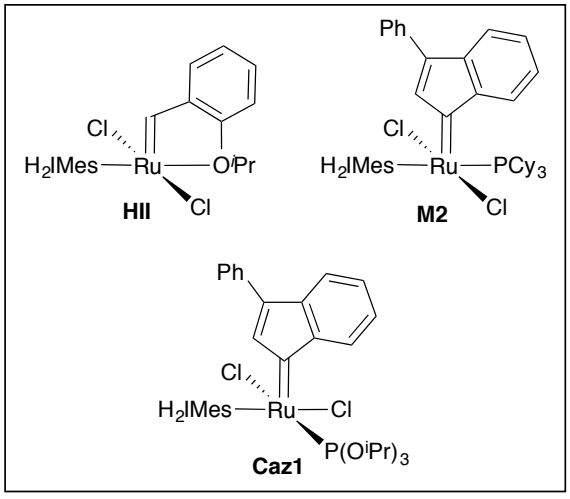

3.2 Results and Discussion

3.2.1 Assessing the Impact of Water on the Metathesis Productivity of HII and GII

The present work began by seeking to establish the broader scope and relevance of the sensitivity to water revealed in the important Cazin study. To that end, the productivity of **HII** and **GII** (chosen as the two dominant metathesis catalysts in current use) was assessed in the presence and absence of water, in metathesis of substrates that span a wide range of difficulty. Test reactions included: (a) the RCM of the benchmark substrate **DDM** (chosen to facilitate literature comparisons),[14] (b) RCM of the more challenging alcohol-functionalized substrate **12**; (c) cross-metathesis (CM) of anethole **14** with methyl acrylate **MA**, and (d) self-metathesis (SM) of styrene. Reaction (c) is of particular interest for the production of cinnamates relevant to the fine-chemical and personal-care sectors. More generally, however, it and the SM reaction (d) permit assessment of the impact of water on *intermolecular* metathesis, which (unlike RCM) does not benefit from the high probability of encounter between olefinic coupling partners.

For the RCM reactions, a catalyst loading of 0.005 mol% was chosen to ensure that catalyst decomposition by water was not masked by the presence of an excessively large catalyst reservoir. The proportion of water added (2.6 μL; 0.13% by volume, or 1,500 ppm) corresponds to ca. 15,000 equivalents relative to catalyst. Reactions were carried out in toluene at 60 °C: to maximize loss of ethylene, the stirred vessels were left open to the glovebox atmosphere. This reduces unproductive cycling via degenerate metathesis with ethylene, and hence the time spent by the catalyst in its most vulnerable methylidene and **MCB** states. Maximum TON values were reached within 2 h, with no subsequent increase by 3 h and 4 h. (Note: under these conditions, ca. 100 μL of solvent (5% by volume) is lost to evaporation over 2 h).

The catalyst loadings used (0.005 mol%) were designed to ensure that RCM of **DDM** and **12** approached completion in the absence of water, but did not reach 100%. The entire catalyst charge is thus required, highlighting any impact of water on catalyst performance. For **HII**, a TON of nearly 19,000 was observed in RCM of **DDM**, as compared to 16,400 for **GII**. In both cases, TON values dropped by ca. 50% in the presence of 15,000 equiv of H_2O (Figure 3.4). For RCM of **12**, an even greater sensitivity emerged, and TON values declined by 85% for **HII**, or 68% for **GII**. As these figures indicate, **HII** proved unexpectedly more sensitive to water-induced decomposition in the cyclization of allylic alcohol substrate **12**. Some protective role for the PCy_3 ligand in **GII** is implied, perhaps greater competition with the pendant hydroxyl group for coordination to the Ru center. This hypothesis could be tested by repeating the RCM of **12** with **HII** in the presence of one equivalent of PCy_3. If the results correspond to those seen in the RCM in the absence of PCy_3, this rules out the possibility that PCy_3 is competing with the hydroxyl group.

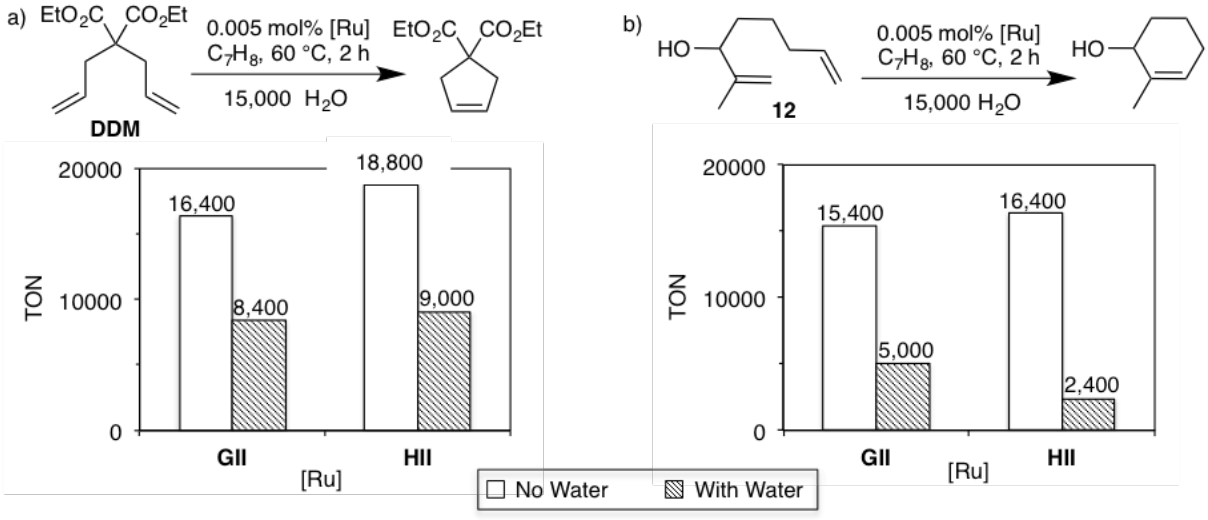

Figure 3.4 Negative effect of water on turnover numbers (TON) in RCM of a) **DDM** and b) allylic alcohol **12**. Proportion of water added corresponds to 2.6 μL in 2 mL; 0.13% by volume. TON is based on replicate runs, ±3%.

The impact of water on styrene self-metathesis was next examined. This experiment can be viewed as catalyst-agnostic, in the sense that $RuCl_2(H_2IMes)(=CH_2)$ is formed following one cycle of metathesis, irrespective of whether the precursor is **HII** and **GII**. To maximize the proportion of the active species, **HII** was chosen. (The relative vulnerability of specific off-cycle catalyst species, including the phosphine- or styrenyl ether-stabilized precatalysts and the resting-state species, is examined in Section 3.2.3).

Metathesis was carried out using 0.005 mol% **HII** under the conditions above; that is, in toluene at 60 °C in a stirred vessel open to the glovebox atmosphere, in the presence or absence of a large excess of water (2.6 μL H_2O; 0.13% by volume, or 1,500 ppm). To gain deeper insight, rate profiles were constructed to assess the impact of adding water once metathesis was under way (4 min; ca. 50% conversion; Figure 3.5). The rate of metathesis diminished relative to the control experiment, and no further activity was observed after 2 h. Total conversion of styrene was 67%, vs. 92% for the control reaction. Water clearly has a detrimental effect on metathesis, but is much less aggressive than (e.g.) the amine poisons explored in related work, which cause much faster knockdown.[15]

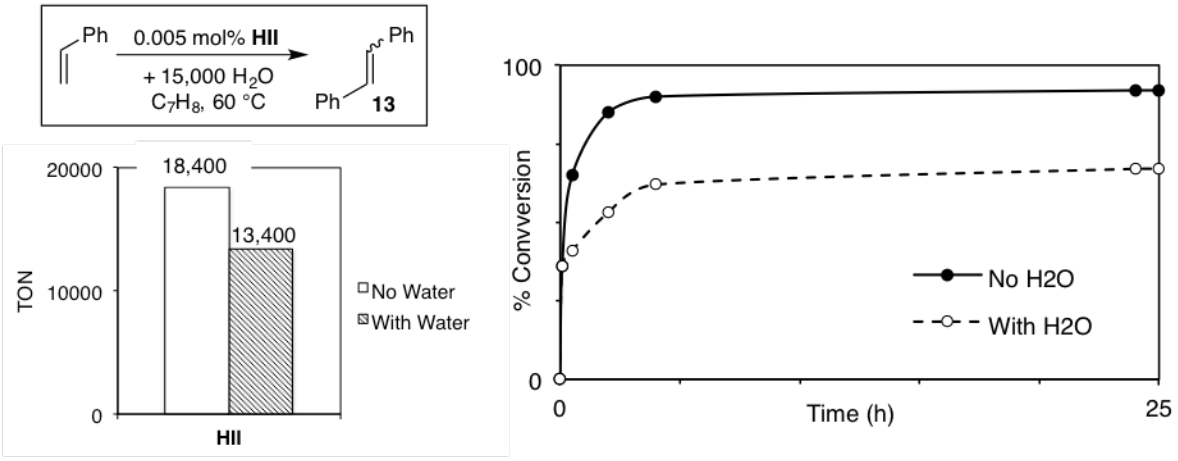

Figure 3.5 Impact of water on the self-metathesis of styrene. Bar graph represents the maximum TON reached in each reaction (TON for formation of product **13**). TON is based on replicate runs, ±3%.

Cross-metathesis of anethole **14** with methyl acrylate is much more challenging, and loadings of **HII** were therefore increased to 0.05 mol%. Given the established vulnerability of **GII** in acrylate metathesis,[16-21] its loading was increased to 0.1 mol% to compensate. For **GII**, the only metathesis product in the absence of water was 68% stilbenoid **15**, formed via self-metathesis of anethole **14** (Figure 3.6).[*] That is, catalyst decomposition was complete prior to any CM of **15** with acrylate. In the presence of water, just 27% **15** was formed.

With **HII**, conversions of anethole reached 90% in the absence of water, and 60% formation of the CM product, cinnamate **16**. In the presence of 15,000 equiv H_2O, conversions of **14** decreased to 60%, and 30% **16** was formed.

∗ Interestingly, a much lower yield of **15** (10%) was observed in this reaction at a catalyst loading of 0.05 mol% **GII**, under otherwise identical conditions.[22] The discrepancy may reflect the presence of trace water in the prior work.

Collectively, these experiments confirm the negative impact of water on the productivity of the widely used catalysts **GII** and **HII**. Moreover, they confirm that the detrimental effect of water is greater as reactions become more challenging.

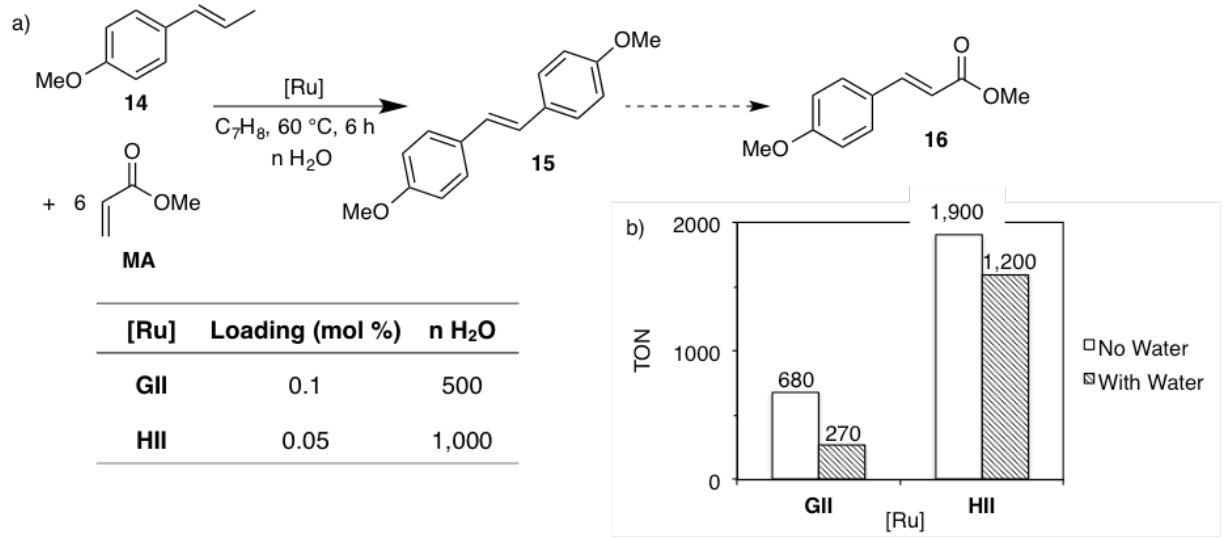

[Ru]	Loading (mol %)	n H_2O
GII	0.1	500
HII	0.05	1,000

Figure 3.6 a) Impact of water on the attempted cross-metathesis of anethole with **MA**. b) TON values refer to formation of **15**: CM product **16** is formed only with **HII**. Proportion of water added corresponds to 2.6 μL in 2 mL; 0.13% by volume. TON is based on replicate runs, ±3%.

3.2.2 Impact of NHC Backbone Saturation on Water Sensitivity

RCM of **DDM** and **12** was repeated as in the preceding section, to assess the relative impact of water on the productivity of the **IMes** complexes **uGII** and **uHII**, relative to the more widely-used **H_2IMes**-containing analogues. Comparison of Figures 3.7 and 3.4 suggests that the **H_2IMes** catalysts are marginally more affected by water. Thus, the drop in productivity in RCM of **DDM** is ca. 30% with the **IMes** catalysts, vs. 50%. The same trend is seen for RCM of **12**, although the difference between the two NHC ligands declines to ca. 10%. These data again suggest a protective role for the phosphine-bound species. Our group recently reported an eightfold smaller

rate constant for loss of PCy_3 from the **IMes** complex $RuCl_2(IMes)(PCy_3)(=CH_2)$ u**GIIm**, relative to its **H_2IMes** analogue **GIIm**.[23]

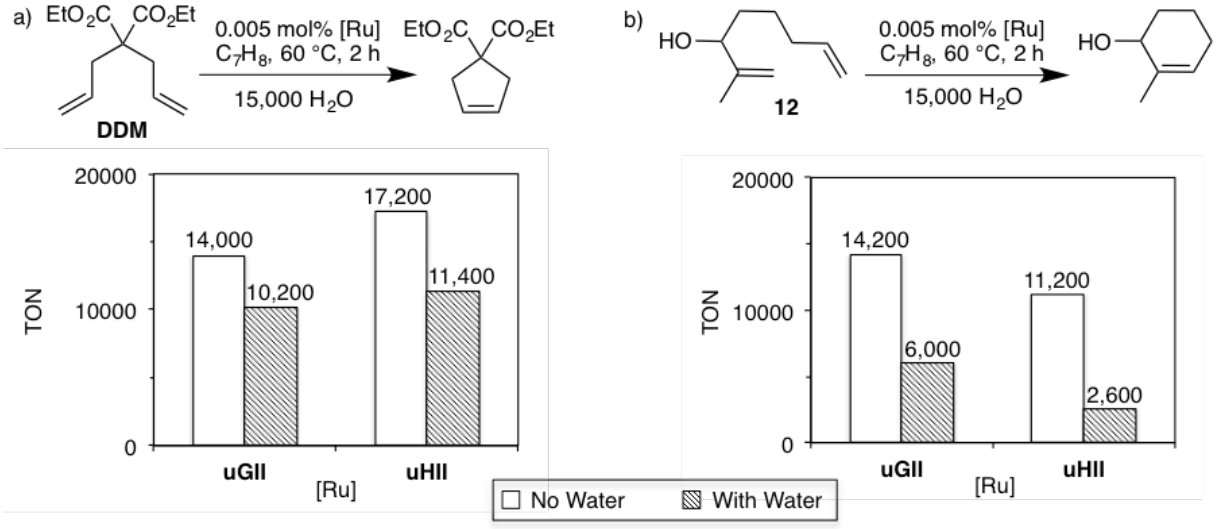

Figure 3.7 Probing the impact of NHC saturation to water-induced decomposition during metathesis. TON is based on replicate runs, ±3%.

We had originally speculated that the **IMes** complexes might be *more* water-sensitive, owing to the weaker Ru–NHC bonding present (a function of the neglible p-acidity)[24,25] of the unsaturated NHC. The greater sensitivity of the **H_2IMes** complexes suggests that NHC decoordination and ensuing hydrolysis (Scheme 3.2)[26] does not contribute to the negative impact of water on catalyst productivity.

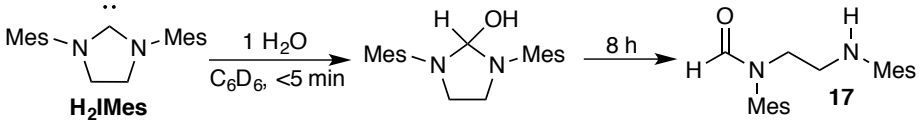

Scheme 3.2 Reported hydrolysis of free **H_2IMes** to form **17**.

3.2.3 Assessing the Water-Sensitivity of Off-Cycle Catalyst Species

3.2.3.1 Water-Sensitivity of Metathesis Precatalysts

In the next phase of this study, efforts focused on identifying which of the various catalyst species present during metathesis were most sensitive to water. Candidate species for **GII** (Scheme 3.3) include the off-cycle pre-catalyst and the five-coordinate, resting-state methylidene complex **GIIm**, to which Dr. Justin Lummiss of this research group has established high-yield, clean synthetic routes.[27] More challenging to study are the catalytic intermediates: four-coordinate methylidene **Ru-2**, and the metallacyclobutane (**MCB**). For the Hoveyda catalyst **HII**, the system is slightly simpler, as the resting-state species is **HII** itself.[22]

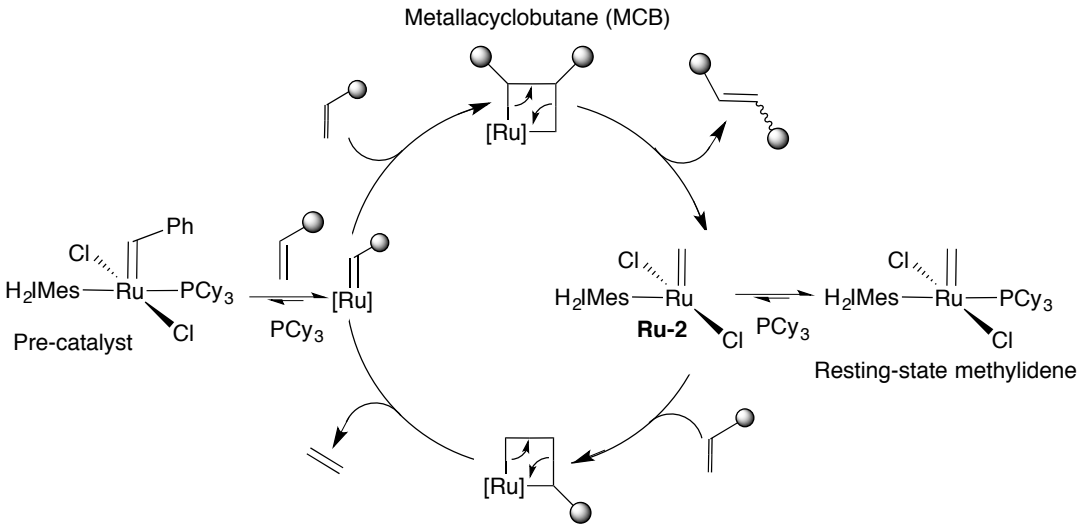

Scheme 3.3 Catalytic cycle for **GII**, showing potentially water-sensitive intermediates.

The impact of water on the longevity of the precatalysts was probed by carrying out reactions at 60 °C in C_6D_6, with 0 or 100 equiv H_2O (Table 3.2). Decomposition was assessed from the integrated intensity of the alkylidene proton relative to that for dimethyl terephthalate (DMT). No change was evident after 24 h at 60 °C for **GII** or **HII**, or their **IMes** analogues **uGII** and **uHII**, ruling out the benzylidene complexes as the vulnerable species.

Table 3.2 Establishing the insensitivity of precatalysts to water.

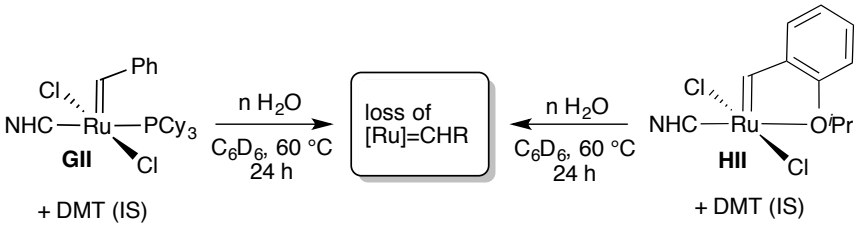

Amount of [Ru]=CHR after 24 h			
		n H_2O	
Catalyst	**NHC**	**n = 0**	**n = 100**
GII	H_2IMes	100	100
uGII	IMes	100	100
HII	H_2IMes	100	100
uHII	IMes	100	100

3.2.3.2 Water-Sensitivity of the Grubbs Resting-State Species, GIIm

Other work from this research group has demonstrated that donor ligands, particularly good donors of relatively small bulk, dramatically accelerate decomposition of the resting-state species **GIIm**. This "donor-accelerated decomposition" pathway is shown in Figure 3.8. Of keen interest is the question of whether water – albeit a rather poor ligand for Ru – can promote such a pathway. Initial studies were carried out at ambient temperatures, to exploit the very low lability of the PCy_3 ligand in **GIIm** at RT, and hence to dissect out the impact of water on the five-coordinate methylidene complex, relative to the four-coordinate species formed by phosphine loss.

Unexpectedly, on treating **GIIm** with 10 equiv H_2O at room temperature (C_6D_6),* the proportion of decomposition at 24 h tripled relative to the water-free control reaction, increasing from 5% loss of alkylidene to 18% (Figure 3.8). The proportion of [$MePCy_3$]Cl **4** observed by $^{31}P\{^1H\}$ NMR analysis tallies with the loss of **GIIm** measured by ^1H NMR analysis, indicating that abstraction of the methylidene ligand by PCy_3 is the sole operative decomposition pathway. In the corresponding experiment with **uGIIm**, the PCy_3 ligand of which is much more strongly bound (i.e. k_1 for PCy_3 loss is nearly an order of magnitude lower, as noted above), water had no impact on the extent of decomposition. Thus, 2% loss of the alkylidene ligand was evident after 24 h at RT, regardless of whether water was present or not.

At 60 °C, the lability of the PCy_3 ligand is enhanced, and decomposition thus reports on both five-coordinate **GIIm** and four-coordinate (**Ru-2** in Scheme 3.3). With 10 equivalents of H_2O, no decomposition was evident after 10 min. After 7 h, however, loss of the alkylidene signal reached 68%, vs. 44% for the control reaction. At 100 equiv H_2O, ca. 5% decomposition was observed even at 10 min, and was complete at 7 h. These data indicate that decomposition occurs via an associative pathway, in which initial binding of H_2O to **GIIm** promotes dissociation of the PCy_3 ligand, as recently established by Mr. William McClennan for the stronger donors dimethylsulfoxide and pyridine.[28]

These findings are remarkable in confirming the deleterious effect of even a poor donor ligand on an otherwise highly stable complex. Their importance stems from the fact that **GIIm**, as the resting-state species in catalysis via the Grubbs catalyst, accumulates during metathesis, and

* Experiment carried out by Mr. William McClennan of this research group, who is examining the scope and generality of donor-accelerated decomposition for phosphine-stabilized Ru metathesis catalysts, including **GIIm**.

from the ubiquity of water as a contaminant in organic synthesis and manufacturing, which is difficult and unfeasibly costly to completely remove.

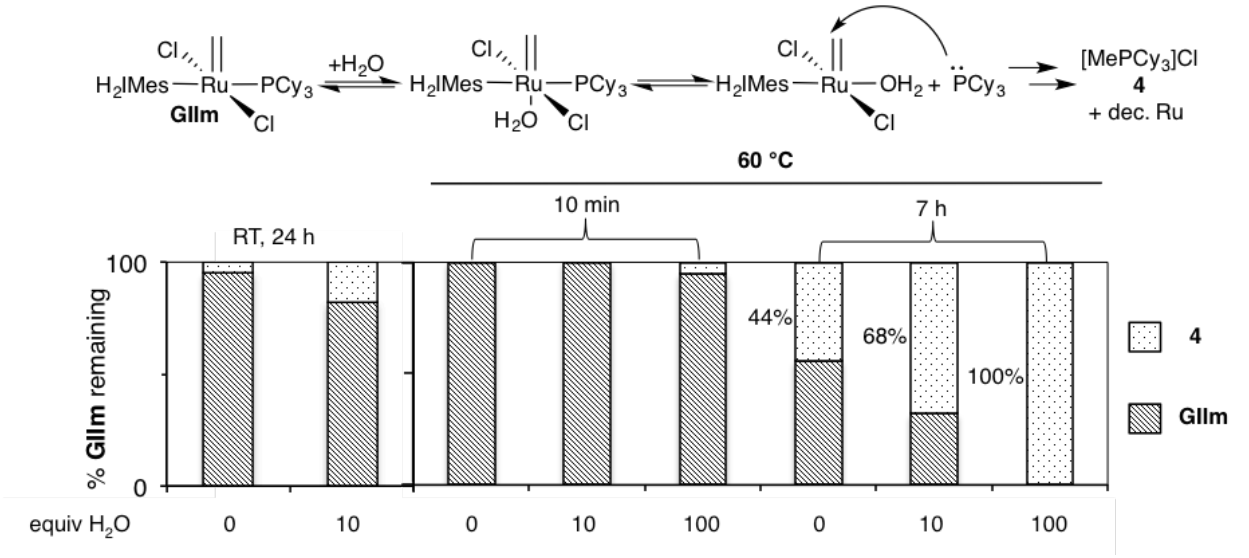

Figure 3.8 Assessing the contribution of water to donor-accelerated decomposition. The increase in % [$MePCy_3$]Cl **4**, relative to the control experiment, reports on this pathway.

3.2.4 Assessing Decomposition of Active-Species by Water During Metathesis

The next set of experiments examined the impact of added water during metathesis. Under these conditions, decomposition of both the metallacyclobutane intermediates, and the four-coordinate methylidene complexes of type **Ru-2** may contribute.

An initial study examined RCM of **DDM** at 60 °C in C_6D_6, in the presence or absence of water (100 equiv), using 1 mol% **GII**. The extent of decomposition was assessed at 10 min, when conversion of **DDM** was ca. 90% complete. As shown in Table 3.3, loss of the alkylidene signal was three times higher in the presence of water: 31%, as compared with 10% in the water-free metathesis experiment. Also notable is the greater extent of decomposition relative to the 5% decomposition seen for **GIIm** in the absence of substrate. This may indicate involvement of the

metallacyclobutane species. (Alternatively, however, the higher PCy_3 lability of **GII** over **GIIm** could be responsible. To rule out this possibility, the experiment should be repeated with **GIIm**, in place of **GII**).

Comparison with other catalysts again shows least decomposition for the slowest-initiating species, **uGII**. For the Hoveyda catalyst **HII**, decomposition is only slightly more extensive than for **GII** (4%, a figure within experimental error). This may reflect the impact on **GII** of the associative reaction with water, which labilizes the PCy_3 ligand, enabling faster entry into the catalytic cycle.

Table 3.3 Impact of added water on catalyst decomposition during metathesis.

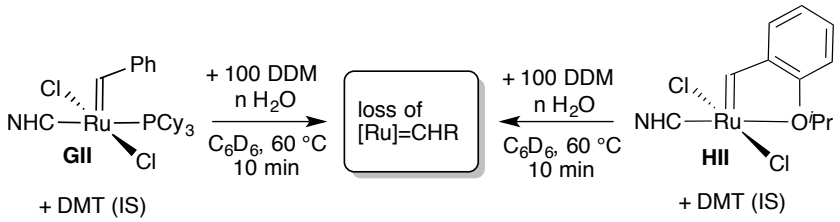

Amount of [Ru]=CHR after 10 min			
		n H_2O	
Catalyst	**NHC**	**n = 0**	**n = 100**
GII	H_2IMes	89	69
uGII	IMes	99	95
HII	H_2IMes	100	65
uHII	IMes	100	75

3.2.5 Determining the Mechanism for Water Promoted Decomposition in Metathesis

3.2.5.1 Donor-accelerated Decomposition for Phosphine Containing GII

For **GII**, both donor-accelerated deactivation and decomposition of the **MCB** were considered as pathways for the observed water sensitivity during catalysis. Markers for these pathways are,

respectively, [$MePCy_3$]Cl **4**, and organic products containing the three carbons of the metallacyclobutane ring (e.g. propylene **18a** and β-methylstyrene **18b**; see below).

Accordingly, NMR experiments involving metathesis of styrene were carried out using **GII** (10 mol %), and a reduced proportion of water (20 equiv) relative to the metathesis experiments of Section 3.2.4, to minimize perturbation of ^{1}H NMR spectra by the water signal. To offset the lower concentration of water present, reactions were carried out in a sealed NMR tube, which minimizes loss of any volatile byproducts (ethylene, propylene), and consequently enhances the proportion of the vulnerable metallacyclobutane species.

In the absence of water, 92% decomposition of **GII** into **4** was observed after 24 h at 60 °C, accompanied by minor amounts of **GIIm** and **18b** (3% and 5%, respectively; Table 3.4). With 20 equiv H_2O, only **4** was present after this time. These data indicate that the sole pathway by which water decomposes **GII** during metathesis is the water-accelerated abstraction of the methylidene group by free PCy_3. In contrast, in the absence of water, **GIIm** remains and abstraction of the methylidene is not the sole decomposition pathway.

Table 3.4 Products of decomposition detected by ^{1}H and ^{31}P{^{1}H} NMR from decomposition of **GII** with and without water.[a]

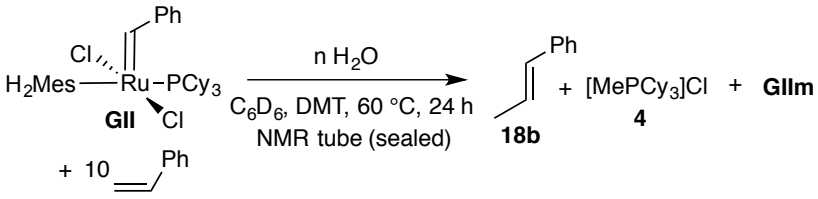

n H_2O	**GII** remaining	**GIIm** remaining	[$MePCy_3$]Cl **4**	MeHC=CHPh **18b**
0 (control)	0%	3%	92%	5%
20	0	0	100	0

[a] Diagnostic ^{1}H signal used to quantify the proportion of of **18b**: PhHC=C*H*CH$_3$ (dq, 6.03 ppm).

3.2.5.1 Decomposition of Metallacyclobutane for HII

The corresponding experiments with **HII** showed no impact of water on catalyst decomposition (Table 3.5). Thus, 92% loss of the alkylidene signals was observed in the presence or absence of water. The water-free experiment revealed ca. 10% each of propylene **18a** and β-methylstyrene **18b**. In the presence of water, the proportion of these "three-carbon markers" reached 39% and 45%, respectively. (Assignment of **18b** was also confirmed by GC-MS from the appearance of a MS signal at *m/z* 118.1 amu). This significant increase indicates that the **MCB** intermediate is the vulnerable species leading to decomposition of **HII**. Literature precedents associating these species with **MCB** decomposition are briefly summarized in the next section. Importantly, however, the decomposition behaviour of **HII** is entirely different from that shown for **GII** above. Thus, decomposition of **GII** appears to be mediated by the methylidene intermediate **GIIm**, while decomposition of phosphine-free catalysts such as **HII** is mediated by the **MCB** intermediate.

Table 3.5 Impact of water on distribution of organic decomposition products observed during metathesis of styrene by **HII**.[a]

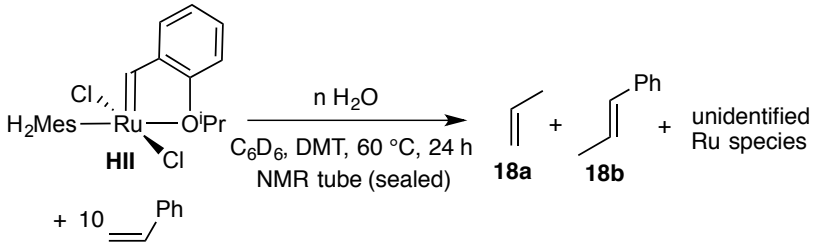

n H_2O	**HII** remaining	H_2C=CHMe **18a**	MeHC=CHPh **18b**
0 (control)	8%	10%	11%
20	8	39	45

[a] Diagnostic ^{1}H signals used to quantify the proportion of **18a**: $CH_3HC{=}CH_2$ (m, 5.72 ppm); of **18b**: PhHC=CHCH$_3$ (dq, 6.03 ppm).

When these reactions were repeated in an open vessel, neither β-methylstyrene nor propylene was detected, pointing toward the involvement of volatile propylene in the sealed-tube reactions. Specifically, β-methylstyrene **18b** is suggested to form via metathesis of **HII** with propylene, followed by metathesis of the ethylidene product **Ru-9** (Scheme 3.4) with styrene. This pathway would limit the amount of propylene generated by the unsubstituted **MCB**.

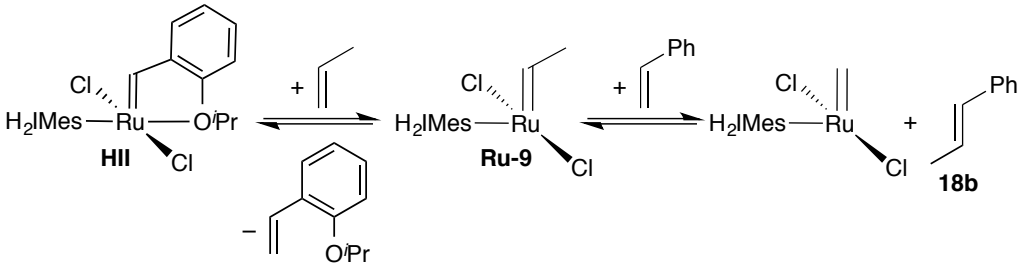

Scheme 3.4 Proposed mechanism for formation of **18b** in the reaction of Table 3.4.

Decomposition of metallacyclobutane intermediates generates products of type **18** if the three carbons of the metallacycle are lost intact. Dr. Benjamin Ireland of this research group observed **18b/c** upon decomposition of **HII** during styrene metathesis in the presence of base (e.g. NEt_3, pyrrolidine, DBU), and attributed their formation to deprotonation of the metallacyclobutane ring at the β-carbon (Scheme 3.5).[15] It is unclear, however, whether the acidity of these protons is sufficient for deprotonation by bases as weak as NEt_3, and other pathways were thus already being investigated. The fact that similar products are seen with water indicates that basicity is irrelevant. As well, the presence of trace water in the Ireland experiments must be considered, and those experiments should be repeated under rigorously anhydrous conditions.

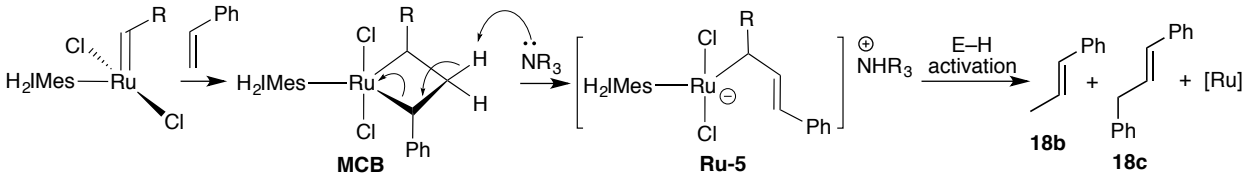

Scheme 3.5 Mechanism for deprotonation of the metallacyclobutane ring at the β-carbon site, proposed by B. Ireland.

The substituents present on the three-carbon backbone depend on the substitution of the **MCB** (Scheme 3.5). Decomposition of the unsubstituted **MCB** would liberate propylene **18a**, while the monosubstituted **MCB** would give rise to β-methylstyrene **18b**, and the disubstituted **MCB** would yield β-benzylstyrene **18c**. Notable is the absence of the latter, which could reflect steric constraints on access to the MCB. The limited decomposition markers seen when volatile olefins are allowed to escape suggests that the unsubstituted **MCB** is the most vulnerable species to water.

3.2.6 Assessing the Vulnerability of the Unsubstituted MCB Towards Water

Pioneering work by the Sasol group reported that in situ-generated **GIIm** decomposes under ethylene to release propylene **18a** as a byproduct.[29] The unsubstituted metallacyclobutane **MCB** was proposed to undergo β-hydride transfer to form allyl hydride **Ru-4**, the ultimate fate of which was not known (Scheme 3.6). DFT analysis supported the energetic accessibility of this pathway. Bespalova subsequently suggested that this behaviour also applies to **HII**.[30]

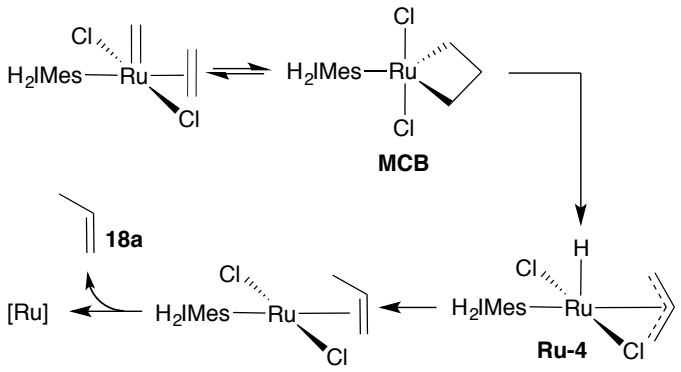

Scheme 3.6 β-hydride transfer mechanism proposed by the Sasol group.

Piers and co-workers confirmed the formation of propylene in NMR studies in which the unsubstituted **MCB** was generated in situ by treating **Ru-10** with ethylene (Scheme 3.7).[31,32] The metallacyclobutane was observed at –50 °C from its characteristic ^{1}H NMR signals. On warming above -25 °C, loss of propylene was observed. Use of ^{13}C-labelled ethylene aided in confirming propylene as the primary decomposition product.

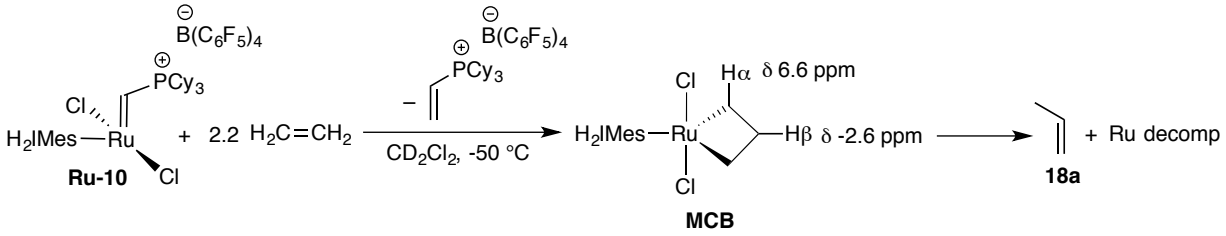

Scheme 3.7 In situ formation of **MCB** and decomposition with loss of propylene.

To assess the impact of water on the unsubstituted **MCB**, **HII** was reacted with ethylene in a gas-saturated C_6D_6 solution (0 or 20 equiv H_2O; 60 °C). Unexpectedly, the rate of decomposition was unaffected by water (Figure 3.9). This is difficult to reconcile with the vulnerability of the MCB inferred from the data above, but tends to suggest that the most vulnerable intermediate is not the unsubstituted **MCB**.

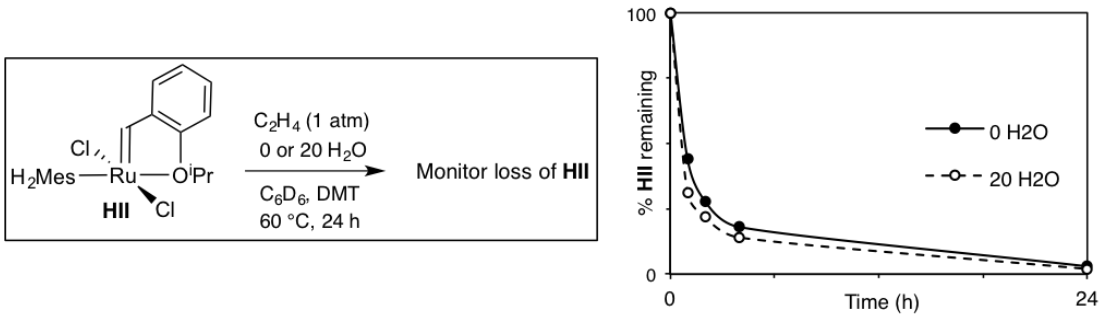

Figure 3.9 Assessing the impact of added water on the rate of decomposition of **HII** under ethylene.

3.2.7 Proposed Mechanism for Water Promoting Formation of Propylene

The fact that the byproducts of type **18** are observed in the presence of water clearly indicates the need to consider an alternative to the base-mediated deprotonation pathway described in Scheme 3.5. One possibility is that water promotes the β-hydride transfer mechanism shown in Scheme 3.6, proposed by the Sasol group to account for liberation of propylene on decomposition of **GIIm** under ethylene, but also invoked for other ruthenacyclobutanes.[33] Crabtree has proposed[34] the following conditions for β-hydride transfer:

1) *The β-carbon of the **MCB** must bear a proton substituent.* Satisfied for all of the **MCB** complexes.
2) *The metal must be electronically unsaturated (≤16-electron), with a vacant site cis to the **MCB***. Satisfied for all of the MCB intermediates, which are trigonal bipyramidal, 14-electron species.
3) *The metal, Cα, Cβ, and β-H atoms must be syn-coplanar*, bringing the *β*-hydrogen into proximity to the metal center. In the **MCB** complex, all carbons are coplanar with respect to Ru, but the *β*-hydrogen is pseudo-axial. While this geometry disfavours *β*-hydride transfer, Piers' NMR data is consistent with an agostic interaction between the Ru center

and the Cα–Cβ bond. Supporting evidence includes the downfield location of the Hα signal, relative to Hβ (6.62 ppm and -2.65 ppm, respectively), and of Cα relative to C*β* (94.0 and 2.30 ppm, respectively),[32] and large values for $^{1}J_{CH}\alpha$ (165 Hz) and $^{1}J_{CH}\beta$ (155 Hz), coupled with a low $^{1}J_{C\alpha-C\beta}$ (15.0 Hz), characteristic of agostic interactions.[35] DFT studies of metathesis-derived ruthenacyclobutanes show shortened Ru–Cα bonds, and elongated Cα–Cβ bonds, resulting in an obtuse Cα–Cβ–Cα' angle.[36,37] These factors shorten the Ru–Cβ distance, increasing the proximity of the Ru and β-hydrogen atoms, and potentially making β-hydride transfer more favorable.

We hypothesize that water could potentially promote this pathway by donating electron density into the C-H antibonding orbital, resulting in a more hydridic β-H that can more readily transfer to Ru (Scheme 3.8). Formation of small proportions of β-methylstyrene and propylene in the absence of water (Table 3.5) points toward a base-level capacity of the metal to back-donate into the antibonding orbital of the C-H bond, albeit to a much smaller extent than where water is present. Following hydride transfer, the cis-disposed hydride and alkyl groups can reductively eliminate.

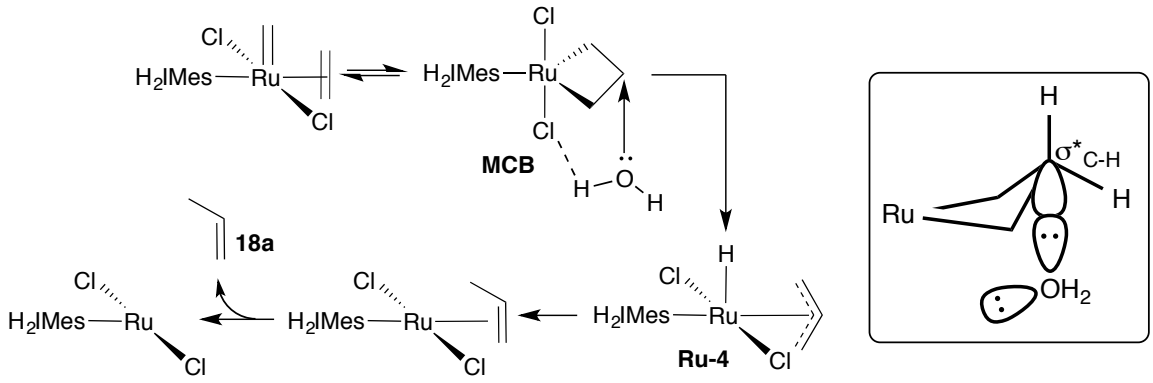

Scheme 3.8 Speculative pathway for water-promoted β-hydride transfer, and (inset) interaction of the lone pair on oxygen with the C-H antibonding orbital.

3.2.9 Exploring the Stability of Hoveyda-type Hydroxide Complexes

While the metathesis literature now contains many examples of Ru-pseudohalide catalysts, none contain a hydroxide ligand. Ruthenium hydroxide species could be envisaged as alternative species accessible via O–H---Cl hydrogen bonding interactions such as that shown in Scheme 3.10. Precedents for outer-sphere H-bonding interactions are well established for E–H···Cl hydrogen bonds, where E = N, and can be conceived for E = O.[38]

3.2.9.1 Attempted Synthesis of Hydroxide Derivatives for HII Using Potassium Hydroxide

Reactions of **HII** with KOH was initially undertaken on NMR scale, by treating a THF solution of **HII** with excess KOH as a degassed aqueous solution (Scheme 3.9). After 3 h, ^{1}H NMR analysis indicated complete loss of **HII**, and formation of two new alkylidene species characterized by singlets at 15.20 and 14.20 ppm (ratio 1:9). At 4 h, only the singlet at 14.20 ppm remained. The alkylidene signal at 15.20 ppm is therefore assigned to mono-hydroxide complex **HII-(OH)**, and the peak at 14.20 ppm to bis-hydoxide species **HII-(OH)$_2$**. The locations of these signals agree well with reported values for related pseudohalide metathesis catalysts containing either one or two aryloxide or thiolate ligands.[39-42]

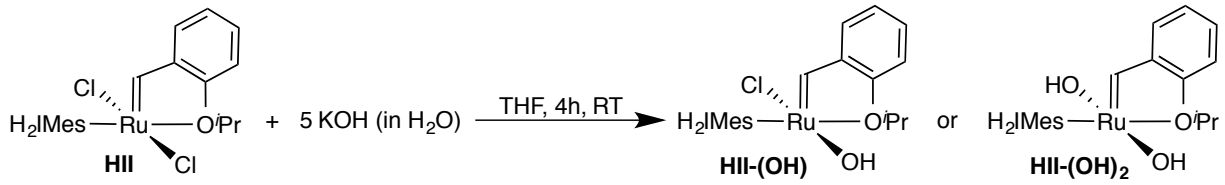

Scheme 3.9 Synthesis of hydroxide derivatives of **HII** via salt metathesis with KOH.

This reaction was repeated on a 110 mg scale, and worked up by evaporating the THF solvent under vacuum, redissolving the residue in benzene, filtering through Celite to remove excess KOH and KCl, and reprecipitating from toluene-pentane at -35 °C. Orange-brown **HII-(OH)$_2$**

was isolated in 52% yield. The origin of the unexpected mass loss was probed by repeating the NMR-scale reaction in THF-d_8 with an internal standard. The in situ yield of **HII-(OH)$_2$** after 4 h was only 70%, indicating competing decomposition to non-alkylidene species. The instability of the complex may be associated with the excess KOH present, as NMR analysis of isolated **HII-(OH)$_2$** showed no evidence of decomposition for at least 24 h in C_6D_6.

3.2.9.2 Improved Synthesis of Hydroxide Derivatives for HII

In the hope of improving stoichiometric control in this reaction, tetra-*n*-butylammonium hydroxide (**19**) was used as an alternative hydroxide source with improved solubility in THF. This salt was purchased as a solution in water (40 wt%), and degassed prior to use. Addition of 2.1 equiv **19** to a THF solution of **HII** at RT caused a colour change from green to brown within seconds, and complete conversion to **HII-(OH)$_2$** within 10 minutes (Scheme 3.10). Work-up as above afforded orange **HII-(OH)$_2$** in 82% yield.

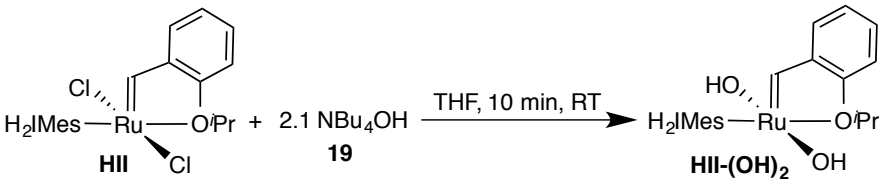

Scheme 3.10 Optimized synthesis of **HII-(OH)$_2$**.

As expected, the ^{1}H NMR signals for **HII-(OH)$_2$** in C_6D_6 correspond closely to those for **HII**, with minor shifts in the ^{1}H signals (Figure 3.10). The exception was a new singlet at 1.1 ppm integrating for two protons, assigned to the two hydrogen atoms on the hydroxide ligands, which exhibited no correlation with other protons or carbons via ^{1}H-^{1}H COSY, or ^{1}H-^{13}C HMQC or HMBC experiments. The assignment of this signal was confirmed by D_2O exchange. While these data are consistent with the proposed structure, satisfactory microanalysis was not

obtained. This likely resulted from decomposition of the compound, as the experimental values were all higher than the calculated values and the colour at the time of analysis was beige instead of orange.

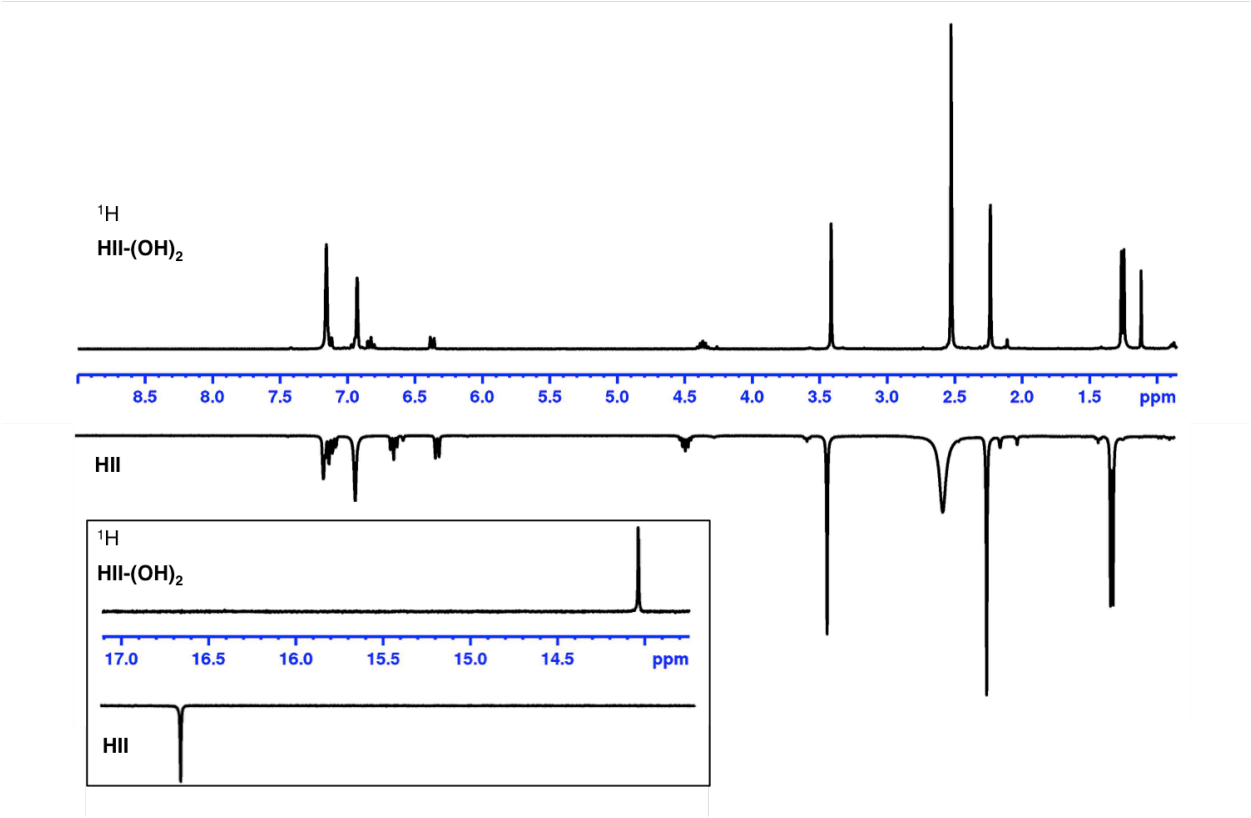

Figure 3.10 ^{1}H NMR spectra (C_6D_6, 300 MHz) of **HII-(OH)$_2$** and (inverted) **HII**. Insert: alkylidene signals.

^{1}H NOESY analysis revealed an NOE interaction between the hydroxide protons and the mesityl *o*-methyl protons, but not between the hydroxide and alkylidene proton. (However, the alkylidene proton interacts with the mesityl *o*-Me, and the aromatic C*H* protons (Figure 3.11). The absence of a through-space interaction between the hydroxide and alkylidene protons suggests the geometry shown, in which H-bonding of the two hydroxy groups is favoured by the mutual disposition of the O*H* protons below the basal plane of the square pyramid.

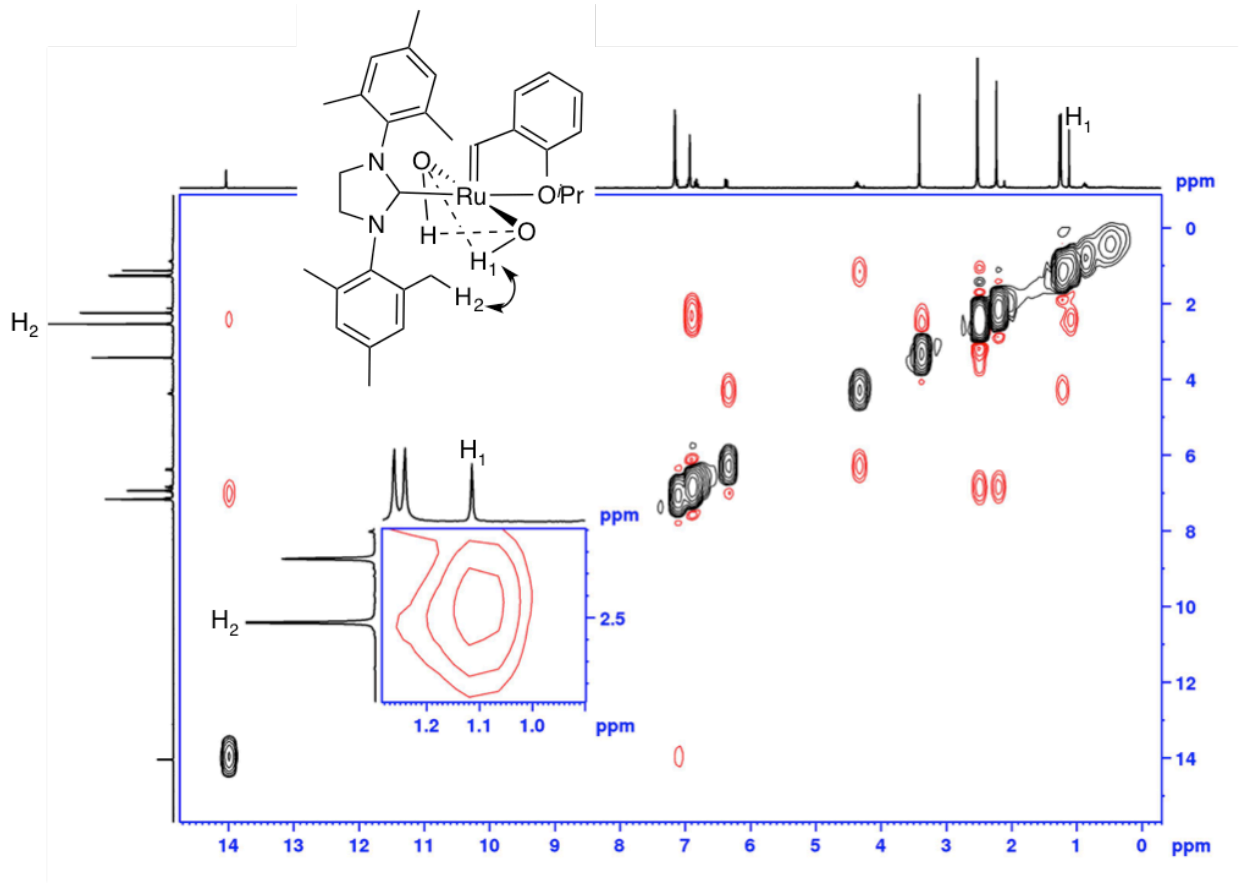

Figure 3.11 NOE interaction involving the hydroxide protons in **HII-(OH)$_2$.**

3.2.9.3 Attempted Synthesis of RuCl(OH)(H$_2$IMes)(=CH-2-O^{i}PrC$_6$H$_4$), HII-(OH).

Selective synthesis of the mono-hydroxide species **HII-(OH)** was originally attempted by treating **HII** with a single equivalent of KOH in water-THF, as in the procedures described above. The rate plot is shown in Figure 3.12. ^{1}H NMR analysis indicated incomplete salt metathesis at 3 h, with a 2:1 ratio of **HII-(OH)** and **HII**. An identical ratio was observed after a further 15 h. Repeating this experiment but with 1.2 equiv KOH resulted in ca. 10% of the bis-hydroxide complex **HII-(OH)$_2$**, but the ratio of **HII-(OH)** to the starting complex **HII** was again ca. 2:1.

Attempts to gain access to clean **HII-(OH)** by treating **HII** with a single equivalent of N^nBu_4OH **19** were also unsuccessful. This reaction resulted in immediate formation of a mixture of **HII, HII-OH**, and **HII-(OH)$_2$**, in a ratio of 4 : 3 : 3. These data point toward an equilibrium system (Scheme 3.11), in which the usual driving force for salt metathesis, precipitation of the chloride salt, is precluded by the solubility of KCl in water. The different ratio, relative to the KOH experiment, is attributed to the higher solubility of the hydroxide ion in THF.

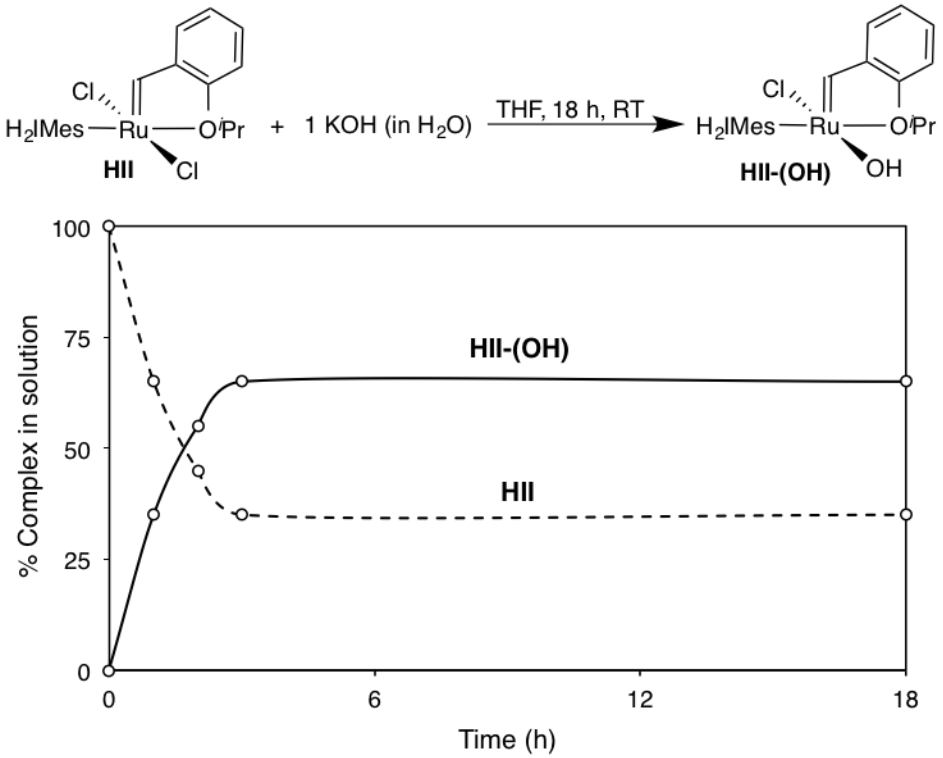

Figure 3.12 Rate plot for reaction of **HII** with 1 equiv KOH.

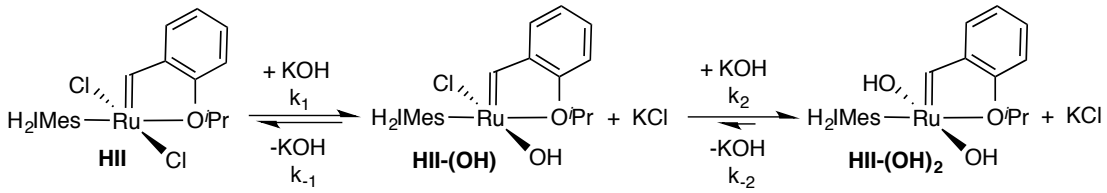

Scheme 3.11 Equilibria in formation of the Ru-hydroxide target complexes.

The equilibrium between **HII** and **HII-(OH)** is a manifestation of the trans effect. While both chloride and hydroxide are relatively weak trans-effect ligands, chloride is higher in the series. Thus when **HII-(OH)** coexists in solution with free chloride and hydroxide ions, the ligand trans to chloride is labilized. Where this ligand is hydroxide, exchange with chloride regenerates **HII**, while exchange with hydroxide has no net effect. Exchange of the chloride ligand (i.e. installation of a second hydroxide ligand) is kinetically disfavoured, owing to the weaker trans effect of the hydroxide ligand. On adding excess KOH, however, **HII-(OH)$_2$** begins to form via a second equilibrium, which lies to the right because both anionic ligands are now poorly trans-labilizing, and anion exchange to re-form **HII-(OH)** is therefore slow. These factors account for the difficulty in accessing solely **HII-(OH)**, which was not pursued further.

3.2.9.4 Instability of Bis-Hydroxide Complex During Metathesis

The catalytic activity of **HII-(OH)$_2$** was assessed in RCM of the benchmark substrate diethyldiallyl malonate, **DDM** (0.1 mol%, RT, toluene). No RCM occurred after 4 h, in comparison, **HII** effects quantitative cyclization of DDM within 30 min under the same conditions. It was shown above that **HII-(OH)$_2$** is stable for 24 h in C_6D_6 solution. The active species formed during metathesis by the hydroxide complex thus appears much more susceptible to decomposition, inhibiting turnover.

3.3 Conclusion

Explored above is the impact of water in metathesis via common ruthenium catalysts. Water was found to promote catalyst decomposition. It was shown that adding water to metathesis reactions was detrimental to both the dominant phosphine-containing catalyst **GII**, and the dominant phosphine-free catalyst **HII**, for a variety of RCM and CM reactions. For **GII**, water was found

to accelerate decomposition by coordinating to the methylidene species, promoting loss of PCy_3, and thus enhancing the rate at which the free phosphine abstracts the methylidene carbon. In the case of **HII**, water promoted decomposition of the metallacyclobutane intermediate. The intimate details of the mechanism remain speculative, but water may promote the known[28-30] β-hydride transfer pathway, perhaps by increasing the hydridic character of the β-hydrogen. Finally, the stability of ruthenium-hydroxide complexes was examined. The bis-hydroxide complex, **HII-$(OH)_2$**, was synthesized. While this complex was stable at RT in solution for 24 h, it was completely inactive for RCM of **DDM**, possibly because of the instability of the metathesis-active intermediates. These findings indicate that water has a much more deleterious effect on Ru-catalyzed metathesis than has generally been presumed.

3.4 References

(1) Higman, C. S.; Lummiss, J. A. M.; Fogg, D. E. *Angew. Chem., Int. Ed.* **2016**, *55*, 3552–3565.
(2) Chang, Y. S.; Graves, B.; Guerlavais, V.; Tovar, C.; Packman, K.; To, K.-H.; Olson, K. A.; Kesavan, K.; Gangurde, P.; Mukherjee, A.; Baker, T.; Darlak, K.; Elkin, C.; Filipovic, Z.; Qureshi, F. Z.; Cai, H.; Berry, P.; Feyfant, E.; Shi, X. E.; Horstick, J.; Annis, D. A.; Manning, A. M.; Fotouhi, N.; Nash, H.; Vassilev, L. T.; Sawyer, T. K. *Proc. Natl. Acad. Sci.* **2013**, *110*, E3445–E3454.
(3) Burtscher, D.; Grela, K. *Angew. Chem. Int. Ed.* **2009**, *48*, 442–454.
(4) Grela, K.; Gulajski, L.; Skowerski, K., Alkene Metathesis in Water. In *Metal-Catalyzed Reactions in Water*, Dixneuf, P. H.; Cadierno, V., Eds. Wiley-VCH: Weinheim, 2013; pp 291–336.
(5) Tomasek, J.; Schatz, J. *Green Chem.* **2013**, *15*, 2317–2338.
(6) Camm, K. D.; Fogg, D. E., From Drug Cocktails to Tissue Engineering: Synthesis of ROMP Polymers for Biological Applications. In *NATO Sci. Ser. II*, Imamoglu, Y.; Dragutan, V., Eds. Springer Verlag: Berlin, 2007; Vol. 243, pp 285–303.
(7) Gulajski, L.; Sledz, P.; Lupa, A.; Grela, K. *Green Chem.* **2008**, *10*, 271–274.
(8) Mohr, B.; Lynn, D. M.; Grubbs, R. H. *Organometallics* **1996**, *15*, 4317–4325.
(9) Jordan, J. P.; Grubbs, R. H. *Angew. Chem. Int. Ed.* **2007**, *46*, 5152–5155.
(10) Skowerski, K.; Szczepaniak, G.; Wierzbicka, C.; Gulajski, L.; Bieniek, M.; Grela, K. *Catal. Sci. Technol.* **2012**, *2*, 2424–2427.
(11) Werner, H.; Grunwald, C.; Stuer, W.; Wolf, J. *Organometallics* **2003**, *22*, 1558–1560.
(12) van Lierop, B. J.; Lummiss, J. A. M.; Fogg, D. E., Ring-Closing Metathesis. In *Olefin Metathesis-Theory and Practice*, Grela, K., Ed. Wiley: Hoboken, NJ, 2014; pp 85–152.

(13) Ulman, M.; Grubbs, R. H. *Organometallics* **1998**, *17*, 2484–2489.
(14) Ritter, T.; Hejl, A.; Wenzel, A. G.; Funk, T. W.; Grubbs, R. H. *Organometallics* **2006**, *25*, 5740–5745.
(15) Ireland, B. J.; Dobigny, B. T.; Fogg, D. E. *ACS Catal.* **2015**, *5*, 4690−4698.
(16) Bailey, G. A.; Fogg, D. E. *J. Am. Chem. Soc.* **2015**, *137*, 7318–7321.
(17) Love, J. A.; Morgan, J. P.; Trnka, T. M.; Grubbs, R. H. *Angew. Chem. Int. Ed.* **2002**, *41*, 4075–4037.
(18) Hoveyda, A. H.; Gillingham, D. G.; Van Veldhuizen, J. J.; Kataoka, O.; Garber, S. B.; Kingsbury, J. S.; Harrity, J. P. A. *Org. Biomol. Chem.* **2004**, *2*, 8–23.
(19) Miao, X.; Fischmeister, C.; Dixneuf, P. H.; Bruneau, C.; Dubois, J. L.; Couturier, J. L. *Green Chem.* **2012**, *14*, 2179–2183.
(20) Bilel, H.; Hamdi, N.; Zagrouba, F.; Fischmeister, C.; Bruneau, C. *Green Chem.* **2011**, *13*, 1448–1452.
(21) Ho, T. T.; Jacobs, T.; Meier, M. A. R. *ChemSusChem* **2009**, *2*, 749–754.
(22) Bates, J. M.; Lummiss, J. A. M.; Bailey, G. A.; Fogg, D. E. *ACS Catal.* **2014**, *4*, 2387−2394.
(23) Lummiss, J. A. M.; Higman, C. S.; Fyson, D. L.; McDonald, R.; Fogg, D. E. *Chem. Sci.* **2015**, *6*, 6739–6746.
(24) Back, O.; Henry-Ellinger, M.; Martin, C. D.; Martin, D.; Bertrand, G. *Angew. Chem. Int. Ed.* **2013**, *52*, 2939 –2943.
(25) Verlinden, K.; Buhl, H.; Frank, W.; Ganter, C. *Eur. J. Inorg. Chem.* **2015**, *2015*, 2416–2425.
(26) van Lierop, B. J.; Reckling, A. M.; Lummiss, J. A. M.; Fogg, D. E. *ChemCatChem* **2012**, *4*, 2020–2025.
(27) Lummiss, J. A. M.; Beach, N. J.; Smith, J. C.; Fogg, D. E. *Catal. Sci. Technol.* **2012**, *2*, 1630–1632.
(28) McClennan, W. L.; Rufh, S.; Lummiss, J. A. M.; Fogg, D. E. *ACS Catal.* **2016**, in preparation.
(29) van Rensburg, W. J.; Steynberg, P. J.; Meyer, W. H.; Kirk, M. M.; Forman, G. S. *J. Am. Chem. Soc.* **2004**, *126*, 14332–14333.
(30) Nizovtsev, A. V.; Afanasiev, V. V.; Shutko, E. V.; Bespalova, N. B., Metathesis Catalysts Stability And Decomposition Pathway. In *NATO Sci. Ser. II*, Imamoglu, Y.; Dragutan, V., Eds. Springer Verlag: Berlin, 2007; Vol. 243, pp 125–135.
(31) Romero, P. E.; Piers, W. E. *J. Am. Chem. Soc.* **2007**, *129*, 1698–1704.
(32) Romero, P. E.; Piers, W. E. *J. Am. Chem. Soc.* **2005**, *127*, 5032–5033.
(33) McNeill, K.; Andersen, R. A.; Bergman, R. G. *J. Am. Chem. Soc* **1995**, *117*, 3625–3626.
(34) Crabtree, R. H., Alkyls and Hydrides. In *The Organometallic Chemistry of the Transition Metals*, University, Y., Ed. John Wiley & Sons, Inc.: Hoboken, NJ, 2014; pp 69–97.
(35) Etienne, M.; Weller, A. S. *Chem. Soc. Rev.* **2014**, *43*, 242--259.
(36) Suresh, C. H.; Koga, N. *Organometallics* **2004**, *23*, 76–80.
(37) Rowley, C. N.; van der Eide, E. F.; Piers, W. E.; Woo, T. K. *Organometallics* **2008**, *27*, 6043–6045.
(38) Gavette, J. V.; Klug, C. M.; Zakharov, L. N.; Shores, M. P.; Haley, M. M.; Johnson, D. W. *Chem. Commun.* **2014**, *50*, 7173–7175.
(39) Conrad, J. C.; Parnas, H. H.; Snelgrove, J. L.; Fogg, D. E. *J. Am. Chem. Soc.* **2005**, *127*, 11882–11883.

(40) Monfette, S.; Camm, K. D.; Gorelsky, S. I.; Fogg, D. E. *Organometallics* **2009**, *28*, 944–946.
(41) Occhipinti, G.; Hansen, F. R.; Törnroos, K. W.; Jensen, V. R. *J. Am. Chem. Soc.* **2013**, *135*, 3331–3334.
(42) Khan, R. K. M.; Torker, S.; Hoveyda, A. H. *J. Am. Chem. Soc.* **2013**, *135*, 10258-10261.

Chapter 4. Revisiting Olefin Metathesis Catalyst Synthesis

4.1 Introduction

Multiple routes have been developed to well-defined Ru alkylidene catalysts that promote olefin metathesis.[1] These routes are based on synthetic methodologies that range from ring-opening of strained cyclopropenes[2] (pathway (a) in Figure 4.1), to alkylidene transfer from diazo derivatives[3] (pathway (b)) or chloroalkane (not shown), or by rearrangement of alkyne reagents[4,5] (pathways (c) and (d)). The majority of synthetic routes start from readily prepared Ru precursors, and afford "first-generation" bis-phosphine catalysts.

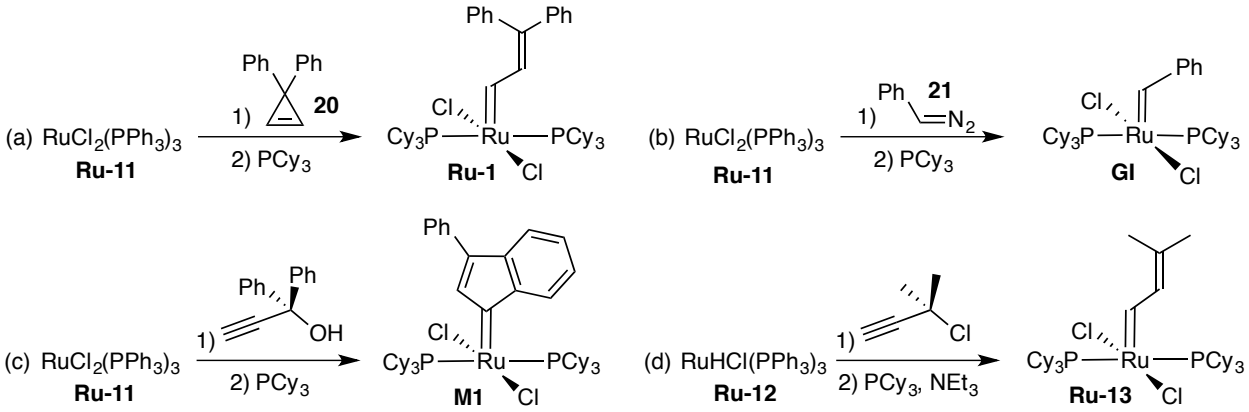

Figure 4.1 Selected examples of different synthetic routes to access ruthenium alkylidene complexes. Routes are based on (a) ring opening, (b) alkylidene transfer, and (c) & (d) alkyne reagents.

The most common ruthenium precursor is $RuCl_2(PPh_3)_3$, **Ru-11**, which can be treated with different alkylidene sources to yield the complexes shown in Figure 4.1. The strategy in pathway (a) implements the use of 2,2-diphenylcyclopropene, **20**, with **Ru-11**. The instability of **20,** a consequence of its ring strain**,** led to the development of diazoalkanes (phenyl diazomethane **21** in Figure 4.1 (b)), a more practical alkylidene-transfer reagent. This alternative source contributed to the discovery of the now-classic first-generation Grubbs catalyst, **GI**. A second

major advances was exchange of the PPh_3 ligands with the stronger σ-donating PCy_3, which greatly enhanced catalyst activity.

The breakthrough benzylidene catalyst **GI** generated a more metathesis-active catalyst than the vinylalkylidene (such as **Ru-1** or **Ru-13)** or indenylidene (**M1)** analogues, without sacrificing the greater ease of handling of these complexes, relative to the high-oxidation-state Schrock catalysts. The synthetic routes utilizing alkyne reagents for **Ru-13** or **M1** may be more attractive than the synthesis of relatively unstable $PhCHN_2$ **21**, but an extra step, involving the cross-metathesis of **Ru-13** or **M1** with styrene, is required to access **GI** (Figure 4.2).

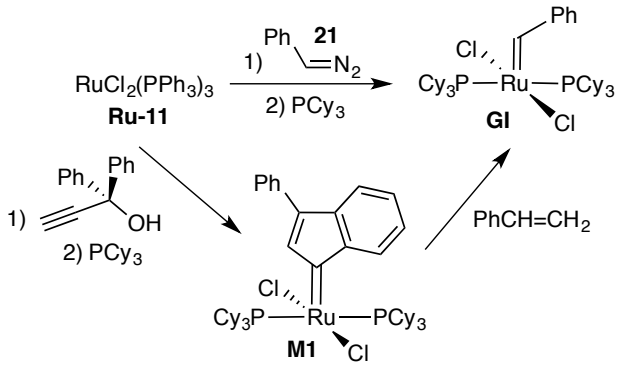

Figure 4.2 Synthesis of **GI**: one-step route involving reaction of $RuCl_2(PPh_3)_3$ with $PhCHN_2$ **21**, or two-step reaction via indenylidene **MI.**

Benzylidene transfer from $PhCHN_2$ **21** is the most widely used methodology.[3] The synthesis of such diazoalkanes via the Bamford-Steven reaction[6] involves reaction of a tosylhydrazone precursor with sodium methoxide at elevated temperature (Scheme 4.1). A major drawback to such diazoalkanes is their sensitivity to decomposition, which results in poor stoichiometric control in the synthesis of **GI**. These issues, and improved synthetic strategies to produce **21** (and hence **GI**) more reliably were therefore examined.

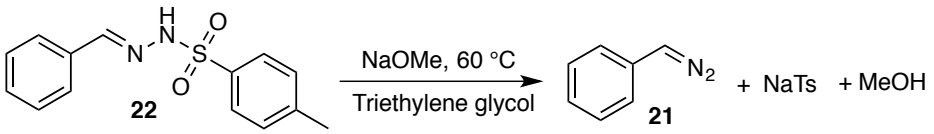

22 **21**

Scheme 4.1 Synthesis of **21** using the Bamford-Stevens reaction.

A major advance in metathesis activity emerged with second-generation Grubbs catalysts such as **GII,** in which one of the PCy_3 ligands on **GI** was replaced with a much more strongly σ-donating *N*-heterocyclic carbene (NHC) ligand such as **H_2IMes**.[7] The most widely used synthetic routes to **GII** employ elevated temperature and a slight excess of strong base (KO*t*Bu or KH) to deprotonate the imidazolium tetrafluoroborate salt **H_2IMes-BF_4**, and install the **H_2IMes** ligand (Scheme 4.2a).[8] However, strong base is known to promote decomposition of metathesis catalysts. Both the Furstner and the Grubbs groups reported formation of Ru–O*t*Bu byproducts arising from unintended reaction with KO*t*Bu.[9,10] In addition, residual base present during the standard methanol rinse is likely to generate methoxide ion, which promotes formation of ruthenium hydrides from **GI** and **GII**.[11,12] (The reaction with methanol itself is much slower, even at elevated temperatures).[13] Catalyst impurities can lead to decreased catalyst potency and can promote undesired side reactions such as isomerization.[14] Formation of impurities and byproducts is endemic to in situ deprotection.

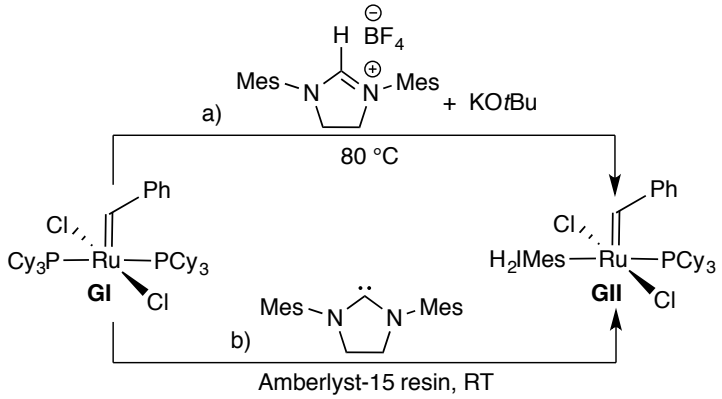

Scheme 4.2 a) Synthesis of **GII** from in situ deprotection of **H_2IMes-BF_4** salt. b) Synthesis of **GII** using "free" carbene route.

In 2012, Dr. Bianca van Lierop of the Fogg group, with her co-workers, developed an updated synthesis for **GII**, its indenylidene analogue **M2**, and the Hoveyda catalyst **HII**, which eliminated the need for in situ deprotection of the NHC precursor.[15] The synthesis employed ligand exchange of a PCy_3 group with free **H_2IMes** (Scheme 4.2b), a methodology previously developed by Dr. Justin Lummiss for synthesis of the methylidene complexes **GIIm**.[16] Workup requires removal of the liberated phosphine, which inhibits catalyst initiation, and has been shown to decompose **GII** during catalysis.[17-19] Conventional workup, by extraction of PCy_3 with cold (-78 °C) pentane, results in materials losses due to the partial solubility of the products in pentane. To improve workup, the liberated phosphine was removed by treating with the Amberlyst-15,[8] a strongly acidic cationic exchange resin. The resin is added once an in situ ^{1}H NMR reveals that no starting material remains, to ensure that the resin does not react with the free **H_2IMes**. Amberlyst-15 resin can be easily removed by filtration once all phosphine has been scavenged.

References page 75

This strategy afforded the target catalysts in high yields and high purity, and indeed our research group has found it to be highly reliable for the synthesis of **HII**, even by relatively inexperienced undergraduate researchers. (The synthesis of **M2** has been essentially unused by our own group). In the ensuing period, however, persistent problems emerged in using this methodology to access **GII**. The origin and solutions to these problems were therefore examined, in addition to the issues with synthesis of **21**.

4.2 Results and Discussion

4.2.1 Phenyldiazomethane Synthesis (21)

Initial efforts focused on improving the synthesis of phenyldiazomethane **21**. The standard approach, a modified version of the Bamford-Stevens reaction (Scheme 4.3),[6] involves treatment of benzaldehyde tosylhydrazone **22** with aqueous KOH at 70 °C in air. The reaction was quenched with water after 20 min, after which the product **21** was extracted with hexanes, concentrated to a red oil, and weighed. The oil was taken up in hexanes and cannula-transferred to a stirred solution of $RuCl_2(PPh_3)_3$ **Ru-11** for the immediate synthesis of **GI**. The yield of **21** is limited to ca. 35% by decomposition.

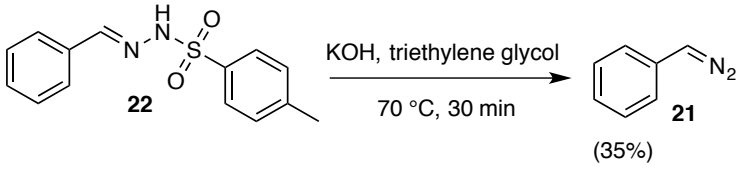

Scheme 4.3 Synthesis of compound **21** under basic conditions and at elevated temperature.

4.2.2 Vacuum Pyrolysis of Isolated Tosylhydrazone Salt to Produce 21

An improved synthesis of **21**, which could lead to improved yields of **GI**, was explored. A priority was handling **21** under inert atmosphere, and maintaining it at low temperature (< -20

°C) wherever possible.[18] In the original Bamford-Stevens reaction, base is used to deprotonate the tosylhydrazone **22**, and elevated temperatures trigger pyrolysis of the in situ-generated salt **23** to generate the diazoalkane (Scheme 4.4a). An alternative synthesis developed by Shechter[21] involves vacuum pyrolysis of the isolated tosylhydrazone salt **23**, and immediate collection of the diazoalkane in a receiving flask cooled at -78 °C (Scheme 4.4b).

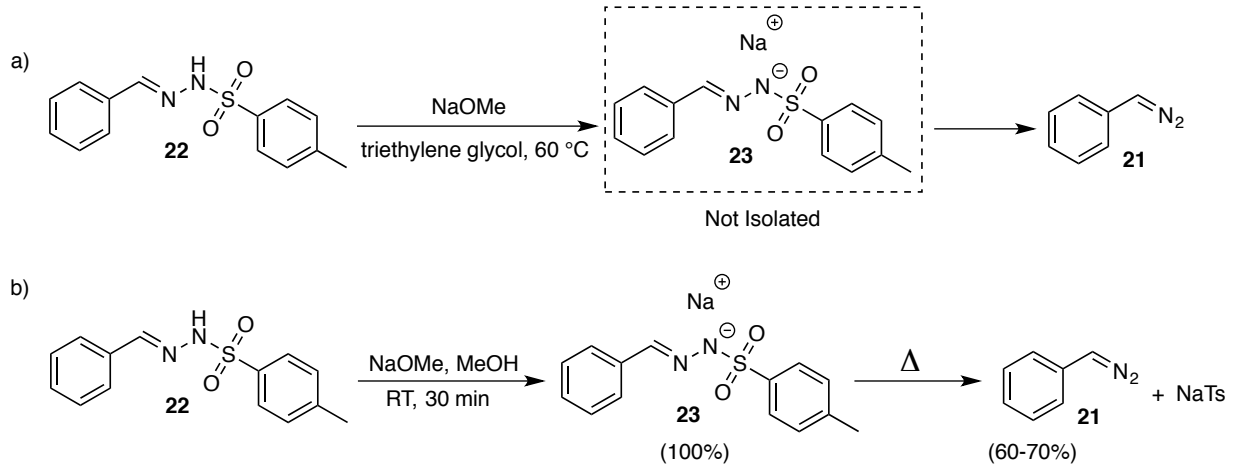

Scheme 4.4 a) Synthesis of **21** via Bamford-Stevens reaction. b) Synthesis of **21** through vacuum pyrolysis of isolated sodium tosylhydrazone salt, **23**.

In following the latter route, the benzaldehyde tosylhydrazone salt **23** was generated in quantitative yield, by treating a solution of **22** in methanol with a slight excess of sodium methoxide in the glovebox (Scheme 4.4b). The methanol was removed under vacuum to deliver **23** as a white powder. This material was dried under vacuum to remove residual solvent prior to vacuum pyrolysis. Compound **23** was stored for several days in the dark, when essential, to inhibit spontaneous photo-induced formation of **21**.

Cracking of **23** to liberate $PhCHN_2$ was then accomplished by suspending **23** in degassed Nujol (an aid to homogeneous heating) in a round-bottomed Schlenk flask, and heating behind a blast shield, in order to distil the diazo reagent via a U-tube into a cooled Schlenk flask open to

vacuum. A schematic is shown in Appendix D. The temperature of the oil bath was slowly increased from 40 °C to 90 °C (at which point red **21** began to distil), and eventually to 110 °C. Increasing the temperature slowly is important to minimize the potential for explosion of the $PhCHN_2$.[20] When production of **21** ceased, the receiving flask was back-filled with N_2 and weighed. The oil was diluted with hexanes, and transferred by cannula to a stirred solution of **Ru-11** in CH_2Cl_2. The alkylidene-transfer reaction was allowed to continue for 1 h while warming from -78 °C to 0 °C, following which PCy_3 was added to effect formation of **GI** (Scheme 4.5).

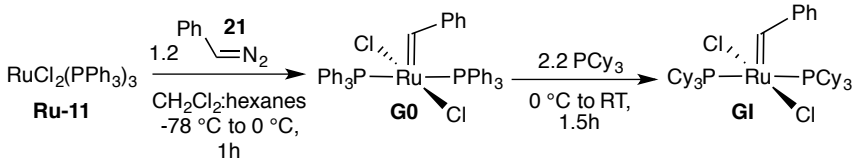

Scheme 4.5 Overall synthesis of **GI** starting from **Ru-11**.

4.2.3 Reproducibility Problems Associated with Residual MeOH

This approach was initially found to yield **21** in highly variable amounts, ranging from essentially quantitative to zero even after extended heating at 110 °C. The problem was traced to the presence of residual methanol in the salt **23**, present even after prolonged exposure to high vacuum. Diazoalkanes are known to react with protic solvents,[22] as shown in Scheme 4.6.

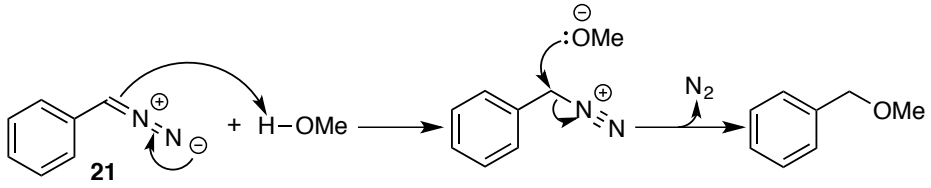

Scheme 4.6 Reaction of compound **21** with methanol leading to decomposition of the phenyldiazomethane.

4.2.4 Updated Synthesis of 21 by Using THF as the Reaction Solvent in the Preparation of 23

To circumvent problems with residual methanol, synthesis of the tosylhydrazone salt **23** was carried out in THF (Scheme 4.7), and **22** was deprotonated with NaH, rather than NaOMe. The synthesis of **21** using the material thus formed showed good reproducibility (yields of **21**: 65-70%), and the ultimate yields of **GI** were routinely ca. 80%.

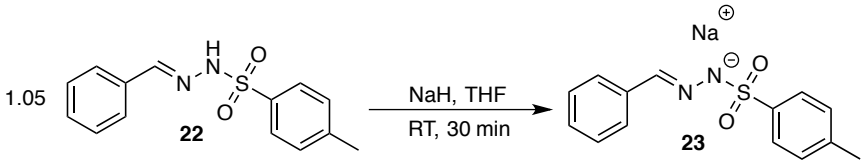

Scheme 4.7 Synthesis of tosylhydrazone salt, **23**, using a modified procedure.

4.2.5 Stoichiometric Control in the Synthesis of GI

Quantifying the mass of **21** in the receiving flask is critical to control the stoichiometry of the benzylidene transfer reaction from **21** to **Ru-11** in the synthesis of **GI**. Use of a slight stoichiometric excess (ca. 1.2 equivalents) proved advisable. Under-addition of **21** results in contamination of the **GI** product with unreacted **Ru-11** (Figure 4.3). While the latter compound can be removed by exhaustive extraction with methanol, yields of **GI** were found to drop to ca. 50%, owing to the partial solubility of **GI** in methanol, as well as incomplete utilization of the precursor **Ru-11**.

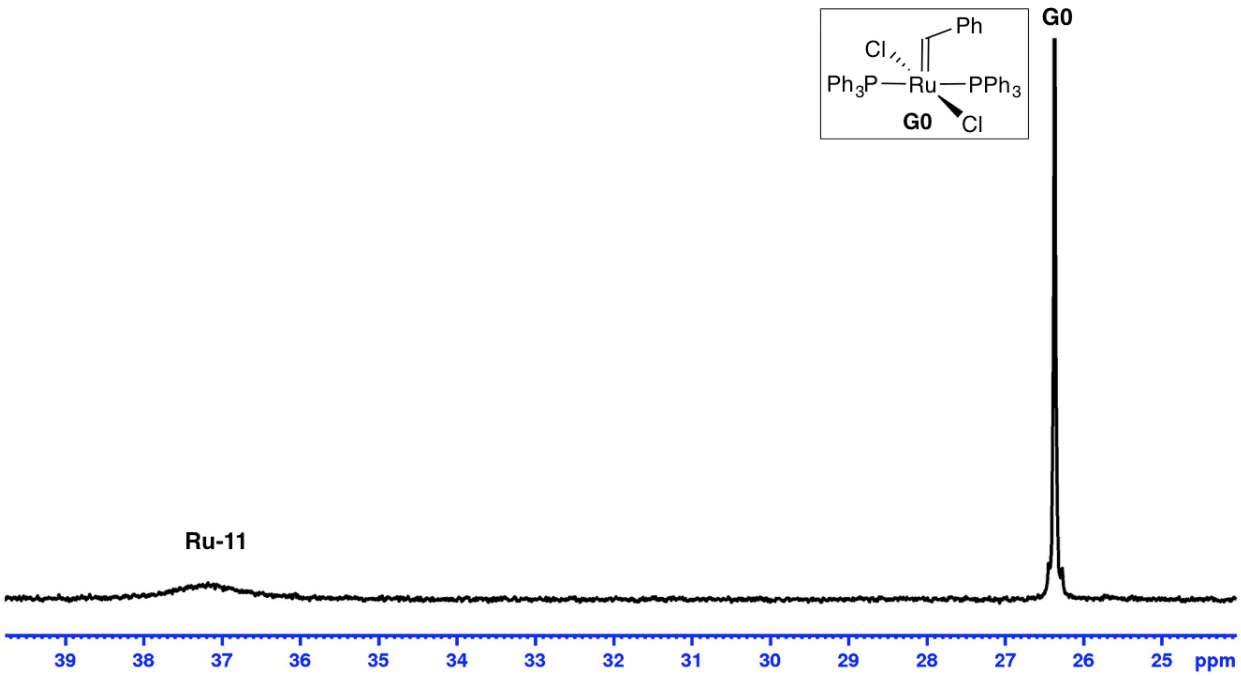

Figure 4.3 $^{31}P\{^{1}H\}$ NMR spectrum of the crude product formed by reaction of **Ru-11** and $PhCHN_2$ **21** (121 MHz, CH_2Cl_2).

Over-addition of **21** also has a negative effect on the yield of **GI**. A second, as-yet unidentified alkylidene species was observed by ^{1}H NMR analysis of the crude product (20.1 ppm; 9% vs. **GI**; Figure 4.4). This compound could be removed by reprecipitation from CH_2Cl_2–methanol, but this occasioned ca. 15% loss, resulting in 50% yield of **GI**.

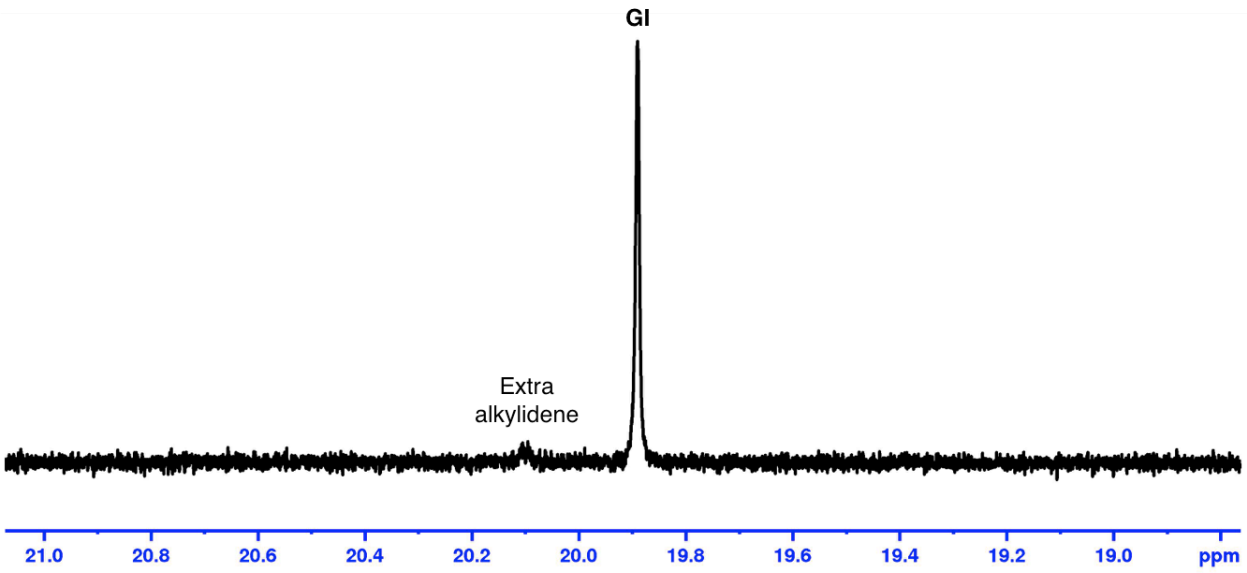

Figure 4.4 ^{1}H NMR spectrum (300 MHz, C_6D_6) of crude **GI** , showing a byproduct arising from use of excess $PhCHN_2$.

A further side-reaction during synthesis of **GI** involves consumption of the diazo reagent **21** via nucleophilic attack by free PPh_3, liberated from **Ru-11** during the alkylidene transfer reaction. This undesired reaction generates the ylide **24**, which accounts for a previously unassigned $^{31}P\{^{1}H\}$ NMR singlet at 23.3 ppm (Figure 4.5). The proposed assignment was confirmed by the deliberate synthesis of **24** (Scheme 4.8) by Ms. Amrah Nasim of this research group. While **24** can be removed by extraction with methanol, it is a hazard to the reaction stoichiometry, which could lead to unreacted **Ru-11**. Slow addition of **21** to **Ru-11** may aid in reducing this side-reaction, and enable preferential reaction of **21** with **Ru-11**.

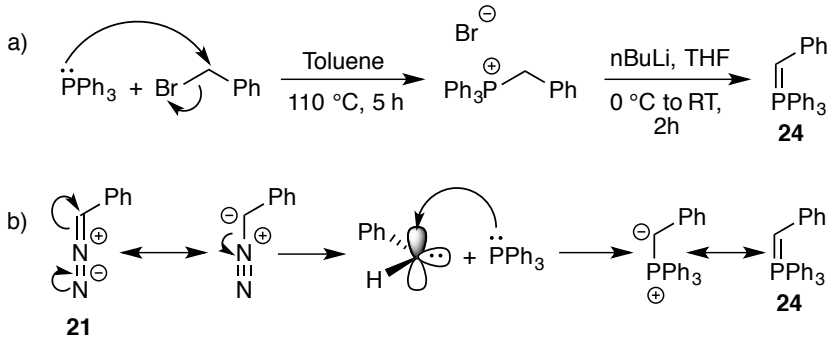

Scheme 4.8 (a) Synthesis of compound **24**. (b) Proposed mechanism for formation of **24** during synthesis of **GI**, via attack of free PPh_3 on **21**.

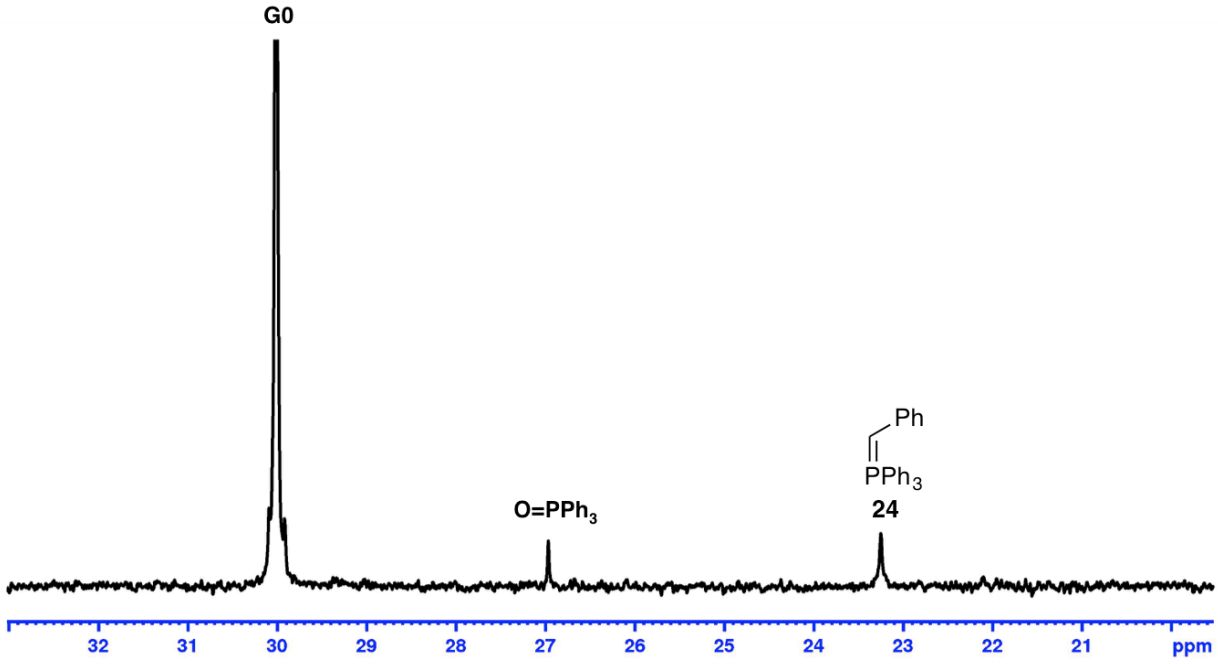

Figure 4.5 In situ $^{31}P\{^{1}H\}$ NMR spectrum (121 MHz, CH_2Cl_2) of crude **GI**, showing **24**.

Higher-yield, higher-purity routes to **GI** will aid in the synthesis of **GII,** as well as other metathesis catalysts (particularly the Hoveyda catalysts **HI** and **HII**). Issues in the synthesis of **GII** via use of Amberlyst as a phosphine scavenger are discussed in the next Section.

4.2.6 Issues Arising in Synthesis of GII via "Free" Carbene and Resin Method

The 2012 van Lierop route to **GII**[15] has been found to exhibit poor control in the reaction of **GI** with free **H_2IMes**. In the published procedure, a slight excess (1.05 equiv) of **H_2IMes** relative to **GI** was used. However, the free carbene is highly sensitive to water, which triggers ring-opening to yield the formamide **17** (Scheme 4.9). If the THF is not scrupulously dry, water will decompose the **H_2IMes**. As **GI** and **GII** are closely similar in solubility, unreacted **GI** is difficult to remove. Adding more than 1.05 equiv of **H_2IMes** to the room-temperature reaction does not result in formation of the bis-carbene complex **Ru-14** (Scheme 4.10), as judged by the ^{1}H NMR analysis. This is unsurprising, given the very low lability of the PCy_3 ligand trans to an NHC donor.[23] Best practices thus involve use of 1.05–1.1 equivalents of the free carbene, with removal of an aliquot for ^{1}H NMR analysis in C_6D_6 after 1 h, at which point the stoichiometry can be corrected, if necessary, by adding the required amount of further free **H_2IMes**.

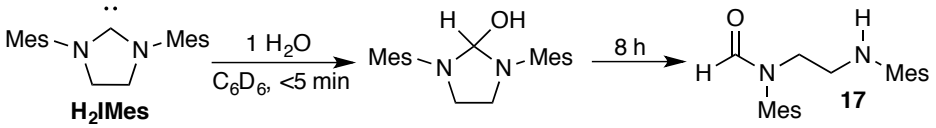

Scheme 4.9 Hydrolysis of **H_2IMes** to afford the formamide product **17**.

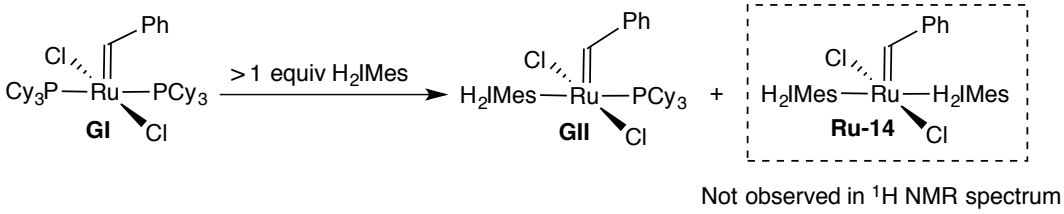

Scheme 4.10 Proposed reaction of **GI** with excess **H_2IMes** to form **Ru-14**.

In the van Lierop procedure, a fourfold excess of the phosphine-scavenging resin Amberlyst-15 was used, relative to **GI**. Subsequent use revealed incomplete scavenging of PCy_3, especially in the 1 h reaction time originally reported. Subsequent optimization indicated that a six-fold

excess, with efficient stirring for 2 h, was required for complete removal of PCy_3. Efficient stirring is essential to control mass transfer. However, stirring with the resin for longer periods resulted in partial catalyst decomposition by unknown pathways, with a ca. 20% decrease in yields.

A further problem was associated with the appearance of trace free PPh_3, where the **GI** was incompletely purified. Unexpectedly, the Amberlyst-15 resin proved unable to scavenge PPh_3, even with six equivalents of resin present. This is very surprising, given the presence of free sulfonic acid groups on the Amberlyst-15 resin, which should suffice to bind PPh_3. At this stage, the reasons remain unclear. While PPh_3 can be extracted with cold pentane, the partial solubility of **GII** in this solvent results in some loss of **GII** in the repeated washings required to successfully remove all the PPh_3.

4.2.7 Common Issues for HI Synthesis Using Amberlyst-15 Resin

As with the **GII** synthesis, four equivalents of resin proved insufficient to remove the free PCy_3 generated during synthesis of **HI** (Scheme 4.11). This amount was increased to six equivalents to successfully remove all of the free PCy_3.

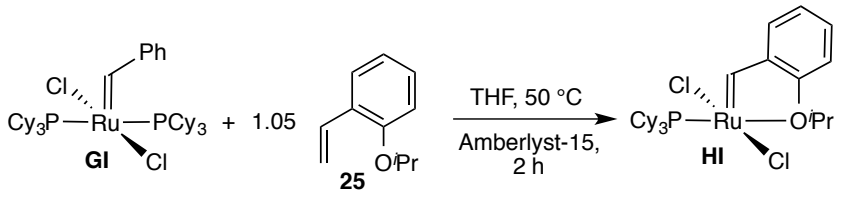

Scheme 4.11 Reported synthesis of **HI** by undergoing CM with **GI** and **25**.

During the reaction, an unidentified impurity was consistently observed by $^{31}P\{^1H\}$ NMR analysis, at 37 ppm (C_6D_6). This species could be removed by chromatography on a short silica

column in the glovebox using 2:1 CH_2Cl_2-hexanes. Alternatively, transformation of **HII** into **HI** can be carried forward, with subsequent chromoatographic purification using 3:1 CH_2Cl_2-hexanes.

4.2.8 Common Issues for HII Synthesis using Amberlyst-15 Resin

The original procedure (Scheme 4.12) was modified, as above, to use six equivalents of resin. A more substantive issue (as seen in the synthesis of **GII**; Section 4.2.7), was the difficulty in controlling the stoichiometry of the reaction between **HI** and free **H_2IMes**. Free **H_2IMes** is readily decomposed by water (see Scheme 4.9 above), and inexperienced users frequently encounter problems with poorly-dried THF (for which the well-known ketyl test can be deceiving, if excessive ketyl is used). Addition of excess **H_2IMes** to the reaction was not detrimental to the yield of **HII**, and excess carbene can be readily removed by the Amberlyst-15 resin treatment.

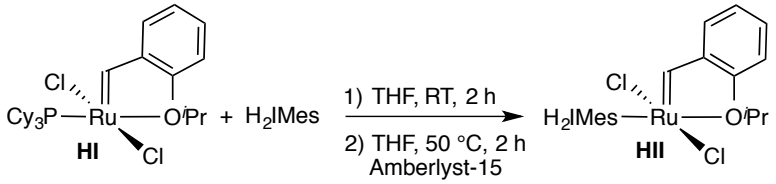

Scheme 4.12 Ligand exchange of **HI** with **H_2IMes** to synthesis **HII**.

4.2.9 Impact of Residual Styrene on Synthesis of HII

Synthesis of **HI** by cross-metathesis of **GI** with styrenyl ether **25** (Scheme 4.13) generates styrene as a co-product. In the 2012 procedure, styrene was extracted with pentane at -35 °C; alternatively, it can be removed by silica-gel chromatography column (Section 4.2.8).

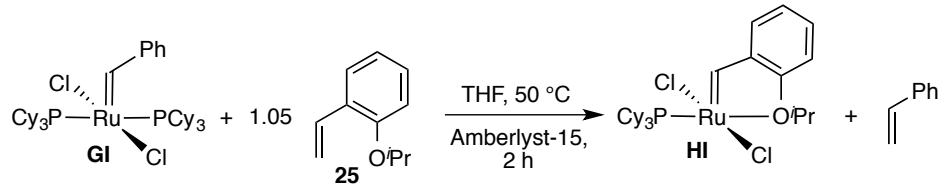

Scheme 4.13 Formation of **HI**, showing the styrene co-product.

Residual styrene was shown to be detrimental in an experiment in which the preparation of **HII** from **HI** was carried out in the presence of a deliberately-added amount of styrene (1 equiv; Scheme 4.14). ^{1}H NMR analysis after 2 h (at which point resin would normally be added) revealed ca. 20% **HII**, 13% of PCy_3-bound **Ru-15**, 50% **GII**, and 17% decomposition. The formation of **GII** is a concern, as its low lability means that it may not completely re-convert to **HII** via recapture of the styrenyl ether when the reaction is terminated. These findings underscore the importance of completely removing residual styrene from **HI** prior to the synthesis of **HII**, to maximize yields and purity.

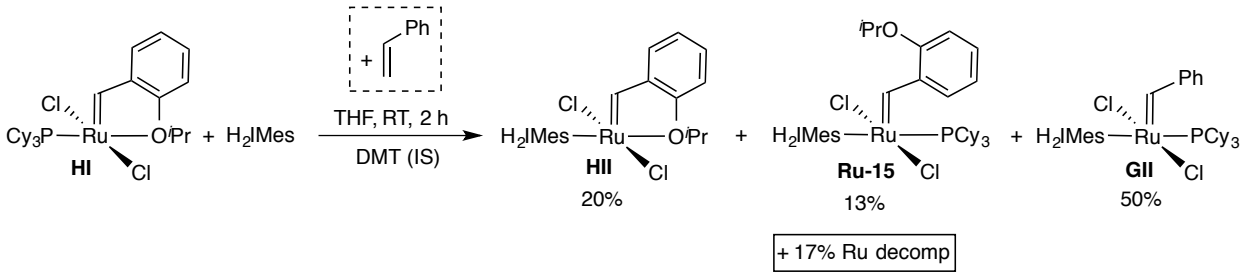

Scheme 4.14 Detrimental effect of added styrene (1 equiv) on the synthesis of **HII**.

4.3 Conclusion

The modifications highlighted in this chapter include better access to **GI** through the improved synthesis of the phenyldiazomethane precursor **21**, increased addition of Amberlyst-15 resin for the syntheses of **GII**, **HI**, and **HII**, and solutions to common problems observed in these

syntheses. The modified procedures permit access to pure catalysts in high yields. These catalysts are of the utmost importance to the scientific community who use these compounds routinely. Simple syntheses to these important catalysts will afford reliable, controlled, reproducible metathesis, thereby advancing the field in both academia and industry.

4.4 References

(1) Fogg, D. E.; Foucault, H. M., Ring-Opening Metathesis Polymerization. In *Comprehensive Organometallic Chemistry III*, Crabtree, R. H.; Mingos, D. M. P., Eds. Elsevier: Oxford, 2007; Vol. 11, pp 623–652.
(2) Nguyen, S. T.; Johnson, L. K.; Grubbs, R. H.; Ziller, J. W. *J. Am. Chem. Soc.* **1992**, *114*, 3974–3975.
(3) Schwab, P.; Grubbs, R. H.; Ziller, J. W. *J. Am. Chem. Soc.* **1996**, *118*, 100–110.
(4) Amoroso, D.; Snelgrove, J. L.; Conrad, J. C.; Drouin, S. D.; Yap, G. P. A.; Fogg, D. E. *Adv. Synth. Catal.* **2002**, *344*, 757–763.
(5) Dorta, R.; Kelly, A., III; Nolan, S. P. *Adv. Synth. Catal.* **2004**, *346*, 917–920.
(6) Bamford, W. R.; Stevens, T. S. *J. Chem. Soc.* **1952**, 4735–4740.
(7) Sanford, M. S.; Ulman, M.; Grubbs, R. H. *J. Am. Chem. Soc.* **2001**, *123*, 749–750.
(8) Scholl, M.; Ding, S.; Lee, C. W.; Grubbs, R. H. *Org. Lett.* **1999**, *1*, 953–956.
(9) Trnka, T. M.; Morgan, J. P.; Sanford, M. S.; Wilhelm, T. E.; Scholl, M.; Choi, T.-L.; Ding, S.; Day, M. W.; Grubbs, R. H. *J. Am. Chem. Soc.* **2003**, *125*, 2546–2558.
(10) Fürstner, A.; Ackermann, L.; Gabor, B.; Goddard, R.; Lehmann, C. W.; Mynott, R.; Stelzer, F.; Thiel, O. R. *Chem. Eur. J.* **2001**, *7*, 3236–3253.
(11) Dinger, M. B.; Mol, J. C. *Eur. J. Inorg. Chem.* **2003**, 2827–2833.
(12) Beach, N. J.; Lummiss, J. A. M.; Bates, J. M.; Fogg, D. E. *Organometallics* **2012**, *31*, 2349–2356.
(13) Beach, N. J.; Camm, K. D.; Fogg, D. E. *Organometallics* **2010**, *29*, 5450–5455.
(14) Higman, C. S.; Lummiss, J. A. M.; Fogg, D. E. *Angew. Chem., Int. Ed.* **2016**, *55*, 3552–3565.
(15) van Lierop, B. J.; Reckling, A. M.; Lummiss, J. A. M.; Fogg, D. E. *ChemCatChem* **2012**, *4*, 2020–2025.
(16) Lummiss, J. A. M.; Beach, N. J.; Smith, J. C.; Fogg, D. E. *Catal. Sci. Technol.* **2012**, *2*, 1630–1632.
(17) Hong, S. H.; Day, M. W.; Grubbs, R. H. *J. Am. Chem. Soc.* **2004**, *126*, 7414–7415.
(18) Lummiss, J. A. M.; McClennan, W. L.; McDonald, R.; Fogg, D. E. *Organometallics* **2014**, *33*, 6738–6741.
(19) Bailey, G. A.; Fogg, D. E. *J. Am. Chem. Soc.* **2015**, *137*, 7318–7321.
(20) Creary, X. *Org. Synth.* **1986**, *64*, 207–216.
(21) Kaufman, G. M.; Smith, J. A.; Stouw, G. G. V.; Shechter, H. *J. Am. Chem. Soc.* **1965**, *87*, 935–937.
(22) Crawford, R. J.; Raap, R. *Can. J. Chem.* **1965**, *43*, 126–132.

(23) Lummiss, J. A. M.; Higman, C. S.; Fyson, D. L.; McDonald, R.; Fogg, D. E. *Chem. Sci.* **2015**, *6*, 6739–6746.

Chapter 5. Conclusions and Future Directions

Ruthenium metathesis catalysts have enabled facile formation of new carbon-carbon double bonds under less demanding conditions than previously required. The ruthenium catalysts have facilitated uptake of olefin metathesis in industrial reactions, albeit nearly two decades after their original discovery. To expand uptake and efficiency, better understanding of their decomposition pathways is essential. Such understanding can teach how to circumvent decomposition, enabling longer-lived, more productive catalysts.

A part of this thesis work was aimed at understanding the impact of water on catalyst performance. Chapter 3 focused on issues of catalyst performance for metathesis in the presence of water. High catalyst loadings (> 1 mol%) are generally required for aqueous metathesis, and solubility issues with either the catalysts or substrates has sometimes been put forward as an explanation. In this work, water was shown to promote catalyst decomposition, leading to lower productivity. The negative impact of water was general for both RCM and CM reactions, and for both phosphine-supported **GII** and phosphine-free **HII** catalysts. The major decomposition pathways were found to be catalyst-dependent. For **GII**, decomposition proceeded through a donor-accelerated pathway, in which coordination of water to the resting-state species **GIIm** promotes PCy_3 loss, and hence accelerates nucleophilic attack of PCy_3 on the methylidene carbon. Ensuing C–H activation results in liberation of $[MePCy_3]Cl$. In the case of **HII**, water-promoted decomposition occurred via the metallacyclobutane complex, as indicated by formation of three-carbon decomposition products that can only originate in the metallacyclobutane ring. Water was suggested to promote a previously-postulated β-hydride transfer pathway, by interacting with the Cβ C–H σ* orbital, and hence rendering this proton

more hydridic. Ruthenium hydroxide species were also examined: a bis-hydroxide derivative of **HII** was isolated and shown to decompose readily during metathesis.

Chapter 4 identifies limitations in current synthetic routes to **GI** and related catalysts, and solutions to these difficulties. The synthesis of phenyldiazomethane, the key alkylidene transfer agent required for synthesis of **GI**, was improved from a yield of ca. 30% to >70% by vacuum pyrolysis and handling under inert atmosphere. The higher purity of the phenyldiazomethane increased the yield of **GI** by ca. 10%. Stoichiometric control in the synthesis of **GI** was discussed, and potential side-reactions, along with methodologies to limit these reactions. The previously established synthetic procedure using the cationic exchange resin, Amberlyst-15, was also modified. As a trivial modification, more resin was shown to be required to completely remove the PCy_3 released by ligand exchange. However, prolonged exposure to the resin was also shown to promote catalyst decomposition, as inferred from decreased yields.

Future work should clarify the mechanism by which water promotes decomposition of the MCB intermediate during metathesis. Three potential pathways can be envisaged to result in the organic decomposition markers observed. These include β-hydride transfer, C-H activation of the mesitylene methyl groups and deprotonation at the **MCB** β-carbon. Deprotonation is unlikely given the low basicity of water and poor acidity of the **MCB** protons. The possibility of C-H activation should be examined by synthesis of deuterated **HII**, in which the **H_2IMes** mesitylene groups are fully deuterated. Incorporation of deuterium into the decomposition products would confirm C-H activation; no incorporation would support the β-hydride transfer pathway. Of

considerable interest is the potential generality of this pathway for **HII** on reaction with other impurities.

Further work on catalyst synthesis should also be undertaken. In the phenyldiazomethane synthesis, more accurate quantification is required to control the stoichiometry of the **GI**–phenyldiazomethane reaction. Use of a less acidic alternative to Amberlyst-15 resin could also be beneficial, to limit decomposition on prolonged exposure to resin. The acidic functionality on the Amberlyst-15 resin is the sulfonic acid moiety, which has a pK_a of approximately -2 in water. The alternative resin Amberlite contains less acidic carboxylic acids groups. Initial tests will be required to determine whether the resin can indeed scavenge PCy_3, and whether pretreatment (e.g. dehydration) affects the rate or efficiency of the process. Exploring the effect of the active functional group of the resins is also suggested, to gain more insight into the stability of the pre-catalysts to these functional groups.

Appendices

A. GC Traces

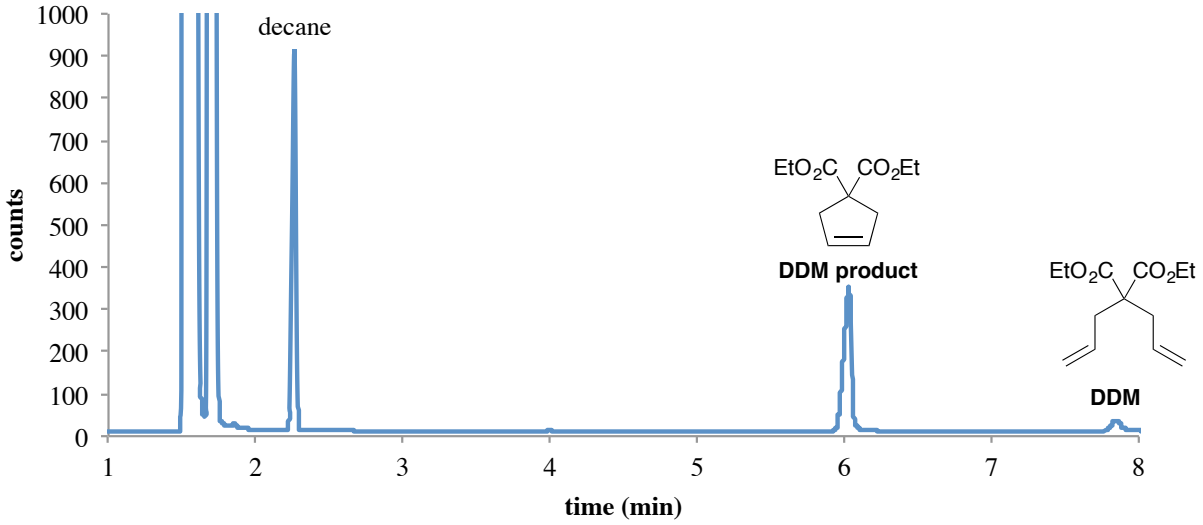

Figure A.1 Representative GC-FID trace for ring-closing metathesis of DDM using **HII**

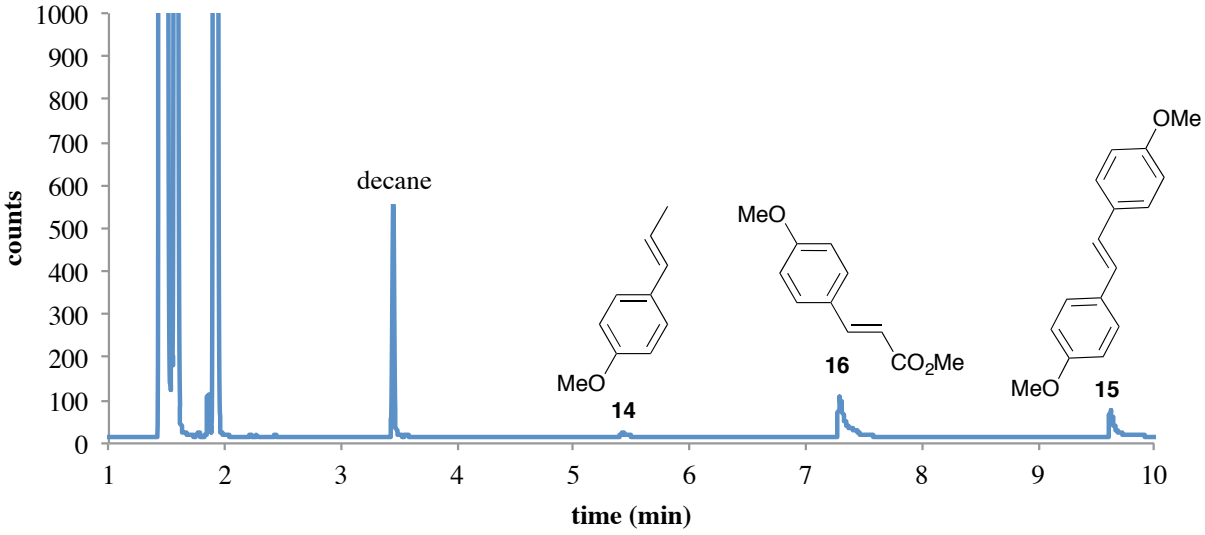

Figure A.2 Representative GC-FID trace for cross-metathesis of anethole **14** to cinnamate **16** using **HII**

B. Identification of Decomposition Products During Metathesis

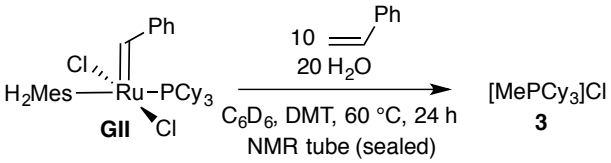

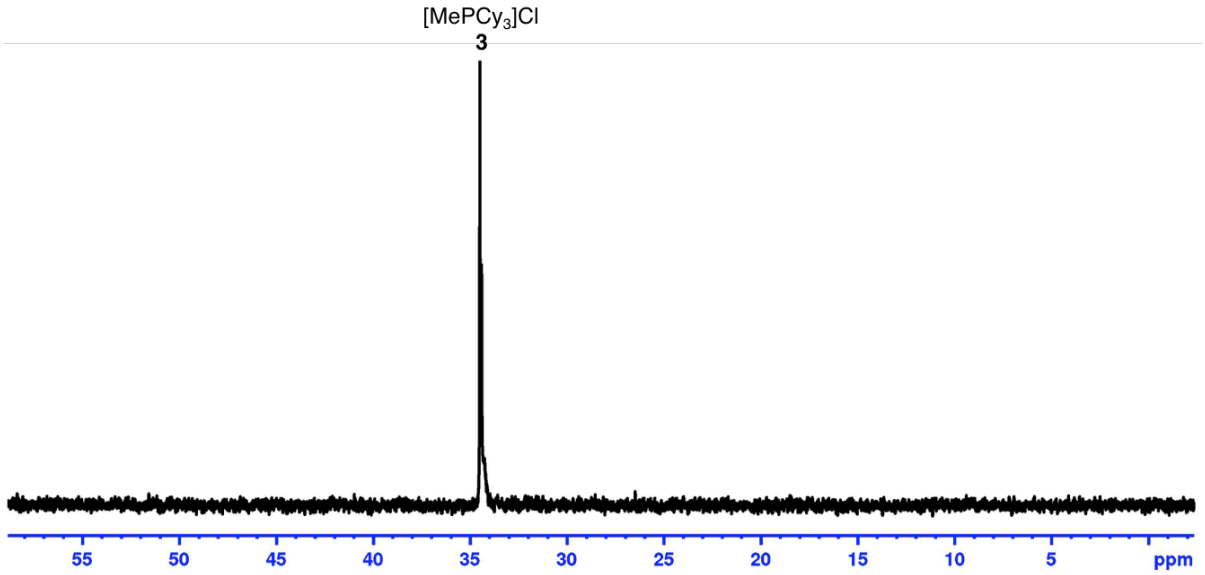

Figure B.1 ^{31}P NMR spectrum (C_6D_6, 121.5 MHz) for the reaction of **GII** with styrene and 20 equiv of water under the conditions above. No **GII** or **GIIm** signals are detected.

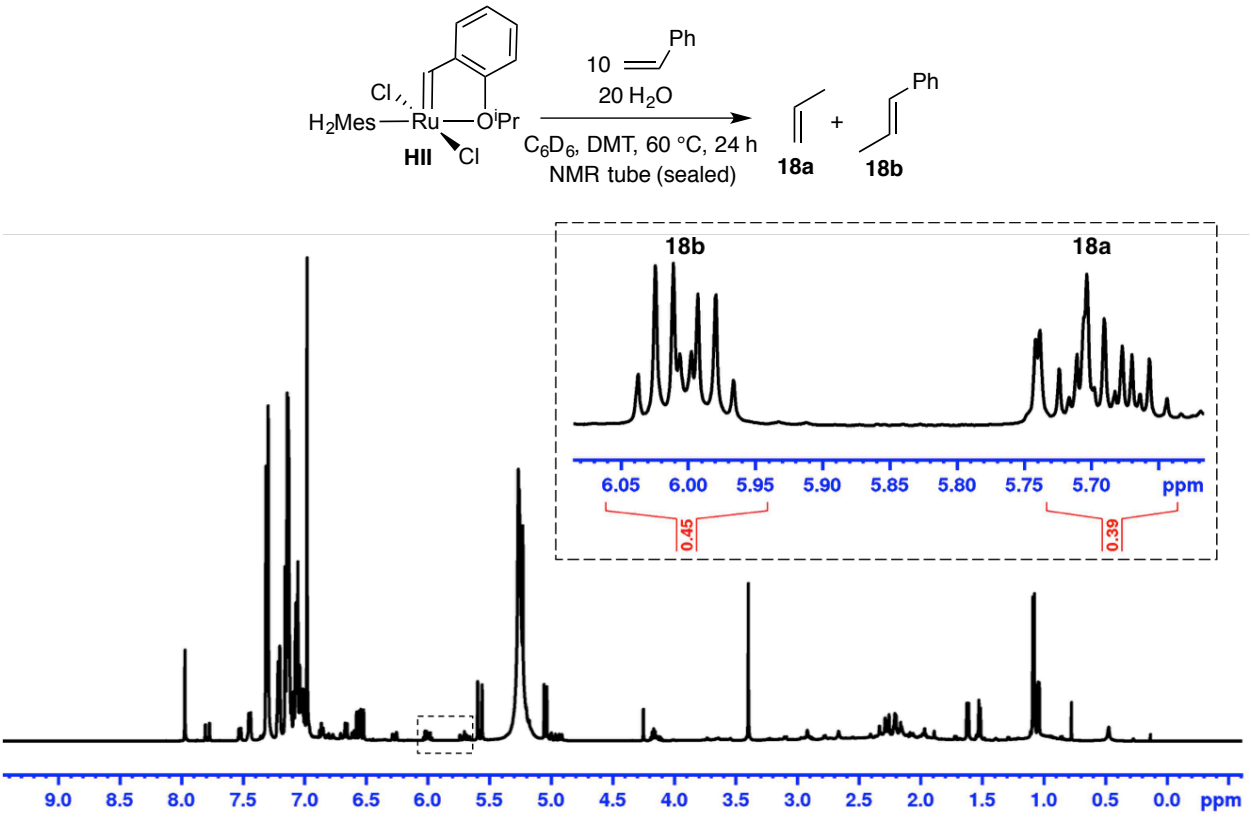

Figure B.2 ^{1}H NMR spectrum (C_6D_6, 300 MHz) for the reaction of **HII** with styrene and 20 equiv of water under the conditions above. Inset shows signals for propene **18a** and β-methylstyrene **18b**

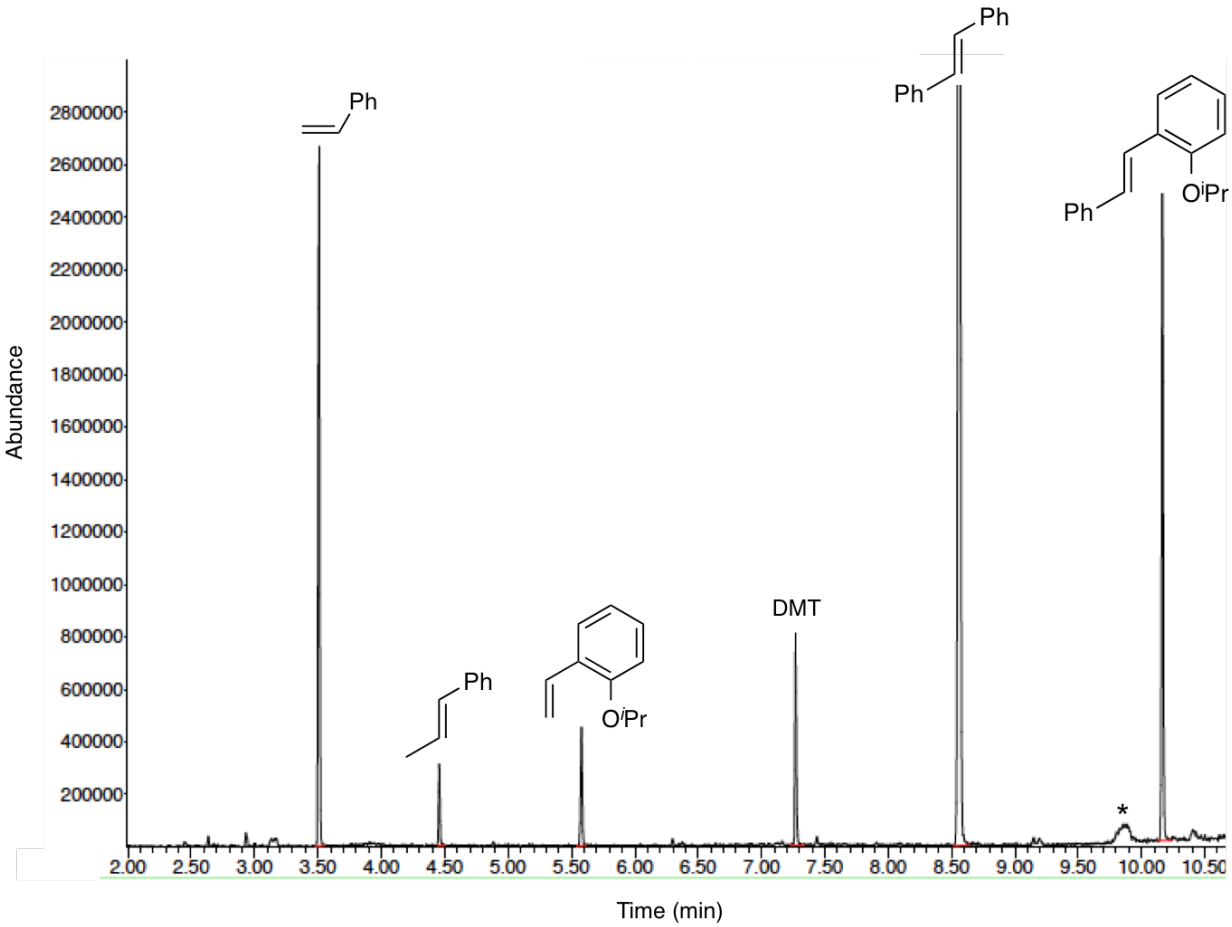

Figure B.3 GC spectrum for reaction of **HII** with 10 equiv styrene and 20 equiv H_2O after 24 h**.** Retention times and MS spectra are consistent with authentic compounds. An unassigned signal (*m/z* 304.2) labeled (*) was also present in a blank GC run.

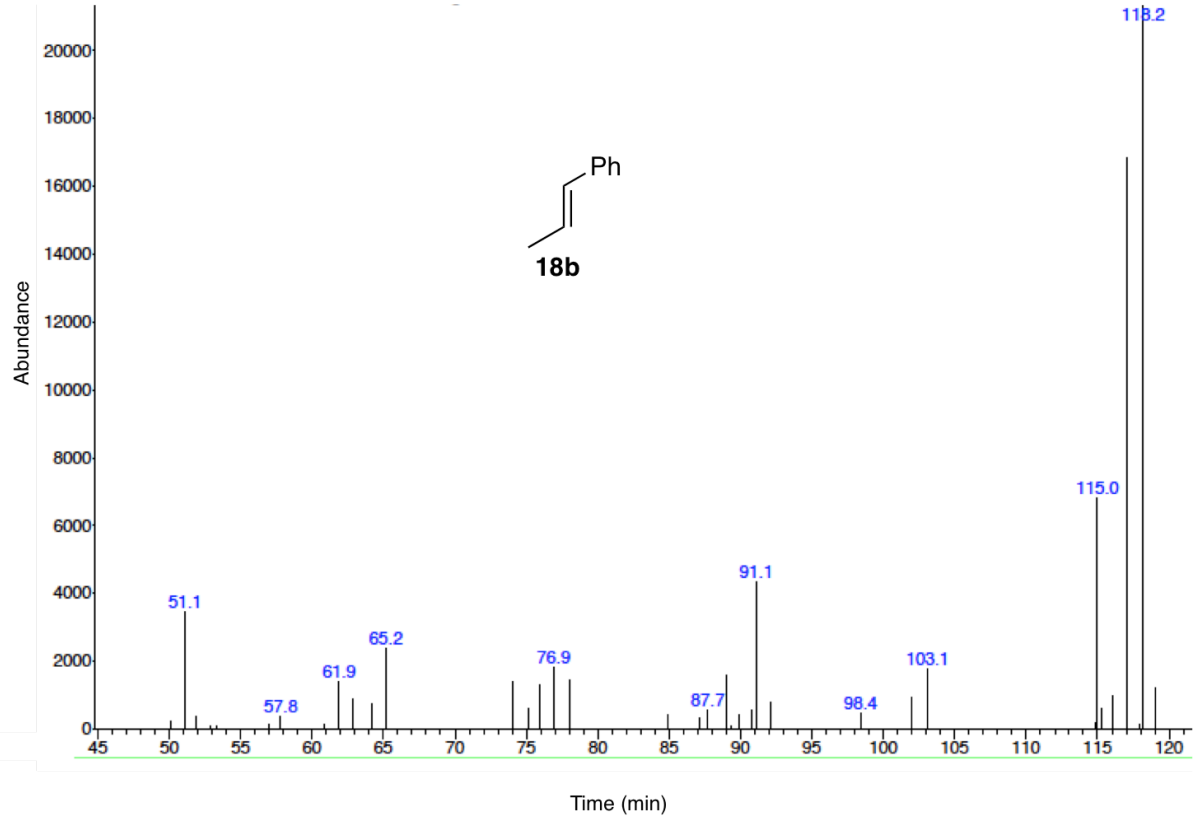

Figure B.4 EI mass spectrum for β-methylstyrene **18b** formed in the reaction stated above. The spectrum of **18b** matches the one in the Wiley Registry of Mass Spectral Data.[1]

C. NMR Characterization for $Ru(OH)_2(H_2IMes)(=CH\text{-}2\text{-}O^iPrC_6H_4)$, HII-$(OH)_2$

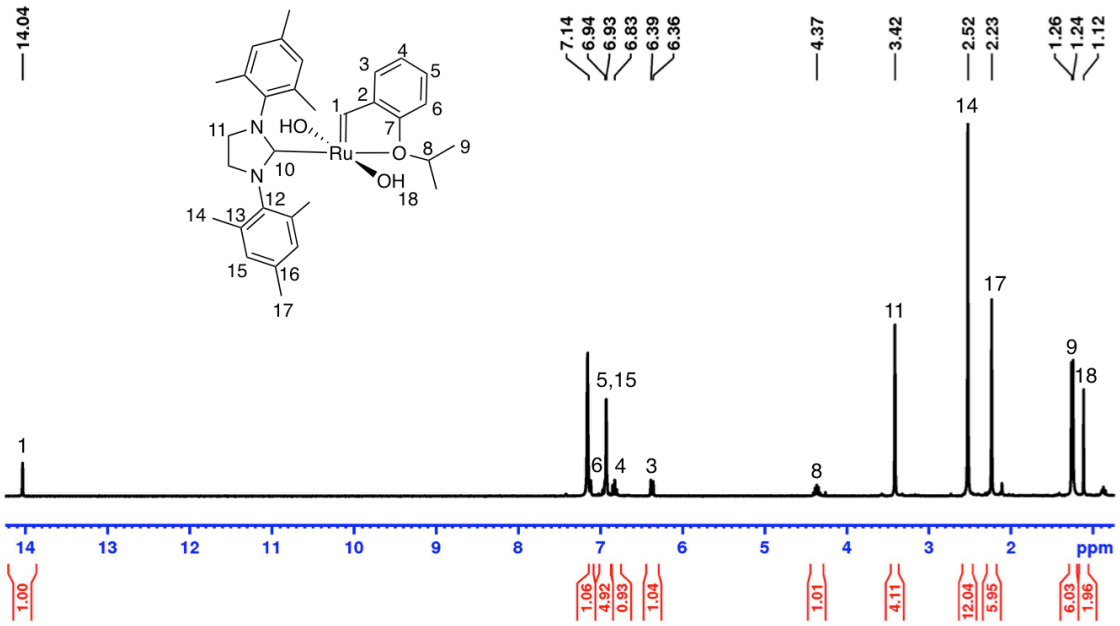

Figure C.1 ^{1}H NMR spectrum (C_6D_6, 300 MHz) for $Ru(OH)_2(H_2IMes)(=CH\text{-}2\text{-}O^iPrC_6H_4)$, **HII-$(OH)_2$**

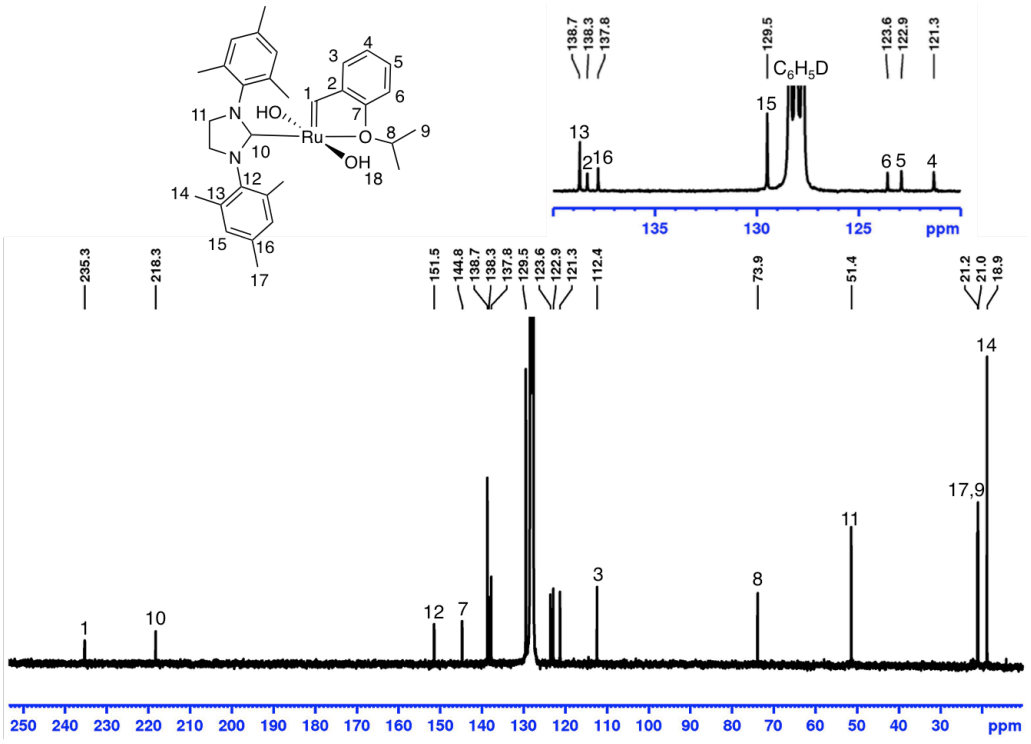

Figure C.2 ^{13}C NMR spectrum (C_6D_6, 75.5 MHz) for $Ru(OH)_2(H_2IMes)(=CH\text{-}2\text{-}O^iPrC_6H_4)$, **HII-$(OH)_2$**

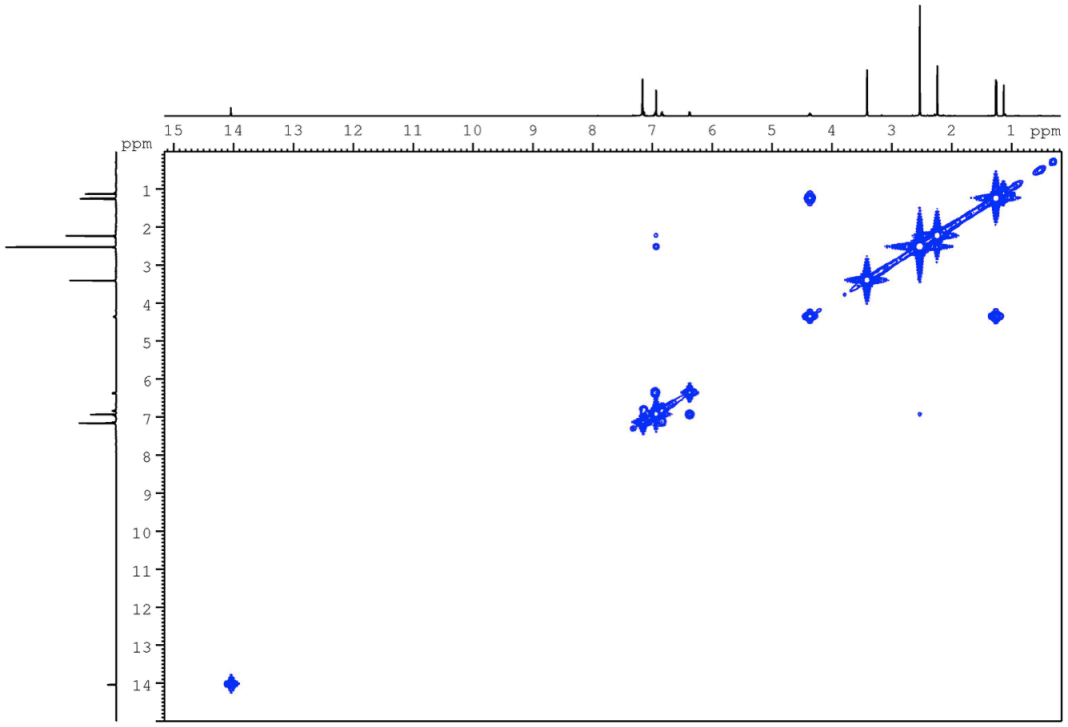

Figure C.3 ^{1}H-^{1}H COSY spectrum (C_6D_6, 300 MHz) for $Ru(OH)_2(H_2IMes)(=CH\text{-}2\text{-}O^{i}PrC_6H_4)$, **HII-(OH)$_2$**

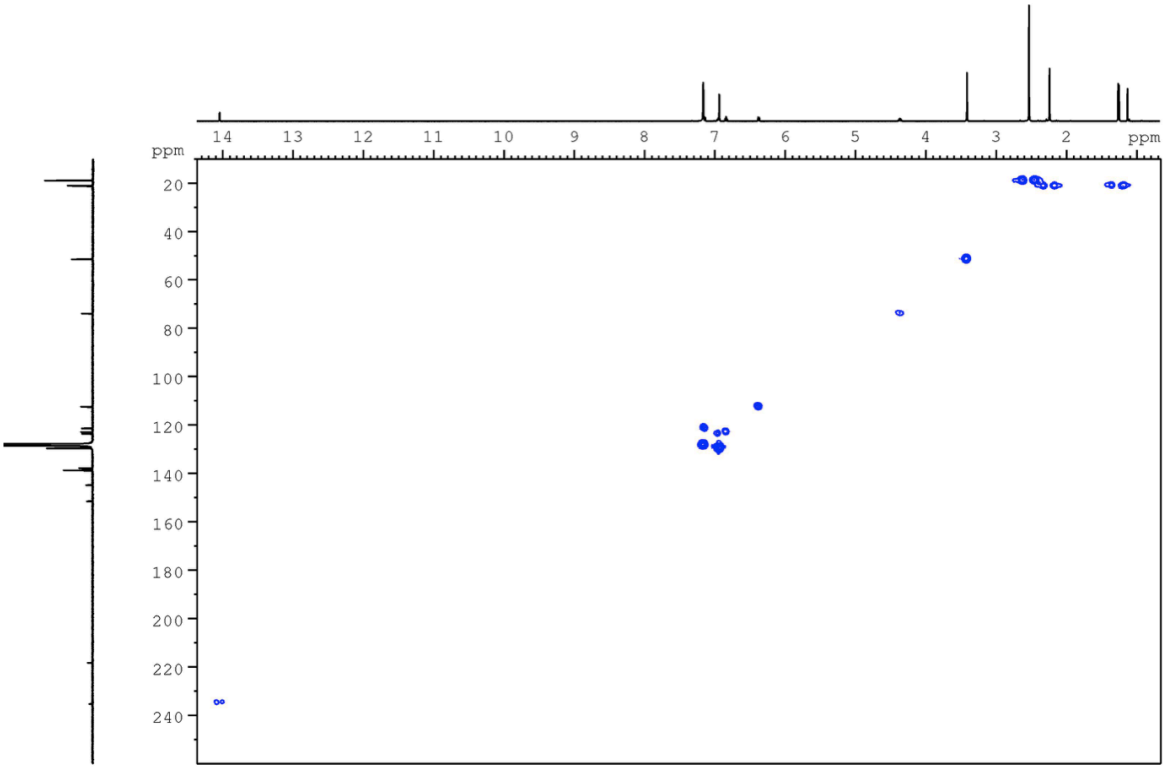

Figure C.4 ^{1}H-^{13}C HMQC spectrum (C_6D_6, 300 MHz) for $Ru(OH)_2(H_2IMes)(=CH\text{-}2\text{-}O^{i}PrC_6H_4)$, **HII-(OH)$_2$**

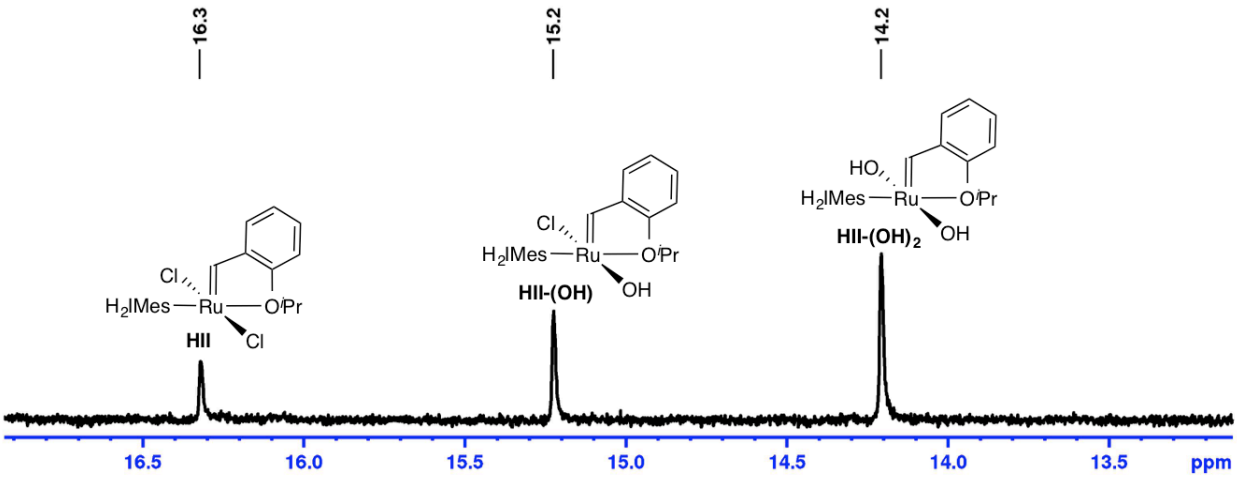

Figure C.5 In situ ^{1}H NMR (THF, 300 MHz) displaying the alkylidene shifts for **HII** and the mono and bis-hydroxide complexes.

D. Apparatus for Synthesis of Phenyldiazomethane

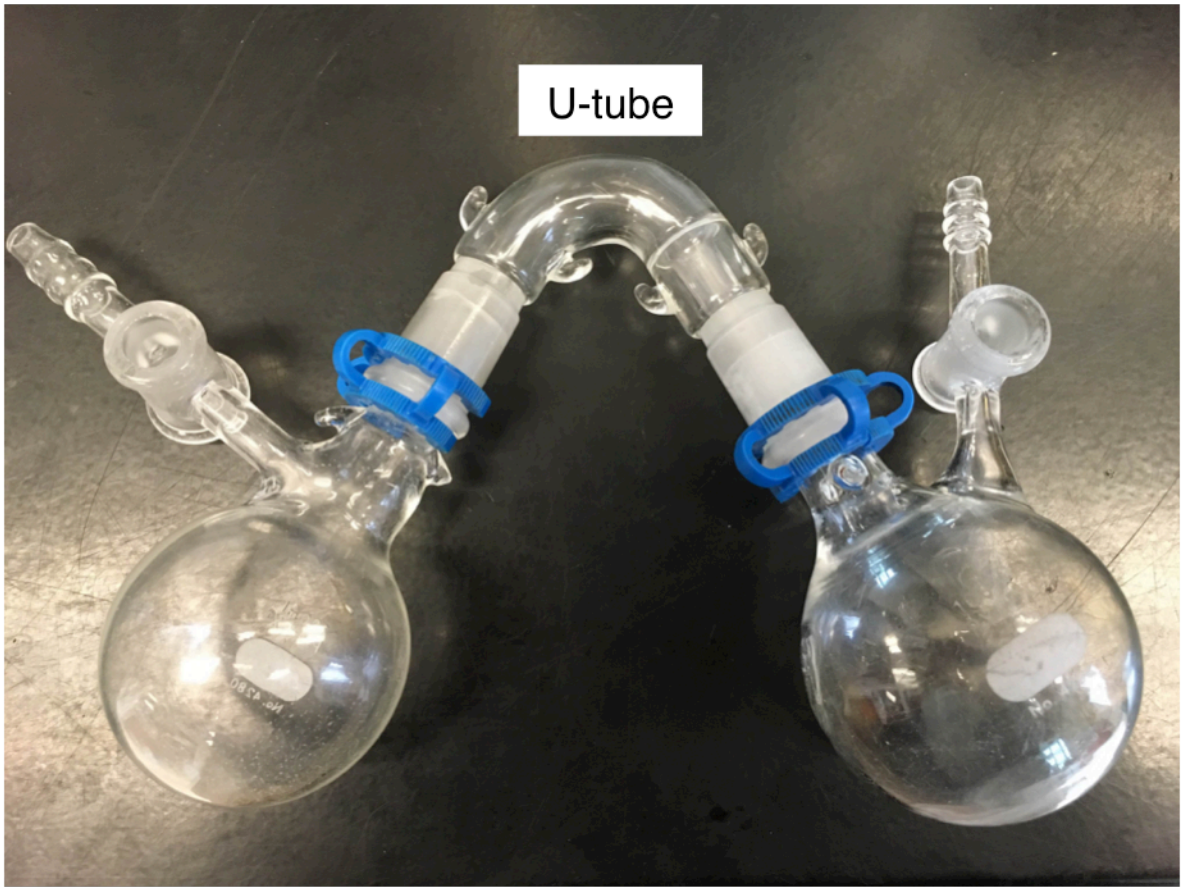

E. References

(1) McLafferty, F. W., *Wiley Registry of Mass Spectral Data*. 9th ed.; Wiley-VCH, 2009.